



**RUSSIAN–GERMAN SEMINAR ON CATALYSIS**  
**“Bridging the Gap between Model and Real Catalysis”**

**ABSTRACTS**

July 9–12, 2007  
Altai Mountains, Russia



SP $\epsilon$ CS<sup>®</sup>



Novosibirsk–2007

Siberian Branch of Russian Academy of Sciences  
Boreskov Institute of Catalysis  
Fritz-Haber-Institut der Max-Planck-Gesellschaft

**RUSSIAN-GERMAN SEMINAR ON CATALYSIS**  
**«Bridging the Gap between Model and Real Catalysis»**

July 9-12, 2007  
Altai Mountains, Russia

**ABSTRACTS**

Novosibirsk-2007

## THE ORGANIZERS



**Boreskov Institute of Catalysis, SB RAS,  
Novosibirsk, Russia**



**Fritz-Haber-Institut der Max-Planck-Gesellschaft,  
Berlin, Germany**

## FINANCIAL SUPPORT



**Russian Foundation for Basic Research, Moscow, Russia**



**Fritz-Haber-Institut der Max-Planck-Gesellschaft,  
Berlin, Germany**



**SPECS GmbH, Berlin, Germany**



**OOO «Rostbiochem», Novosibirsk, Russia**

## INTERNATIONAL ADVISORY COMMITTEE

R. Imbihl	Institute of Physical Chemistry and Electrochemistry, Hannover University, Hannover, Germany
H. Knözinger	Munich University, Munich, Germany
O.V. Krylov	Semenov Institute of Chemical Physics, RAS, Moscow, Russia
V.A. Likholobov	Institute of Hydrocarbons Processing, SB RAS, Omsk, Russia
V.V. Lunin	Lomonosov Moscow State University, Moscow, Russia
V.N. Parmon	Boreskov Institute of Catalysis, SB RAS, Novosibirsk, Russia
N. Rösch	Technical University of Munich, Munich, Germany

## ORGANIZING COMMITTEE

Chairmen:	Valerii I. Bukhtiyarov	Boreskov Institute of Catalysis, SB RAS, Novosibirsk, Russia
	Robert Schlögl	Fritz-Haber-Institut der Max-Planck-Gesellschaft, Berlin, Germany
	V.V. Kaichev	Boreskov Institute of Catalysis, SB RAS, Novosibirsk, Russia
	I.E. Beck	Boreskov Institute of Catalysis, SB RAS, Novosibirsk, Russia
	D. Su	Fritz-Haber-Institut der Max-Planck-Gesellschaft, Berlin, Germany
	A.Yu. Stakheev	Zelinsky Institute of Organic Chemistry, RAS, Moscow, Russia
Secretaries:	L.Ya. Startseva	Boreskov Institute of Catalysis, SB RAS, Novosibirsk, Russia
	S. Wrabitz	Fritz-Haber-Institut der Max-Planck-Gesellschaft, Berlin, Germany

## **PLENARY LECTURES**

PL-1

**OXYGEN ELECTRONIC STATES ON THE SURFACE OF CATALYSTS:  
A QUANTUM-CHEMICAL VIEW**

**Zilberberg Igor**

*Boreskov Institute of Catalysis, Novosibirsk, Russia*

*E-mail: [Zilberberg@catalysis.ru](mailto:Zilberberg@catalysis.ru)*

As generally accepted, oxidative processes on the surface of metal-oxide catalysts are determined mostly by the local properties of the “active” center. Among such properties the energy of oxygen binding on the active center was suggested by Boreskov to be responsible for the whole scenario: full oxidation is attributed to weakly bound oxygen whereas partial oxidation is only possible with strongly bound oxygen. The oxygen binding energy is in turn determined by the electronic state of the oxygen-containing active center. The electronic states of the oxygen center are in general divided into two distinct classes: those arising from close-shell configurations and open-shell states. To distinguish between these cases by quantum-chemical means the multi-determinant wave-function-based approach is a general prescription. At the same time the broken-symmetry spin-polarized Hartree-Fock or Kohn-Sham approach in the paired-orbital basis set represents a promising alternative which can be equally applied for a cluster model and periodic system.

The following examples will be discussed in this presentation. (1) The  $[\text{FeO}]^{2+}$  oxo ferrous species to model “alpha-center” (first introduced by Panov and coworkers) formed on the Fe-ZSM5 catalyst as a result of the  $\text{N}_2\text{O}$  decomposition of iron-containing sites of zeolite. This center exhibits superactivity in the oxidation of benzene to phenol and methane to methanol. (2) Models of the nucleophilic and electrophilic oxygen species on the metallic silver surface discussed in connection with the ethylene epoxidation.

**TOWARDS AN UNDERSTANDING OF STRUCTURE-REACTIVITY  
RELATIONSHIPS IN CATALYSIS: MODEL STUDIES**

**Shaikhutdinov Shamil**

*Fritz-Haber-Institut der Max-Planck-Gesellschaft, Abteilung Chemische Physik,  
Berlin, Germany*

*E-mail: [shamil@fhi-berlin.mpg.de](mailto:shamil@fhi-berlin.mpg.de)*

In attempts to understand the reactivity of oxide and metal/oxide surfaces, we develop model systems where metal and/or oxide particles are deposited on thin, well-defined oxide films under controlled conditions. The model systems have been studied by various “surface science” techniques. Case studies of alkyne hydrogenation and CO oxidation on the model systems will be discussed. In particular, the particle size, support and environmental effects on structure and reactivity of metal nanoparticles will be highlighted.

Our studies are focused on an understanding of structure-reactivity relationships in catalysis using well defined model systems, involving metal particles deposited on ordered oxide films grown on single crystal substrates. We are employing many experimental techniques such as scanning tunneling microscopy (STM), temperature programmed desorption (TPD), infrared reflection absorption spectroscopy (IRAS), and X-ray photoelectron spectroscopy (XPS).

Small metal particles typically exhibit strong size-dependent properties. In addition, the reactivity of the metal particles may depend on the support nature, for example, non-reducible (e.g., alumina, silica) vs reducible (e.g., iron, niobium, cerium) oxides. The size and support effects on adsorption and reactivity of the metal particles are the primary objectives of our studies. In order to understand these phenomena, we deposit metal (Pd, Au, Pd-Ag alloy, etc) particles on various supports and study the adsorption properties of the metal particles as a function of the particle size and dimensions. On the other hand, we compare the adsorption behavior of the metal deposits on the different supports (alumina, silica, iron oxides, ceria, etc) for a given particle size. The nature of the oxide support may influence the reaction (for example, by supplying oxygen species or active sites at metal/oxide periphery) and also alter the nucleation and growth of the metal particles and therefore affect thermal stability of the smallest particles.

Another important issue is the possible reconstruction of the catalysts surface in a reaction atmosphere. These phenomena have been studied by STM *in situ*. Case studies for Au deposited on iron oxides and ceria will be shown.

## PL-3

# INTENSITIES OF IR STRETCHING BANDS AS A NEW SPECTRAL CRITERION OF CHEMICAL ACTIVATION OF ADSORBED MOLECULES VIA THEIR POLARIZATION BY THE ACTIVE SITES IN THE ACID HETEROGENEOUS CATALYSIS

**Kazansky V.B.<sup>1\*</sup>, Subbotina I.R.<sup>1</sup>, Jentoft F.C.<sup>2</sup>, Schlögl R.<sup>2</sup>**

<sup>1</sup>*Zelinsky Institute of Organic Chemistry of the Russian Academy of Sciences,  
Leninsky prospect 47, Moscow 119071, Russia*

*\*E-mail: [vbk@ioc.ac.ru](mailto:vbk@ioc.ac.ru)*

<sup>2</sup>*Fritz Haber Institute of the Max Planck Society, Department of Inorganic Chemistry,  
Faradayweg 4-6, 14195 Berlin, Germany*

It is suggested to utilize as a spectral criterion of perturbation of adsorbed molecules in addition to the low-frequency shifts of their IR stretching bands also the intensities of these bands. The latter are directly connected with polarizability of chemical bonds. Therefore, they are a better indication of chemical activation of adsorbed molecules in acid catalysis than the low-frequency shifts. The examples of such approach are presented for proton transfer to  $\pi$ -bonded olefins, for molecular and dissociative adsorption of paraffins and for their dehydrogenation on cationic forms of zeolites.

Chemical activation of adsorbed molecules is the central problem of heterogeneous catalysis. One of the generally used ways of its solution is the correlation of the perturbation of chemical bonds by the active sites with the low-frequency shifts of the corresponding IR stretching bands. Despite these shifts are directly connected with the force constants of chemical bonds and therefore properly characterize their weakening, the mechanism of such weakening remains unclear. Therefore, we suggest to use as a spectral criterion of chemical activation of adsorbed molecules in addition to low-frequency shifts the intensities of the stretching bands. The latter are proportional to polarizability of chemical bonds upon their stretching or compression. Therefore, they are directly connected with chemical activation of adsorbed molecules in heterogeneous acid catalysis, when the chemical activation of adsorbed molecules arises from their polarization. In the present lecture such possibility is discussed for adsorption of hydrocarbons on acidic and cationic forms of zeolites.

In this connection, our first example is devoted to characterization of acidity strength of hydrogen forms of zeolites [1]. The obtained results indicate that the extinction coefficients of the strongly acidic hydroxyl groups in mordenite are very much higher than for the silanol groups. This demonstrates the utility of our approach as a measure of the OH acidity strength.

The spectral study of ethylene oligomerization on hydrogen forms of zeolites demonstrates that interaction of acidic protons with the double bonds of  $\pi$ -bonded olefins results also in the very strong polarization of the combination of double bond stretching vibrations with the bending vibrations of  $\text{CH}_2$  groups [2]. This indicates the concerted mechanism of proton transfer to adsorbed molecules, which involves strong polarization of hydroxyl groups and the double bond in the  $\pi$ -bonded ethylene in combination with polarization of C-H bending vibrations of one of  $\text{CH}_2$  groups upon its transformation into methyl group via proton addition.

Our final example is devoted to the study of molecular and dissociative adsorption of light paraffins on gallium oxide [3] and cationic forms of zeolites [4]. The obtained results indicate that interaction of adsorbed paraffin with Lewis acid sites is accompanied by different polarization of different C-H stretching bands. This results in the IR spectra with the very unusual distribution of the C-H stretching bands in intensity. Those most strongly polarized by Lewis active sites are unusually strongly low-frequency shifted and are very intense. In contrast the intensity of weakly perturbed bands is very weak. It was also demonstrated that at elevated temperatures the most strongly perturbed and polarized vibrations are involved in heterolytic dissociative adsorption of light paraffins, which represents the first step of their dehydrogenation. Thus, the intensities of IR bands could be also used as a reactivity index of adsorbed molecules, while they are much more sensitive to their perturbation by active sites in comparison with the low-frequency shifts of IR stretching bands. Indeed, the low-frequency shifts correspond only to several percents of their absolute values, while the change in intensity can reach one order of magnitude. Therefore, they present a better way for characterization of polarization of chemical bonds involved in elementary steps of acidic catalysis.

## References

1. B. Kazansky, A.I. Serykh, J. Fraissard, V. Semmer-Herledan, PCCP 5 (2003) 966.
2. V.B. Kazansky, I.R. Subbotina, F. Jentoft, J. Catal. 2409 (2006) 66.
3. V.B. Kazansky, I.R. Subbotina, A.A. Pronin, R. Schlögl, F.C. Jentoft, J. Phys. Chem. B 110 (2006) 7975.
4. V.B. Kazansky, I.R. Subbotina, F.C. Jentoft, R. Schlögl, J. Phys. Chem. B 110 (2006) 17468.



## THE ROLE OF SUBSURFACE SPECIES IN HETEROGENEOUS CATALYTIC REACTIONS

**Hävecker M., Teschner D., Vass E., Knop-Gericke A., Zafeiratos S.,  
Gabasch H., Schnörch P., Schlögl R.**

*Fritz-Haber-Institut der Max-Planck-Gesellschaft,  
Department of Inorganic Chemistry, Berlin, Germany*

*E-mail: [knop@fhi-belin.mpg.de](mailto:knop@fhi-belin.mpg.de)*

The role of subsurface species in heterogeneous catalytic oxidation and hydrogenation reactions will be discussed. The application of synchrotron radiation based in situ X-ray photoelectron spectroscopy (XPS) has allowed the identification of subsurface species under reaction conditions. The correlation of their abundance with the catalytic activity was studied. It was shown, that the selectivity in the hydrogenation of pentyne to pentene over Pd catalysts is controlled by the formation of a PdC phase. A similar phase was observed during the ethylene oxidation over Pd(111).

In situ XPS allows the investigation of correlations between the catalytic performance and the electronic surface structure of working catalysts. By synchrotron radiation facilities the photon energy and therefore the information depth of the detected photoelectrons can be varied to some extent. This variation offers the possibility to detect depth concentration profiles of species occurred under reaction conditions. In hydrogenation and oxidation

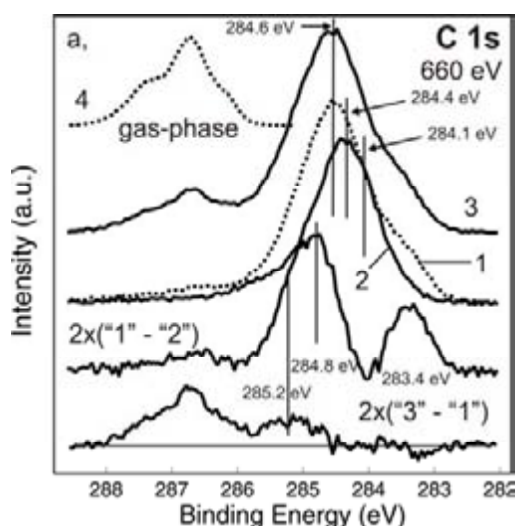


Figure 1: C1s region of Pd foil at different conditions. 1: in the reaction mixture; 2: after switching off 1-pentyne (only H<sub>2</sub>); 3: after switching off H<sub>2</sub> (only 1-pentyne). All the spectra were recorded at 358 K. Some difference spectra are also shown.

reactions subsurface species could be identified by this technique under reaction conditions. These subsurface species show a dynamic response of changes of the reaction conditions as shown in Fig. 1 and they show a strong correlation with the catalytic performance of the catalyst.

A correlation of the abundance of subsurface oxygen and the yield of formaldehyde was found in the methanol oxidation over Cu foil [1]. The CO oxidation over Ru(0001) is characterized by a monotonous increase of the catalytic activity with the abundance of subsurface oxygen [2]. Under selective hydrogenation reaction conditions of pentyne to pentene over Pd catalyst (T = 358 K,

$p_{\text{H}_2} = 0.85$  mbar,  $p_{\text{pentyn}} = 0.05$  mbar) the formation of a dissolved C in Pd was observed [3].

The thickness of the phase was estimated to be about 1.5 nm. This phase is metastable and can be observed only under reaction conditions. When the pentyn is switched off, the PdC phase decomposes (see Fig. 1). It was shown, that the hydrogen, that is dissolved in Pd is very reactive, but not selective. The hydrogen provided by the gas phase to the surface of the catalyst is selective. Therefore it was concluded that the PdC phase, which forms under reaction conditions of the selective hydrogenation hinders the diffusion of the dissolved hydrogen to the surface.

The oxidation reaction of ethylene on Pd(111) single crystal was investigated in the temperature range from 330 – 930 K in a reaction mixture of  $5 \times 10^{-4}$  mbar  $\text{C}_2\text{H}_4$  and  $1.5 \times 10^{-3}$  mbar  $\text{O}_2$ . At 500 K the formation of a PdC phase indicated by a shift of the C1s signal and the diffusion of C into the Pd bulk was observed. The abundance of the PdC phase coincidences with a shift of the selectivity towards CO formation. Above 660 K the dissolved carbon species decomposed and the reaction took place on an adsorbate-depleted Pd metal surface, with CO as the main product.

The examples demonstrate the potential of in situ XPS for the investigation of metastable subsurface species involved in heterogeneous catalytic processes.

## References

1. H. Bluhm, M. Hävecker, A. Knop-Gericke, E. Kleimenov, R. Schlögl, D. Teschner, V.I. Bukhtiyarov, D.F. Ogletree, M. Salmeron, *J. Phys. Chem. B* 108 (2004) 14340.
2. R. Blume, M. Hävecker, S. Zafeiratos, D. Teschner, E. Kleimenov, A. Knop-Gericke, R. Schlögl, A. Barinov, P. Dudin, M. Kiskinova, *J. Catal.* 239 (2006) 354.
3. D. Teschner, E. Vass, M. Hävecker, S. Zafeiratos, P. Schnörch, H. Sauer, A. Knop-Gericke, R. Schlögl, M. Chamam, A. Wootsch, A.S. Canning, J.J. Gamman, S.D. Jackson, J. McGregor, L.F. Gladden, *J. Catal.* 242 (2006) 26.

## ACTIVATING LIGHT ALKANES – NEW OPPORTUNITIES THROUGH MOLECULAR UNDERSTANDING

**Lercher Johannes A.**

*TU München, Department of Chemistry, Lichtenbergstr. 4, 85748 Garching, Germany*

*E-mail: johanneslercher@hotmail.com*

The activation and catalytic transformation of light alkanes is a demanding and important problem at the boundary of the petroleum and petrochemical industry. The high availability of light alkanes and the push for higher feedstock diversity in the petrochemical industry requires a better understanding of the underlying chemical principles of the catalytic chemistry. In many cases, thermodynamic boundary conditions dictate that the reaction temperatures for hydrocarbon transformation reactions are low, which requires highly active catalysts.

Alkanes interact with oxide surfaces primarily through Dispersion forces. This is best seen in the interaction of alkanes with zeolites, in which the interaction of n-alkanes contributes the majority of the heat of adsorption the molecule generates upon adsorption. Figure 1 shows such a dependence of the heat of adsorption of n-alkanes on various zeolites

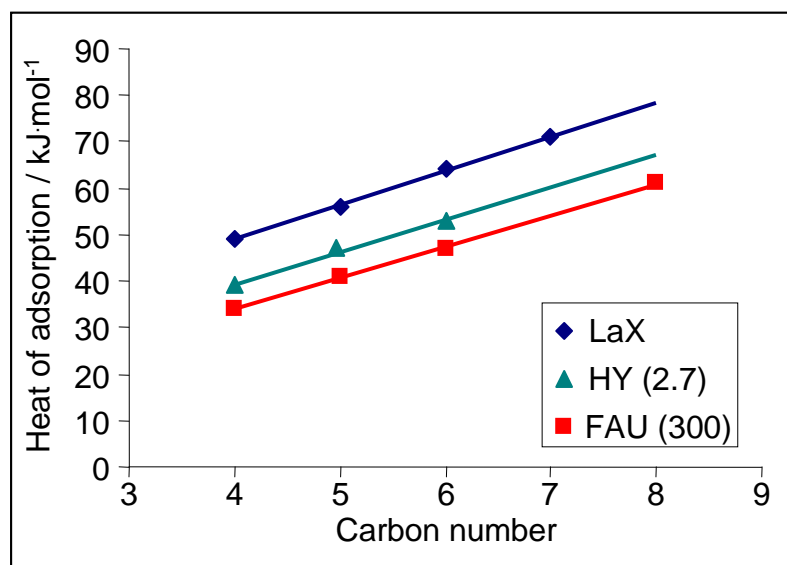


Figure 1. Heat of adsorption of n-alkanes adsorbed on faujasite type zeolites

with faujasite structure. The figure indicates that the direct contribution of the interactions with the Brønsted acidic hydroxy groups does only contribute few kJ per mol adsorbed alkanes [1]. This relatively weak interaction explains also, why it is so difficult to directly activate alkanes *via* this route. The direct (protolytic) conversion of alkanes has true energies of

activation of approximately 200 kJ/mol, largely independent of the zeolite structure and the size of the alkane [2]. However, the experiment also indicates that the rate of reaction is primarily dependent on the concentration of the reactants in the zeolite pores, i.e., the larger the alkane and the better the fit between the alkane and the zeolite, the higher the

concentration of alkanes in the pores and with it the higher the rate of reaction normalized to the concentration of Brønsted acid sites will be.

In order to be able to convert alkanes at low temperatures hydride transfer reactions from carbenium ions (formed by olefins present in traces or by an additional process) have to be utilized. The best known and most discussed case is the isomerization of alkanes by sulfated zirconia. In this case, sulfated zirconia generates the olefins from alkanes during the reaction in extremely small quantities by a stoichiometric redox process converting chemisorbed  $\text{SO}_3$  into chemisorbed  $\text{SO}_2$  and water. The olefins generated isomerize to iso-olefins and are being removed from the surface *via* hydride transfer. For every olefin created approximately 500 hydride transfer cycles occur. The overall true energy of activation for this process is around 115 kJ/mol [3]. This hydride transfer is also the dominating route of transition metals are used as integral part of the catalysts.

Direct addition of olefins to enable this reaction route is hardly possible with fixed bed reactors, but can be industrially realized if a backmixed reactor is used for operation. The best example for that chemistry is the alkylation of isobutane with n-butene over a solid acid catalyst. In order to achieve stable operation, the concentration of the olefin has to be in the low ppm range, which is only possible with backmixed reactors at high conversions [4].

Generation of the olefins, however, is not mandatory to be catalyzed by redox active oxides or metals. The polarization by large multiply charged cations (such as  $\text{La}^{3+}$ ) is so much stronger than the interaction with the Brønsted acidic hydroxyl groups that this interaction induces direct dehydrogenation of the sorbed alkanes [5]. The strong polarization is already seen in Figure 1, which shows that the heat of adsorption of the alkanes increased by approximately 10 kJ/mol. The interaction involves polarizing C-H groups at secondary and tertiary carbon atoms, while the C-H groups of primary carbon atoms are even strengthened. At temperatures as low as 340 K evolution of molecular hydrogen and cracking of adsorbed molecules has been observed. DFT calculations indicate that the true energy of activation is approximately the same as observed for butane isomerization with sulfated zirconia.

Finally, a new potential route to activate the primary carbon atom is opened *via* the oxidative chlorination of methane using  $\text{LaCl}_3$  as catalysts and  $\text{HCl}$  and  $\text{O}_2$  as co-reactants [6]. The role of the oxidation process appears to be to generate positively charged surface chlorine atoms, which can be exchanged in an electrophilic substitution for one hydrogen in methane. The process is selective with very little oxidation and a small extent of generating carbon oxides.

## PL-5

Overall, it will be shown that multifunctional catalysts and closely coupled reaction steps are needed to activate alkanes at mild temperatures. Only the subtle control of the functions and actions lead to active and stable catalysts. New catalytic materials and new potential process routes can be developed using the rigorous understanding of the elementary steps as guiding principle.

### References

1. F. Eder, M. Stockenhuber and J.A. Lercher, *J. Phys. Chem. B* 101 (1997) 5414.
2. Th.F. Narbeshuber, H. Vinek and J.A. Lercher, *J. Catal.* 157 (1995) 388.
3. X. Li, K. Nagaoka, L.J. Simon, A. Hofmann, J. Sauer and J.A. Lercher, *J. Am. Chem. Soc.* 127 (2005) 16159.
4. A. Feller, A. Guzman, I. Zuazo and J.A. Lercher, *J. Catal.* 224 (2004) 80.
5. C. Sievers, A. Onda, A. Guzmán, K.S. Otilinger, R. Olindo and J.A. Lercher, *J. Phys. Chem. B*, accepted for publication (2007).
6. E. Peringer, S.G. Podkolzin, M.E. Jones, R. Olindo and J.A. Lercher, *Topics in Catalysis* 38 (2006) 211.

## APPLICATION OF IN SITU METHODS FOR THE INVESTIGATION OF ELECTROCATALYTIC REACTIONS

**Savinova Elena R.**

*Boreskov Institute of Catalysis, Novosibirsk, Russia*

*E-mail: [elensav@catalysis.ru](mailto:elensav@catalysis.ru)*

*Université Louis Pasteur, LMSPC-UMR 7515, Strasbourg, France*

*E-mail: [Elena.Savinova@ecpm.u-strasbg.fr](mailto:Elena.Savinova@ecpm.u-strasbg.fr)*

Electrocatalytic processes have recently attracted considerable attention due to their technological importance in a number of applications, in particular polymer electrolyte membrane fuel cells (PEMFC). The lecture gives a selected review of in situ methods utilized for the investigation of heterogeneous electrocatalytic reactions occurring at solid/liquid interfaces.

Heterogeneous electrocatalytic processes occur at the electrode/electrolyte interface. These are of utmost importance in a variety of technologically important applications including energy conversion, electrosynthesis, electrochemical sensors, etc. The mechanisms of electrocatalytic processes may be similar to those of heterogeneous catalytic reactions. This is however not always the case since application of electric potential across the interface may exert strong influence on the nature of the adsorbates and the rates of their transformations. In contrast to heterogeneous catalytic, electrocatalytic processes allow an additional degree of freedom namely the electric potential drop across the interface. The latter can be utilized as a tool for controlling the rates and selectivities of surface reactions.

In this presentation we will mainly focus on the investigation of solid/liquid electrified interfaces. Their in situ spectroscopic investigation is hindered by absorption of incoming and outgoing radiation in a layer of liquid electrolyte. Despite this difficulty application of various in situ spectroscopies for studying solid/liquid interfaces has flourished during recent decades resulting in considerable advancement of the understanding of the mechanisms of electrocatalytic reactions [1-3].

In this lecture we will consider selected examples demonstrating possibilities of in situ methods for the investigation of the structure and composition of solid/liquid electrified interfaces and the mechanisms of electrocatalytic reactions. Both cathodic (oxygen reduction reaction) and anodic (carbon monoxide and methanol oxidation) processes will be discussed. We will start from electrochemical methods, their advantage being high sensitivity, while disadvantage – limited selectivity [4]. We will then move to the infrared spectroscopy and

## PL-6

discuss its application to the understanding of CO and methanol adsorption and oxidation at monometallic Pt [5] and bimetallic PtRu [6] electrodes. The last example refers to the oxygen reduction reaction at Ru and Se-modified Ru nanoparticles as studied using in situ X-ray absorption spectroscopies [7].

### Acknowledgements

The contribution of N. Alonso-Vante, H. Boennemann, O.V. Cherstiouk, S.V. Cherepanova, A.N. Gavrilov, F. Hahn, V.V. Kriventsov, A.N. Kuznetsov, D.I. Kochubey, K.N. Loponov, F. Maillard, K.S. Nagabhushana, S.N. Pronkin, P.A. Simonov, U. Stimming, V.I. Zaikovskii is highly appreciated. Funding from RFBR under grant No. 06-03-32737 is gratefully acknowledged.

### References

1. Structure of Electrified Interfaces, J. Lipkowski, P.N. Ross (Eds.), Wiley VCH, New York, 1993.
2. Interfacial Electrochemistry: Theory, Experiment and Applications, A. Wieckowski (Ed.), Marcel Dekker, New York, 1999.
3. Handbook of Fuel Cells. Fundamentals, Technology and Applications, Vol. 2: Electrocatalysis, W. Vielstich, A. Lamm, H.A. Gasteiger (Eds.), John Wiley & Sons, Chichester, 2003.
4. S.N. Pronkin, P.A. Simonov, V.I. Zaikovskii, E.R. Savinova, *J. Mol. Catal. A* 265 (2007) 141.
5. F. Maillard, E.R. Savinova, P.A. Simonov, V.I. Zaikovskii, U. Stimming, *J. Phys. Chem. B* 108 (2004) 17893.
6. E.R. Savinova, F. Hahn, N. Alonso-Vante, in press.
7. V.V. Kriventsov, K.N. Loponov, D.I. Kochubey, K.S. Nagabhushana, H. Boennemann, and E.R. Savinova, in press.

## REVEALING STRUCTURE-ACTIVITY RELATIONSHIP IN SUPPORTED METAL CATALYSTS BY ANALYSIS OF XPS LINE SHAPE

**Stakheev Alexander<sup>1</sup>, Grunert Wolfgang<sup>2</sup>, Tkachenko Olga<sup>1</sup>, Teleguina Natalia<sup>1</sup>**

<sup>1</sup>*Zelinsky Institute of Organic Chemistry, Moscow, Russia*

<sup>2</sup>*Ruhr-University Bochum, Bochum, Germany*

*E-mail: [st@ioc.ac.ru](mailto:st@ioc.ac.ru)*

The presentation is devoted to application of XPS lineshape asymmetry analysis for revealing structure-activity relationship for supported Pt and Pd catalysts. The method allows gathering valuable information on electronic state of supported metal particles and provides new insight into metal-support interaction effects.

Several examples of application of this approach are discussed:

1. Study of SMSI effect for Pt/TiO<sub>2</sub>
2. Metal-support interaction in Pd/carbon
3. Deactivation of Pt/HPA/Al<sub>2</sub>O<sub>3</sub>
4. Alloying in Pd-Ag/carbon and Pd-Ag/Al<sub>2</sub>O<sub>3</sub>

Advantages and limitations of XPS lineshape analysis are considered.



## **ORAL PRESENTATIONS**

- Study of the mechanisms of heterogeneous catalytic reactions at atomic-molecular level
- Application of the Surface Sensitive Methods to study the formation, activation and degradation of the active sites in heterogeneous catalysts
- Computational chemistry to study the catalytic reactions

QUANTUM CHEMICAL MODELING OF NANOSIZED TRANSITION METAL  
CATALYSTS: DENSITY FUNCTIONAL CALCULATIONS OF Pd AND Cu  
NANOCLUSTERS

**Yudanov I.V.<sup>1</sup>, Neyman K.M.<sup>2</sup>, Rösch N.<sup>3</sup>**

<sup>1</sup>*Boreskov Institute of Catalysis, Novosibirsk, Russia*

<sup>2</sup>*Institució Catalana de Recerca i Estudis Avançats (ICREA) and Departament de Química  
Física, Universitat de Barcelona, Barcelona, Spain*

<sup>3</sup>*Department Chemie, Technische Universität München, Garching, Germany*

*E-mails: [ilya@catalysis.ru](mailto:ilya@catalysis.ru), [konstantin.neyman@icrea.es](mailto:konstantin.neyman@icrea.es), [roesch@ch.tum.de](mailto:roesch@ch.tum.de)*

To study catalytic properties of nanosized metal catalysts, we developed an approach based on the calculations of three-dimensional symmetric clusters of fcc metals terminated by low-index surfaces. Our nanocluster model strategy allows us to calculate the electronic structure of particles and catalytic reactions on them with a diameter of 1 nm and beyond at an accurate DFT level. This modeling technique is applied to study mechanisms of catalytic reactions on Pd and Cu nanoparticles.

With a CO probe on cuboctahedral Pd particles we demonstrated that such symmetric three-dimensional cluster models of ~100 metal atoms quantitatively describe various adsorption properties of a single crystal (111) surface or of (111) facets of model catalyst particles (which are usually more extended than our model clusters). On the other hand, CO adsorption characteristics calculated for sites at edges, kinks and (001) terraces of these cluster models permit an interpretation of peculiarities of the experimental C-O vibrational spectra obtained for defect-rich and well-defined model catalysts [1,2].

Furthermore, we investigated the mechanism of Pd nanosized catalyst poisoning by carbon and carbonaceous species which are formed at small rates as byproducts of methanol dehydrogenation. We considered the adsorption of monoatomic carbon and carbonaceous CH<sub>x</sub> (x = 1, 2, 3) fragments at different sites of nanoparticles as well as in subsurface (in the case of carbon) interstitial positions [3-6]. CH<sub>3</sub> and CH<sub>2</sub> species were found to occupy preferentially positions at edges of nanoparticles [5,6]. We also considered the mechanism of C-O bond scission in different intermediates (CH<sub>3</sub>O, CH<sub>2</sub>O, CHO and CO) of methanol dehydrogenation, in particular the thermodynamics of these reactions and the corresponding activation barriers [5,6]. According to calculations, C-O bond scission is likely to proceed as a slow byprocess parallel to the faster dehydrogenation pathway in intermediates exhibiting single (σ-type) C-O bond, i.e. methoxide and hydroxymethyl species [6].

## OP-1

Finally, we applied our cluster modeling technique to study catalytic properties of Cu and Pd nanoparticles which are modified by pre-adsorbed oxygen.

### References

1. I.V. Yudanov, R. Sahnoun, K.M. Neyman, and N. Rösch, *J. Chem. Phys.* 117 (2002) 9887.
2. I.V. Yudanov, R. Sahnoun, K.M. Neyman, N. Rösch, J. Hoffmann, S. Schauermann, V. Johánek, H. Unterhalt, G. Rupprechter, J. Libuda, and H.-J. Freund, *J. Phys. Chem. B* 107 (2003) 255.
3. I.V. Yudanov, K.M. Neyman, and N. Rösch, *Phys. Chem. Chem. Phys.* 6 (2004) 116.
4. K.M. Neyman, C. Inntam, A.B. Gordienko, I.V. Yudanov, and N. Rösch, *J. Chem. Phys.* 122 (2005) 174705.
5. I.V. Yudanov, K.M. Neyman, N. Rösch, *Phys. Chem. Chem. Phys.* 8 (2006) 2396.
6. I.V. Yudanov, A.V. Matveev, K.M. Neyman, N. Rösch, submitted.

**ON THE IMPACT OF Pd ON THE MAGNETIC PROPERTIES OF Co PARTICLES  
ON A THIN ALUMINA FILM ON NiAl(110)**

**Martyanov O. N.<sup>1\*</sup>, Risse T.<sup>2</sup>, and Freund H.-J.<sup>2</sup>**

<sup>1</sup>*Boriskov Institute of Catalysis, Novosibirsk, Russia*

<sup>2</sup>*Fritz-Haber-Institut der Max-Planck-Gesellschaft, Berlin, Germany*

\*E-mail: [oleg@catalysis.ru](mailto:oleg@catalysis.ru)

Changes of the magnetic properties of ferromagnetic Co particles deposited at room temperature on a thin alumina film grown on a NiAl(110) substrate were investigated as a function of Pd coverage by subsequent deposition of Pd onto deposited Co particles. From comparison with previous XPS, IR, and TPD experiments as well as measurements on annealed samples it is concluded that Pd which tend to form a shell on top of Co particles induces structural rearrangements within the Co particles which may also involve the intermixing of small amounts of Pd into the Co particles.

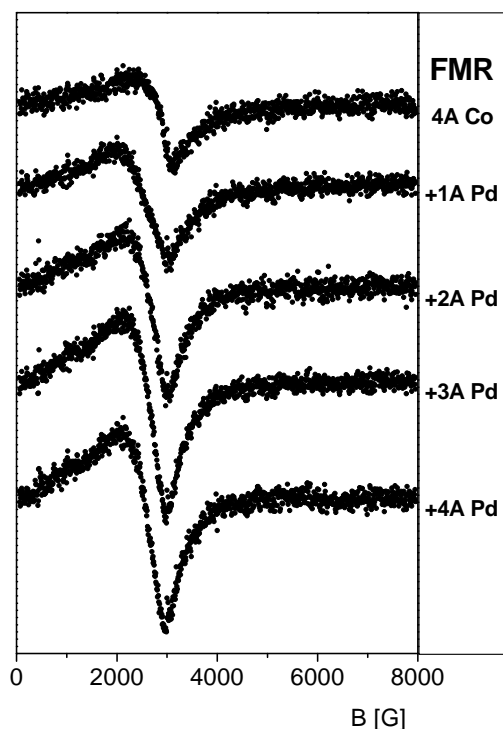
The interest to nanometer scale bimetallic particles is on the one hand driven by the prospects these systems have to improve technologically important applications and on the other hand these systems pose a variety of important problems for fundamental science. Cobalt and bimetallic Co-Pd systems are well-known Fischer-Tropsch catalysts. Compared to Co, the bimetallic systems exhibit an increased activity towards CO- hydrogenation and methane conversion, attributed to resistance against oxidation. To gain more insight into the microscopic properties of this complex system a model system was prepared using a well defined thin alumina surface, which was proven to be a suitable model system [1]. Co and Pd were deposited onto this substrate under UHV conditions and the properties of the particles were previously explored using XPS, STM, TPD, and IR spectroscopy for different preparation conditions [2-4]. From the abovementioned experiments it was concluded that Pd grown on top Co particles form a shell while the reversed deposition order gives rise to a substantial intermixture of Pd and Co due to the tendency of Pd to segregate to the surface of the particles. In the present investigation we looked into this growth using the magnetic properties as a sensitive probe to investigate structural properties of the abovementioned bimetallic particles.

The ferromagnetic resonance (FMR) experiments were carried out in a specially designed UHV apparatus which has been described previously [5]. The thin aluminum oxide film was grown on a NiAl(110) single crystal as described in detail elsewhere [6]. The particles were grown at 300 K by an electron beam evaporator (Focus/Omicron EFM3) with a deposition

## OP-2

rate of 1 Å/min as calibrated by a quartz microbalance. The base pressure in the apparatus was better than  $2 \cdot 10^{-10}$  mbar.

It is known that Co particles formed by deposition of 2 Å Co at room temperature have to be considered superparamagnetic, however, due to the particle size distribution not all of them are in the isotropic limit of FMR spectroscopy giving rise to a size dependence of the resonance position within the ensemble. An analysis of the angular dependence, assuming superparamagnetic particles with a uniaxial anisotropy, results in a  $g$ -value of  $2.22 \pm 0.015$  which is in a good agreement with previously obtained data and indicates that the structure of the clusters is perturbed as compared to bulk like situations where a smaller  $g$ -value is expected [7]. The FMR spectra observed for 4 and 10 Å Co deposited on the  $\text{Al}_2\text{O}_3/\text{NiAl}(110)$  surface show a strong increase of the FMR intensity as compared to the 2 Å case. The apparent resonance position shifts monotonously towards lower fields with increasing amount of Co. Concomitantly, the line shape becomes more asymmetric indicative for an increase of the magnetic anisotropy.



FMR spectra of Pd deposited at 300 K on top of 4 Å Co on  $\text{Al}_2\text{O}_3/\text{NiAl}(110)$

The Figure on the left shows the changes of the FMR spectra of 4 Å Co upon subsequent deposition of Pd at 300 K. The addition of 1 Å Pd results in an increase of the line width from 800 G to 960 G accompanied by a shift of the apparent resonance position to 2450 G. In addition, the integral intensity of the spectrum increases by about 40%. The FMR intensity increases further upon addition of Pd and levels off at about 3 Å Pd. At this point the intensity has approximately doubled. Despite of differences in the changes of resonance position and line width upon Pd co-deposition the relative intensities of all systems behave rather similar. The FMR intensity increases by a factor of 2 for particles formed upon deposition of 2 Å Co to a factor of 2.5 for the 10 Å case, after addition of 2 and 4 Å Pd, respectively.

This increase in FMR intensity is due to an increase of the projection of the magnetization along the static magnetic field for these superparamagnetic particles. In principle this increase could either be governed by an increase of the magnetic anisotropy or

by an increase of the magnetic moments of the metal particles. Due to the rather small change in the resonance positions observed it is unlikely that the effect is dominated by an increase of the anisotropy constants. Furthermore, the absolute change of the FMR intensity for the larger particles is about three orders of magnitude larger than for the small particles while the amount of Pd necessary to achieve this increase differs only by a factor of two which renders this explanation even more unrealistic for the bigger particles.

We have shown that Pd deposited on top of Co particles grown at 300 K changes the magnetic properties of the Co particles considerably, in particular with respect to the magnetic moment of the particles. This increase in the magnetic moment could be correlated to structural rearrangements within the pristine Co particles which are induced by Pd and it is likely that Pd does not simply form a shell on top of the Co particles as inferred from XPS, STM, TPD and IR results, but is incorporated into the Co particles to facilitate structural rearrangements. This is corroborated by comparing the abovementioned pristine particles to structurally relaxed systems created by thermal annealing. In this case no increase of the magnetic moment was observed, however, similar changes of the resonance position and the line width were observed in both cases, indicating the importance of the Co/Pd interface for the magnetic anisotropy of the system. For a reversed deposition order previous experiments had already shown that a substantial intermixing of Co and Pd takes place. This intermixture of Pd and Co leads to systems with a considerably enhanced magnetic anisotropy. On the other hand the line width, characterized by an inhomogeneous superposition of resonance lines, indicates that a substantial deviation of the magnetic properties exists which is due to the spread in chemical composition and structural inhomogeneities of these systems grown under kinetically controlled situations.

## References

1. H.-J. Freund, J. Libuda, M. Bäumer, T. Risse, A. Carlsson, *Chem. Rec.* 3 (2003) 181.
2. A.F. Carlsson, M. Naschitzki, M. Bäumer, H.-J. Freund, *J. Phys. Chem. B* 107 (2003) 778.
3. A.F. Carlsson, M. Bäumer, T. Risse, and H.-J. Freund, *J. Chem. Phys.* 119 (2003) 10885.
4. M. Heemeier, A.F. Carlsson, M. Naschitzki, M. Schmal, M. Bäumer, and H.-J. Freund, *Angew. Chem. Int. Ed.* 41 (2002) 4073.
5. J. Schmidt, T. Risse, H. Hamann, and H.-J. Freund, *J. Chem. Phys.* 116 (2002) 10861.
6. J. Libuda, F. Winkelmann, M. Baumer, H.-J. Freund, T. Bertrams, H. Neddermeyer, and K. Muller, *Surf. Sci.* 318 (1994) 61.
7. T. Hill, T. Risse, and H.-J. Freund, *J. Chem. Phys.* 122 (2005) 164704.

## OP-3

### THE OXIDATION OF RHODIUM SUPPORTED ON ALUMINA IN REACTION WITH NO<sub>x</sub> STUDIED BY XPS

**Kalinkin A.V., Smirnov M.Yu., Bukhtiyarov V.I.**

*Boreskov Institute of Catalysis, Novosibirsk, Russia*

*E-mail: [avkalinkin@mail.ru](mailto:avkalinkin@mail.ru)*

It is found that NO<sub>x</sub> reacts with model Rh/Al<sub>2</sub>O<sub>3</sub> catalysts to produce nitrate and nitrite species on the alumina surface. Parallel, rhodium particles are oxidized. Depending on the concentration of rhodium deposited, the oxidation results in a solution of oxygen atoms in the bulk of rhodium particles or in Rh<sub>2</sub>O<sub>3</sub>-like oxide. It is found that rhodium particles deposited on Al<sub>2</sub>O<sub>3</sub> can be oxidized by the nitrate species produced in the reaction of NO<sub>x</sub> with the alumina surface.

The abatement of NO<sub>x</sub> in automobile exhaust gases gains in increasingly more significance in view of implementation of engines operating in the presence of a great excess air. In this connections, the actual tasks are the development of catalytic systems for NO<sub>x</sub> utilization and the studies of the mechanism of NO and NO<sub>2</sub> reactions with other components of automobile catalysts designed for the exhaust purification. This work is aimed to identify products forming under the reaction of NO<sub>x</sub> with Rh/Al<sub>2</sub>O<sub>3</sub> – a traditional component in the automobile catalysts – using X-ray photoelectron spectroscopy (XPS).

Samples of Rh/Al<sub>2</sub>O<sub>3</sub> model catalysts were prepared by evaporation of different amounts of rhodium onto a thin alumina film grown on a tantalum foil. In the course of Rh deposition, a photoemission line Rh3d appears first at a binding energy BE(Rh3d<sub>5/2</sub>) 308.2 eV and then shifts to the value typical of massive metallic rhodium (307.2 eV) as the rhodium concentration grows. The increased BE(Rh3d<sub>5/2</sub>) values observed for low concentrations of Rh deposited are due to a so-called ‘size-effect’ resulting from a difference in properties of small metallic particles and corresponding massive metal.

Thus prepared samples of Al<sub>2</sub>O<sub>3</sub> and Rh/Al<sub>2</sub>O<sub>3</sub> were treated in a preparation chamber of a photoelectron spectrometer with a NO<sub>x</sub> mixture composed of O<sub>2</sub> (10 Torr) and NO (10 Torr) at room temperature and then transferred into an analyzer chamber for spectra measurement. Al<sub>2</sub>O<sub>3</sub> reacts with NO<sub>x</sub> to produce surface nitrate and nitrite species revealed by N1s lines with BEs 407.2 and 404.7 eV, respectively. A characteristic change is observed also in the O1s spectrum. Before the reaction, the O1s spectrum is composed of two lines possessed by oxygen anions in the structure of alumina (a strong line at 531.1 eV) and surface hydroxyl and

water species (a minor shoulder at 533.1 eV). After the reaction with  $\text{NO}_x$ , the latter line becomes much stronger that can be assigned to formation of the nitrate and nitrite species.

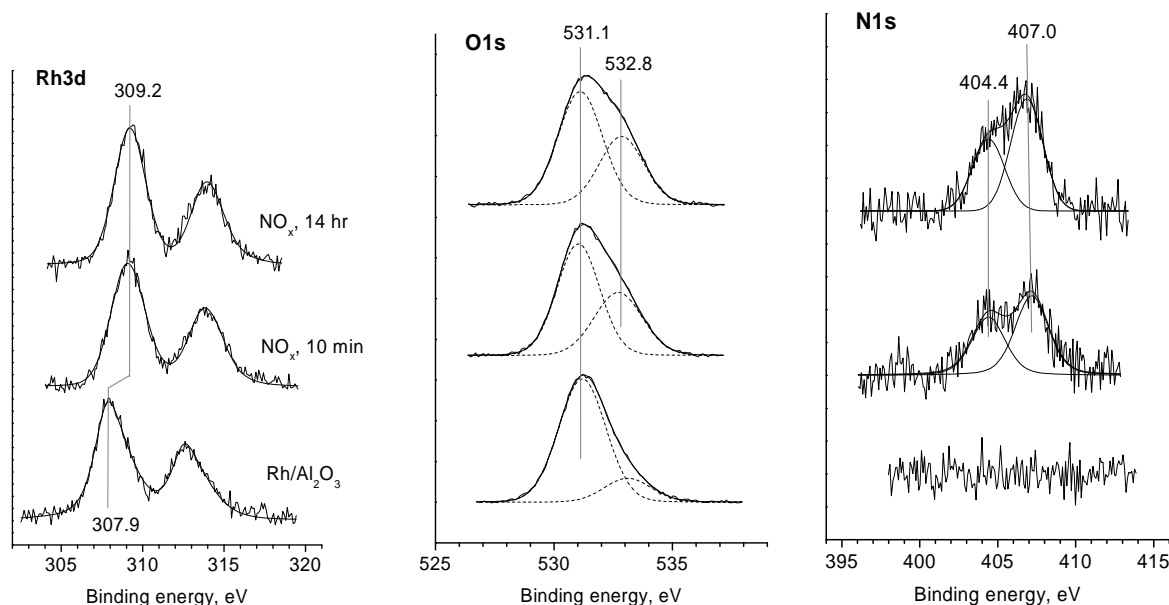


**Fig. 1.** Rh3d, O1s and N1s spectra of Rh/Al<sub>2</sub>O<sub>3</sub> (Rh/Al 0.11) before and after the reaction with NO<sub>x</sub> at room temperature for 10 min and 14 hours.

Parallel with nitrate and nitrite formation, the reaction of Rh/Al<sub>2</sub>O<sub>3</sub> with NO<sub>x</sub> changes the chemical state of supported rhodium. Fig. 1 exhibits Rh3d, O1s and N1s spectra recorded for a Rh/Al<sub>2</sub>O<sub>3</sub> sample before and after the reaction with NO<sub>x</sub> at room temperature. A Rh/Al atomic ratio in the sample is equal to 0.11 that corresponds to relatively small rhodium particles. After 10 min of the reaction, the Rh3d<sub>5/2</sub> line shifts from the initial value of 307.9 eV upward by ~ 1.2 eV, i.e. becomes typical of rhodium oxide, Rh<sub>2</sub>O<sub>3</sub>. Increase in the reaction time period to 14 hours results in a negligible additional shift of the Rh3d line until the BE(Rh3d<sub>5/2</sub>) 309.2 eV. As compared with the 10 min time period, some increase (~10-15%) in the nitrate species concentration is observed that is revealed in the behaviour of the N1s (BE ~ 407.0 eV) and O1s (~ 532.8 eV) lines.

The chemical state of rhodium after the reaction with NO<sub>x</sub> depends on the surface concentration of Rh and, hence, on an average size of rhodium particles. Fig. 2 exhibits Rh3d spectra recorded for a Rh/Al<sub>2</sub>O<sub>3</sub> sample characterized by the Rh/Al ratio of 0.45 before and after the reaction with NO<sub>x</sub> at room temperature. Like in the case of Rh/Al 0.11, the reaction causes the Rh3d line to shift upward, however, the increase in the Rh3d<sub>5/2</sub> binding energy,  $\Delta\text{BE}$ , is significantly smaller and is dependent on the reaction time. Thus, the  $\Delta\text{BE}$  value is equal to 0.6 eV with the reaction lasts 20 min, and increases to 0.9 eV after the prolonged



## OP-3

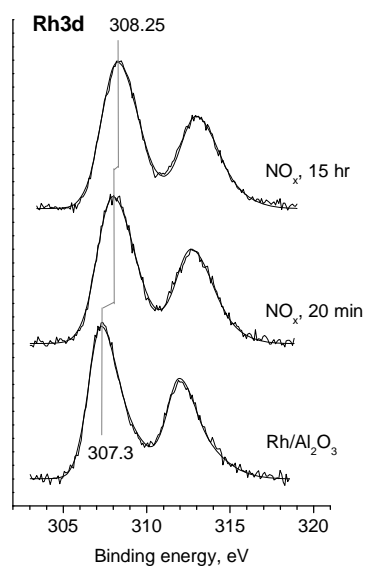


**Fig. 2.** Rh3d spectra of Rh/Al<sub>2</sub>O<sub>3</sub> (Rh/Al 0.45) before and after the reaction with NO<sub>x</sub> at room temperature for 20 min and 15 hours.

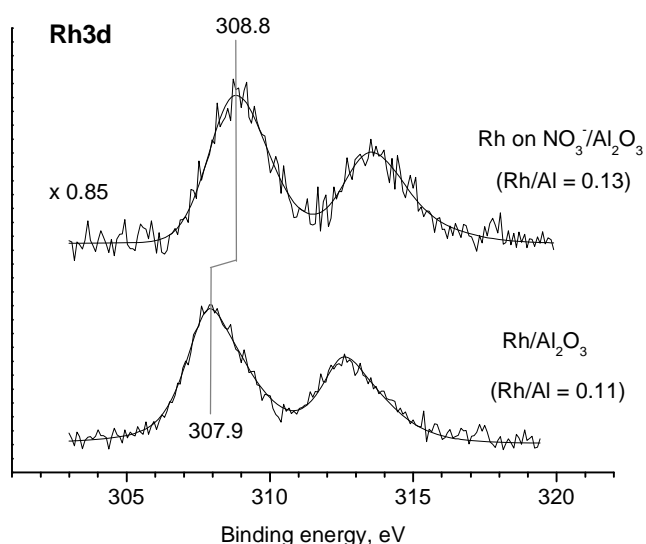


**Fig. 3.** Rh3d spectra recorded under deposition of rhodium onto the clean and nitrated surfaces of alumina.

treatment in NO<sub>x</sub> for 15 hours (Fig. 2). Thus, in the case of relatively big Rh particles, the first state of rhodium oxidation is assumed to result in a solution of oxygen atoms in the bulk. Apparently, the concentration of oxygen dissolved increases with the reaction time approaching the formation of Rh<sub>2</sub>O<sub>3</sub> at the limit.

When the concentration of rhodium is very high (Rh/Al ~ 5), the treatment of Rh/Al<sub>2</sub>O<sub>3</sub> in NO<sub>x</sub> even for 15 hours changes insignificantly the chemical state rhodium. That might be due to an extremely low reaction ability of such a big Rh particles. Other reason could be a requirement of free sites on the alumina surface for the Rh oxidation to take place. To verify participation of the support in rhodium oxidation, rhodium was deposited by evaporation onto the alumina surface pre-treated in NO<sub>x</sub>. Fig. 3 exhibits the Rh3d spectra recorded after rhodium deposition in comparable amounts onto the clean and nitrated surfaces of alumina. The Rh3d line characterizing rhodium on the nitrated surface is shifted upwards by ~ 0.9 eV with respect to the case of rhodium deposited onto the clean alumina surface. This fact indicates that oxidation of rhodium particles supported on alumina can proceed via interaction with the surface nitrate species formed in the reaction of Al<sub>2</sub>O<sub>3</sub> with NO<sub>x</sub>.

The financial support of the Russian Foundation for Basic Research (Grant No 07-03-00266) is gratefully acknowledged.

**MODELING ACTIVE CENTERS ON OXIDE SURFACES IN CLUSTER  
APPROACH OF DENSITY FUNCTIONAL METHOD**

**Shor E.I.<sup>1</sup>, Shor A.M.<sup>1</sup>, Laletina S.M.<sup>1</sup>, Shulimovich T.A.<sup>1</sup>, Nasluzov V.A.<sup>1</sup>,  
Rösch N.<sup>2</sup>**

<sup>1</sup>*Institute Chemistry and Chemical Technology, Krasnoyarsk, Russia*

<sup>2</sup>*Chemical Department, Munich Technical University, Garching, Germany*

*E-mail: [nasluzova@4net.ru](mailto:nasluzova@4net.ru), [as@icct.ru](mailto:as@icct.ru)*

Results of embedded cluster density functional calculations on properties of oxide supported small transition metal particles are reported. Nucleation of gold clusters Au<sub>n</sub> (n = 1-6) on a perfect surface  $\alpha$ -Al<sub>2</sub>O<sub>3</sub>(0001) is considered. To explore anchoring of metal particles in zeolite materials we described the adsorption of M<sub>6</sub> (M = Rh, Ir, Au) metal clusters on faujasite. To study active metals species coordinated at various surface defects of amorphous SiO<sub>2</sub> we developed and investigated cluster models based on structure of MCM-41 material.

During period of last several years we a developing cluster approach computational schemes for modeling active sites on oxide surfaces with embedding in polarizable lattice of crystalline environment. These schemes for ionic substrates like surfaces of MgO and Al<sub>2</sub>O<sub>3</sub> [1] and for polar covalent SiO<sub>2</sub> [2,3] framework substrates are aimed at accurate reproduction of embedding lattice environment effect which provide quantitative character of the calculational results by criterion of correspondence to hypothetical exact model with the same level of treating of the exchange correlation interactions. Our recent research effort was focused on a detailed theoretical characterization of complexes and clusters on the surface of oxide supports as well as in zeolite cavities. The main subjects of these investigations were surface species of the group of coinage metal.

We investigated the nucleation of gold clusters on a perfect surface of the ionic oxide Al<sub>2</sub>O<sub>3</sub>. For this purpose, we carried out GGA DFT calculations on embedded cluster models of adsorption complexes Au<sub>n</sub>/ $\alpha$ -Al<sub>2</sub>O<sub>3</sub>(0001) (n = 1-6). The calculated binding energies, E<sub>b</sub>, vary between 0.3 and 1.2 eV. The geometric structure of adsorbate Au to Au<sub>3</sub> in these surface complexes does not prevent an efficient interaction with the substrate. Thus, for such cluster sizes E<sub>b</sub> is proportional to number of the gold atoms. Adsorption of the clusters Au<sub>4</sub> to Au<sub>6</sub> is accompanied by a deformation of the structure from those of the planar gas phase structures. The adsorbate deformation energies are 0.2-0.9 eV. The binding energy E<sub>b</sub> for Au<sub>4</sub> to Au<sub>6</sub> is less than 1.0 eV and decreases with the increasing number of gold atoms. In all cases studied, the substrate deformation energy is a considerable contribution, about half of the interaction

## OP-4

energy of the deformed substrate and adsorbate. According to the calculated strength of the substrate-adsorbate interaction of gold clusters on a perfect  $\alpha\text{-Al}_2\text{O}_3(0001)$  surface does not strongly affect the nucleation energies.

According to the experiment, gold species of different oxidation state are able to participate in reactions as catalytically active centers in zeolites. To characterize such species we studied the interaction of mononuclear gold species in different oxidation states with a six-member ring of the sodalite cage in faujasite. We calculated the adsorption energy for complexes of  $\text{Au}^0$  close to zero with the distances to oxygen centers being longer than 3 Å. Cations  $\text{Au}^{1+}$  are localized in the plane of the faujasite six-ring, forming dominating bonds with two oxygen atoms of the substrate. Complexes  $\text{Au}^{1+}\text{CO}$  are predicted to form only a single bond with one substrate oxygen atom. Such changes in coordination of Au species are in agreement with results of EXAFS measurements.

To explore anchoring of poly-nuclear metal particles in zeolite materials we described the adsorption of  $\text{M}_6$  ( $\text{M} = \text{Rh}, \text{Ir}, \text{Au}$ ) metal clusters on faujasite with two models of  $\text{C}_3$  symmetry, a “unhydrogenated” (bare) cluster  $\text{Au}_6$  and a “reacted” cluster  $\text{Au}_6\text{H}_3$  with three protons transferred to the metal cluster from bridging OH groups of the zeolites framework. The latter structure represents reverse hydrogen spillover from the zeolite support to the metal particle. The quantum mechanical region of the systems comprised 12 tetrahedral (T) centers, including a faujasite six-ring accessible from the supercage. Upon coordination to a zeolite wall, the cluster  $\text{Au}_6$  retains its open, almost planar structure which is characteristic for such particles in the gas phase. The cluster  $\text{Au}_6$  forms bonds with oxygen atoms outside of the ring. We calculated the adsorption energy at 0.9 and 0.4 eV when the metal particle is coordinated to a substrate containing acidic OH groups in crystallographic positions  $\text{O}_4\text{H}$  (inside six-ring) and  $\text{O}_3\text{H}$  (outside six-ring), respectively. A surface complex with a hydrogenated gold cluster formed after hydrogen spillover is 0.5 eV more stable than the initial unhydrogenated complex with  $\text{O}_3\text{H}$  groups while it is 0.3 eV less stable than the corresponding unhydrogenated complex with  $\text{O}_4\text{H}$  groups. We mention for comparison that similarly coordinated clusters  $\text{Rh}_6$  and  $\text{Ir}_6$  exhibit compact structures of regular and distorted trigonal prism, respectively. Clusters  $\text{Rh}_6$  and  $\text{Ir}_6$  form six metal-oxygen bonds with centers of the faujasite six-ring and the hydrogenated complexes are always considerably more stable than the corresponding “bare” adsorbed metal particles.

Computational models were developed based on the structure of an idealized wall of cavities of the mesoporous material MCM-41 to study active metals species coordinated at various surface defect sites of amorphous  $\text{SiO}_2$  such as oxygen vacancies  $\text{V}_\text{o}$ , non-bridging

oxygen (NBO), silanolate group ( $\text{NBO}^-$ ) as well as Si dangling bonds ( $\text{E}'$ ). Such a surface is represented by two layers with honeycomb structure of interconnecting tetrahedrons  $\text{SiO}_4$ .  $\text{V}_o$  center is formed by deleting oxygen atoms in bridging positions of the “top” layer. To form terminal surface silanol groups  $\text{SiOH}$ , one deletes an O atom of an Si-O-Si bridge which connects tetrahedrons of the top and bottom layers; subsequently, two Si centers of the bridge are brought out from the slab to the surface by reflection with respect to an external  $\text{O}_3$  plane and finally adding two OH groups on either side of the slab. Consequently,  $\text{E}'$  and  $\text{NBO}^-$  defects are obtained when OH and  $\text{H}^+$ , respectively, are removed from the top layer  $\text{SiOH}$  group. Adsorption of small particles  $\text{Ag}_n$  ( $n = 1, 2, 4$ ) and  $\text{Au}_n$  ( $n = 1, 2$ ) at defects of  $\text{SiO}_2$  surface have been studied. Accordingly, silver dimers are adsorbed in upright orientation. The planar rhombic structure of  $\text{Ag}_4$ , characteristic for such a particle in the gas phase, is preserved after adsorption at  $\text{V}_o$  and  $\text{NBO}^-$  defects.  $\text{Ag}_4$  is tetrahedral when it interacts with  $\text{E}'$  defects. Substrate-adsorbate bonds of intermediate strength are formed upon interaction with  $\text{NBO}^-$  and  $\text{E}'$  centers with binding energies of 1 to 2 eV. Weak bonds are formed when silver species interact with  $\text{V}_o$  centers. Nucleation is hindered by strong interaction with defect; it was calculated unfavorable for metal species bound to  $\text{E}'$  centers. It was shown that the direct interaction of an adsorbed gold dimer with two adjacent defects as compared to interaction with an isolated defect can result in energy gain up to 0.2 eV. Atomic gold and a gold dimer form strong bounds with  $\text{E}'$  centers of 3.9 and 2.6 eV, respectively. The corresponding bonding energies for NBO defects are 3.1 and 2.4 eV; for  $\text{NBO}^-$ , these energies drop to 0.7 and 1.6 eV, respectively.

## References

1. V.A. Nasluzov, V.V. Rivanenkov, A.B. Gordienko, K.M. Neyman, U. Birkenheuer, N. Rösch, J. Chem. Phys. 115 (2001) 8157.
2. V.A. Nasluzov, E.A. Ivanova, A.M. Shor, G.N. Vayssilov, U. Birkenheuer, N. Rösch, J. Phys. Chem. B 107 (2003) 2228.
3. E.A. Ivanova-Shor, A.M. Shor, V.A. Nasluzov, G.N. Vayssilov, N. Rösch, J. Chem. Theory Comp. 1 (2005) 459.

## OP-5

### STM AND XPS STUDY OF Pt/Al<sub>2</sub>O<sub>3</sub> AND Pt-Sn/Al<sub>2</sub>O<sub>3</sub> MODEL CATALYSTS PREPARED BY “WET CHEMISTRY” METHODS ON ALUMINA THIN FILMS

**Nartova A.V., Beck I.E., Bukhtiyarov A.V., Kvon R.I., Bukhtiyarov V.I.**

*Boreskov Institute of Catalysis, Novosibirsk, Russia*

*E-mail: [nartova@catalysis.nsk.su](mailto:nartova@catalysis.nsk.su)*

Thin alumina films grown on polycrystalline foil of FeCrAl alloy were applied for preparation of Pt/Al<sub>2</sub>O<sub>3</sub> and Pt-Sn/Al<sub>2</sub>O<sub>3</sub> model catalysts using “wet chemistry” methods. Investigation of these samples with STM and XPS shows that Pt particle size distribution depends on morphology and chemical composition of the support, as well as on the preparation conditions.

Application of the surface science approach to heterogeneous catalysis uses simplified model versions of real catalysts. They have been studied under well-defined UHV conditions with very powerful methods, which have allowed chemical and structural characterization down to atomic level. Recently developed scanning probe microscopy methods (STM and AFM) occupy a special place among the surface science methods, since they allow *in situ* probing the morphology of both metal active component and the support (including corrugations of the support texture, sintering of metal particles, SMSI effects, etc.) [1,2]. Combination of SPM with chemical analysis methods such as Auger and X-ray photoelectron spectroscopy is a rather powerful tool for understanding the catalyst life from the very first steps of the catalyst preparation until its deactivation.

The major drawback of this approach is the so-called ‘material gap’. The real catalysts are morphologically complex multi-component systems, often with microscopic dimensions, whereas the fundamental surface science studies focus on the catalytic behaviour of well-structured and, most often, single crystal metal, alloy or oxide materials. Surface Science community is making strong efforts to overpass this problem, including the elaboration of the new type of model supports (planar oxides) and of many methods to deposit and stabilize the metal nanoparticles on the surface of oxide supports (cryotechniques, grafting, soft landing, lithography and so on) [1,3,4].

Application of the “wet chemistry” methods, when active component is introduced from the aqueous precursor [5,6]) seems to be one of the very challenging and promising approaches in this field. Indeed, the same precursors and methods as those used for preparation of porous catalysts can be applied in this case. However, the model supports applied for these methods has to meet several conditions. First of all, the support has to be stable under ambient conditions and during treatments in solution. On the other hand, it should be suitable for investigation with surface science methods.

Recently, we developed the original preparation procedure of new model support – alumina thin film grown on polycrystalline foil of FeCrAl-alloy [7-9]. Its study by combination of STM (Scanning Tunneling Microscopy) and XPS methods has shown that contrary to the model systems described in literature our support is characterized by rough surface and high stability during air and solution treatments. As consequence, this support could be used for preparation of the model catalysts (metal particles on alumina) with “wet chemistry methods”.

In this communication we present the first results on preparation and study of the model Pt/Al<sub>2</sub>O<sub>3</sub>/FeCrAl catalysts prepared by the “wet chemistry” methods. Platinum(IV) nitrate solution stabilized by HNO<sub>3</sub> was used as a precursor of active component. Pretreatment and drying conditions were very close to the conditions used during the deposition of active component on the porous supports [10]. Subsequent reduction of the impregnated support was carried out in  $\sim 5 \times 10^4$  Pa of H<sub>2</sub> at temperature of 470 K. The mechanisms of Pt particles formation during the preparation were investigated using STM and XPS.

In the case of three-hour adsorption of platinum from relatively concentrated solution ( $1 \times 10^{-4}$  M), the bimodal particles size distribution, which is considerably differed from statistic distribution for thermally deposited metal particles, was finally formed. Very small platinum particles (the mean size of  $\sim 1$  nm) and very large objects up to 50 – 60 nm in diameter were found on the surface of the model support. Detailed STM analysis showed that small Pt particles are located on the flat regions of the supports, while large objects are formed as result of precursor accumulation in curvatures of the support relief. Comparison of STM and XPS data allows us to assume that in both cases there is a strong interaction of the precursor with the model alumina support.

The dilution of the initial platinum (IV) nitrate solution (up to 10 times) and changing of the solution pH allowed preparation of the sample, maximal sizes of Pt particles in which does not exceed 25 nm. This result demonstrates that variation of the deposition conditions make s it possible to prepare model catalysts with different particle size distribution. It should be mentioned that XPS shows a similarity of the chemical state of the precursor (platinum nitrate) adsorbed on the surface of following supports with different crystal structures and surface areas: Al<sub>2</sub>O<sub>3</sub>/FeCrAl,  $\alpha$ -Al<sub>2</sub>O<sub>3</sub> (surface area - 5.3 m<sup>2</sup>/g),  $\theta$ -Al<sub>2</sub>O<sub>3</sub> (110 m<sup>2</sup>/g) and  $\gamma$ -Al<sub>2</sub>O<sub>3</sub> (244 m<sup>2</sup>/g).

Similar approach was used for the modification of the model support with tin that was adsorbed from Sn(II) acetate solution in glacial acetic acid followed by annealing in air at 390 K. XPS shows that SnO<sub>2</sub> is formed on the support surface under these conditions. The model modified support prepared by such manner was used for platinum adsorption followed by hydrogen reduction (see above). The non-modified Pt/Al<sub>2</sub>O<sub>3</sub> catalysts prepared using the same conditions was used as the reference sample.

## OP-5

STM shows bimodal size distribution of the objects (Pt particles) on the modified support surface. The sizes of smaller objects are ranged from 1 to 12 nm (the mean size of ~ 5 nm) and larger objects with the sizes from 10 to 60 nm (the mean size is around 25-30 nm). In the case of the non-modified sample (Pt/Al<sub>2</sub>O<sub>3</sub>) size distribution of Pt particles was much narrower (from 1 to 9 nm) with maximum at 5 nm. The comparison of the STM data for the different samples allows us to interpret the results obtained. Most probably, first maximum of the distribution (sizes up to 12 nm) corresponds to platinum particles located directly on alumina, while the second maximum (10 – 60 nm) can belong to platinum particles which are connected with or lies on stannic oxide.

The Pt/Al<sub>2</sub>O<sub>3</sub> sample is characterized by Pt4f<sub>7/2</sub> binding energy of 71.5 eV that corresponds to metallic particles of Pt. In the case of the Pt/Sn/Al<sub>2</sub>O<sub>3</sub> sample two features with binding energy of 71.3 and 72.0 eV are observed in Pt4f<sub>7/2</sub> spectrum. The species with lower binding energy can be attributed to the metal particles of Pt, whereas the second species – to platinum interacted with SnO<sub>2</sub>. Thus, the developed “wet chemistry” approach provides the method of preparation of the model catalysts with direct interaction of Pt with modifier (SnO<sub>2</sub>) that is used for stabilization of active component in real catalysts [11].

### Acknowledgements

Some part of the study was performed on the equipment granted by Russian Science and Innovation Agency (Rosnauka) under the program “Development of the instrumental base of scientific organizations” (Decision № 09.255.02/053). The authors are grateful to Dr. S.A. Tiis for his experimental assistance and appreciate the financial support of research by CRDF (grant NO - NO-008-X1 and The 2006 BRHE Fellowship Program, RNP.2.2.2.3.10032), RFBR (grant No 07-03-00398) and Interdisciplinary Integration project of fundamental investigations # 79 of Siberian Branch of RAS.

### References

1. M. Baumer, H.- J. Freund, Prog. Surf. Sci. 61 (1999) 127.
2. Sh.K. Shaikhutdinov, D.I. Kochubei, Russian Chem. Rev. 62 (1993) 443.
3. D.R. Rainer, D.W. Goodman, J. Mol. Catal. A 131 (1998) 259.
4. S. Abbet, K. Judai, L. Klinger, U. Heiz, Pure Appl. Chem. 74 (2002) 1527.
5. D.P.C. Bird, Castilho de C.M.C., R.M. Lambert, Surf. Sci. 449 (2000) L221.
6. S. Wodiuning, J.M. Keel, T.S.E. Wilson, F.W. Zemichael, R.M. Lambert, Catal. Lett. 87 (2003) 1.
7. A.V. Nartova, R.I. Kvon, Chemistry for Sustainable Development 11 (2003) 209.
8. A.V. Nartova, R.I. Kvon, Kinet. Catal. 45 (2004) 771.
9. A.V. Nartova, R.I. Kvon, E.I. Vovk, V.I. Bukhtiyarov, Bulletin of the Russian Academy of Sciences. Physics. 69 (2005) 524.
10. D. Dou, D.-J. Liu, W.B. Williamson, K.C. Kharas, H.J. Robota, Appl. Catal. B 30 (2001) 11.
11. O.A. Barias, A. Holmen, E.A. Blekkan, J. Catal. 158 (1996) 1.

## SIMULATION OF CATALYTIC PROCESSES OVER METAL NANOPARTICLES: STATE OF THE ART

**Elokhin V.<sup>1,3</sup>, Kovalyov E.<sup>1</sup>, Myshlyavtsev A.<sup>2</sup>**

<sup>1</sup>*Boriskov Institute of Catalysis, Novosibirsk, Russia*

<sup>2</sup>*Omsk State Technical University, Omsk, Russia*

<sup>3</sup>*Novosibirsk State University, Novosibirsk, Russia*

*E-mail: [elokhin@catalysis.ru](mailto:elokhin@catalysis.ru)*

A brief review would be given reflecting the approaches to the simulation of physicochemical processes proceeding over the supported metal nanocatalysts. The statistical lattice model for the adsorption and reaction processes over the supported metal nanoparticle has been elaborated which permits one to take into account the dynamic change in the shape and surface morphology of the nanoparticle under the influence of the reaction media.

In heterogeneous catalysis, adsorption and reaction processes usually occur on supported metal nanoparticles. Along with the appearance of high-precision techniques for surface characterisation, considerable progress in manufacturing of model catalysts with well-defined properties like particle size, shape and separation has been achieved in the last decade of the 20th century. Despite this progress, the cognitive potential of the experimental studies in itself is still limited because the measurements are usually indirect and the information derived demands quantitative processing and interpretation. This can be done only with the use of mathematical models. The peculiarities of reaction performance over supported metal nanocatalysts, including the inherent heterogeneity of metal crystallites as well as spontaneous and adsorbate-induced changes of the shape and surface morphology [1], dictate the special requirements to the theoretical models aimed at the simulating of catalytic properties of nanoparticles [2-4]. Application of the conventional mean-field models is rather limited here. Despite the potential power of molecular dynamics, the use of this technique for the analysis of the physicochemical processes over supported particles is also limited due to the short length and time scales typical for this approach. Under such circumstances, the most effective are stochastic simulations based on the Monte-Carlo technique.

Often as a model of the supported particle a top projection of the truncated pyramid has been considered, i.e., the pyramid is represented by a  $N \times N$  square lattice, where the central  $M \times M$  array of sites mimics the top facet (active surface of the particle) and the periphery corresponds to the support (or to the side facets with different catalytic properties). Despite of



## OP-6

the simplicity of such models, both predictable and unexpected result has been obtained by modelling of different peculiarities of the reaction performance over the supported particles. Such factors as reactant supply due to the diffusion over the support (spillover) [5], interplay of the reaction kinetics on the different facets of the supported particle due to the adsorbed species diffusion between the facets [6], the jump-wise reshaping of the active particle under the influence of the adlayer composition [7], the influence of geometric parameters of the supported particles on the reactivity and selectivity of the multi-route catalytic reactions [8], reciprocal effect of the surface morphology and adsorption-reaction processes over the catalytic particle [9], were examined in various studies. However, the theoretical models taking into account the dynamic change of the shape and surface morphology of the catalytic particles under the influence of adsorbed species and temperature action are practically lacking.

The statistical lattice model of the supported catalyst particle which takes into account the change of the shape and surface morphology of the nanoparticles under the influence of the reaction media has been elaborated [10, 11]. To model the active metal particle the Kossel crystal located on the inert support has been chosen. The morphology of the particle's surface is determined by the heights of the metal atom columns. The change of morphology can be caused by the diffusion of the surface atoms (the metal atoms attract each other and the atoms of support with some interaction energies). As a result, some «dynamically» equilibrium shape of the particle arises, depending on the temperature, size of the crystal and the ratio of interaction energies between metal and support atoms. At the intermediate range of temperatures ( $T \cong 500$  K) the surface of the particle is flat enough but the corners and edges are partly rounded. The surface of the metal particle becomes extremely rough at the hemispherical shape ( $T \cong 900$  K). The beginning of the dispersal of metal particle over the support surface in our model is located between  $T = 900$  K and  $T = 1100$  K. The radius of the dispersal remain unchanged (within statistical fluctuations) during the process of the equilibration. When these radii overlap we can observe the coalescence of closely situated particles at high temperatures (Ostwald ripening). After the reduction of the temperature (from 1100 K to 500 K or from 900 K to 500 K) the particle shape returns to the initial equilibrium characteristic for the given temperature. The distribution of the particles sizes after the reduction of the temperature is determined by the procedure of cooling (stepwise or gradual cooling).

Kinetic dependencies of the catalytic reactions on the “roughened” particles are qualitatively and quantitatively different from the kinetics on the flat rigid surfaces. In the

case of “adsorbate-metal” interactions adsorption can induce the change of the shape and surface morphology of the supported particle, at that the adsorption isotherms differ noticeable from the ideal Langmuir isotherm. After the removing of the adsorbed layer the particle shape returns to the initial equilibrium characteristic for the given temperature, similar to the experimentally observed reversible reshaping of active nanoparticles [12]. The adsorption-induced reshaping of the nanoparticles could be explained by the joint actions of following factors: diffusion of the surface atoms of the metal particle, attractive interaction between metal atoms and adsorbed species, and possibility of desorption of the adsorbed species (in test experiments, when the desorption of the adsorbed species was prohibited, any remarkable change of the particle shape and surface morphology has been not observed).

Besides, the simulation of oscillatory reaction ( $\text{CO} + \text{O}_2/\text{Pd}$ ) with the detailed mechanism taking into account the formation and consumption of the subsurface oxygen has been provided. The influence of the particles shape and surface morphology, as well as spillover effects, on the characteristics of oscillations and surface waves has been studied.

The study was partly supported by RFBR grant 05-03-32971.

## References

1. J. Libuda, S. Schauermaun, M. Laurin, T. Schalow, J. Hartmann, H.-J. Freund, *Monatshefte für Chemie*, 136 (2005) 59.
2. V.P. Zhdanov, B. Kasemo, *Surf. Sci. Rep.* 39 (2000) 25.
3. V.P. Zhdanov, *Surf. Sci.* 500 (2002) 966.
4. V.I. Elokhin, A.V. Myshlyavtsev, In: *Dekker Encyclopedia of Nanoscience and Nanotechnology*. J.A. Schwarz, C.I. Contescu and K. Putyera, Eds.; Marsel Dekker, Inc.: New York, 2004. pp. 621-632.
5. V.P. Zhdanov, B. Kasemo, *J. Catal.* 170 (1997) 377.
6. V.P. Zhdanov, B. Kasemo, *Surf. Sci.* 405 (1998) 27.
7. V.P. Zhdanov, B. Kasemo, *Phys. Rev. Lett.* 81 (1998) 2482.
8. A.S. McLeod, L.F. Gladden, *J. Catal.* 173 (1998) 43.
9. F. Gracia, E.E. Wolf, *Chem. Eng. Jour.* 82 (2001) 291.
10. E.V. Kovalyov, V.I. Elokhin, A.V. Myshlyavtsev, B.S. Bal'zhinimaev, *Dokl. Phys. Chem.* 381 (2001) 309.
11. E.V. Kovalyov, E.D. Resnyanskii, V.I. Elokhin, B.S. Bal'zhinimaev, A.V. Myshlyavtsev, *Phys. Chem. Chem. Phys.* 5 (2003) 784.
12. P.L. Hansen, S. Helveg, A.K. Datye, *Adv. Catal.* 50 (2006) 77.

**NEW CATALYSTS BASED ON ENSEMBLES OF NANOPARTICLES:  
FROM MODEL TO REAL CATALYSIS**

**Rostovshchikova T.<sup>1</sup>, Smirnov V.<sup>1</sup>, Lokteva E.<sup>1</sup>, Gurevich S.<sup>2</sup>, Kozhevnikov V.<sup>2</sup>, Mitina L.<sup>3</sup>**

<sup>1</sup>*Lomonosov Moscow State University, Moscow, Russia*

<sup>2</sup>*Ioffe Physico-Technical Institute, St-Petersburg, Russia*

<sup>3</sup>*ISTC, Moscow, Russia*

*E-mail: [rtn@kinet.chem.msu.ru](mailto:rtn@kinet.chem.msu.ru)*

The catalytic behavior of nanoparticles depends not only on a cluster size (usual size effect) but also on an average intercluster distance. This effect associated with intercluster interactions should be taken into account for prediction of catalytic properties of nanoparticle system. The advantages of catalysis by ensembles of nanoparticles are demonstrated in tested reactions of chlorohydrocarbons and hydrogenation with model catalysts consisting of uniform metal clusters (Cu, Ni, Pd) deposited on silicon or carbon supports by means of laser electrodispersion technique. Based on these results new unusually efficient and stable catalysts for utilization of toxic polychlorinated wastes are developed.

Recently it was found that, in addition to the well known size effect, the catalytic activity of nanostructured metal catalysts strongly depends on an average distance between metal particles or an average surface particle density [1-3]. The reason for this phenomenon named as a new type of the size effect is that the intercluster distance determines a possibility of the interaction between nanoclusters. As a result of thermally stimulated electron tunneling between closely located nanoparticles the highly active charged species may occur in ensembles of nanoparticles. This effect is applied to the development of new highly effective catalysts for conversion of hydrocarbons and their halogen derivatives.

For fabrication of model catalysts based on ensembles of metal (Cu, Ni, Pd) clusters the laser electrodispersion (LED) technique [4] has been used. This method based on cascade fission of metal microdrops charged in laser torch plasma let us deposit uniform amorphous spherical nanoparticles on solid supports (Si, SiO<sub>2</sub>, C). The particle size was 2-5 nm depending on metal. The typical image of Ni/SiO<sub>2</sub> film and particle size distribution is shown in fig.1. The films consisting of densely packed aggregates (ensembles) of granules become conducting due to electron tunneling between nearby granules. Inter-grain electron tunneling leads to a redistribution of charges and to formation of a significant amount of the charged particles within ensembles. These charged states provide unique catalytic properties of nanostructured films. The main features of the films consisting of ensembles of nanoparticles

in chlorohydrocarbon reactions (Cu, Ni) and hydrogenation (Ni, Pd) are the unusually high catalytic activity ( $10^4$ - $10^5$  product Mol/Me Mol·h); the strong influence of an average intercluster distance, solvent polarity and support type (dielectric or conductive) on catalytic behavior as well as the correlation between catalytic properties and film conductivity [1-3]. The similar data have been obtained previously for Cu- and Pd-polymer nanocomposites [5]. The catalytic activity of the ensembles of nanoparticles stabilized both on  $\text{SiO}_2$  surface and in polymer matrix is many times higher compared to that for separated copper clusters and highly loaded films (Fig. 2).

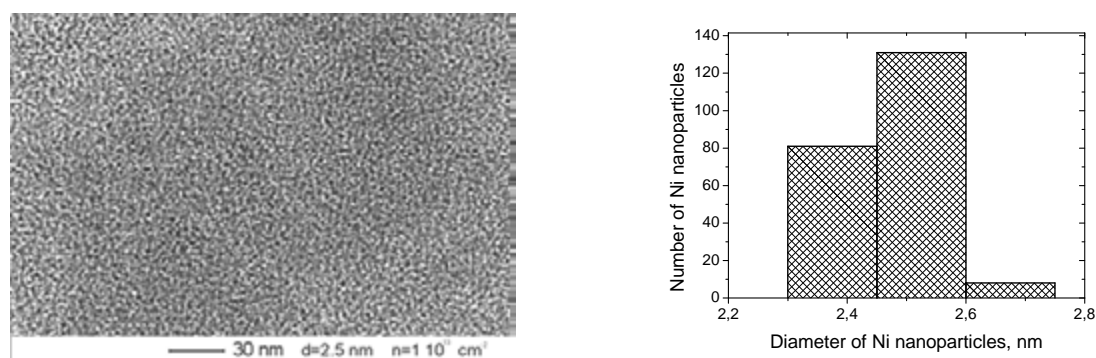


Fig. 1. TEM image and particle size distribution of Ni/SiO<sub>2</sub>/Si.

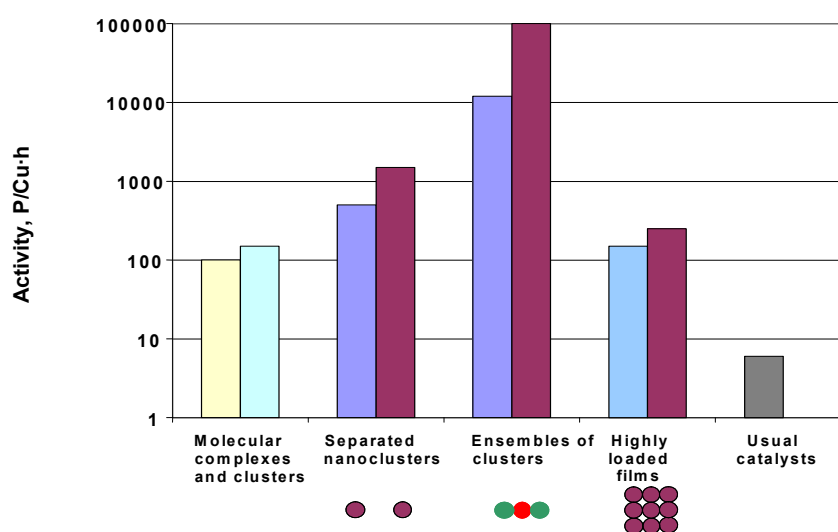


Fig. 2. Catalytic activities of different Cu catalysts in chlorinated alkenes isomerization.

These results are in good agreement with the theoretical estimates indicating that there is an optimum average inter-particle distance in one-layer film at which, due to electron tunneling between closely located particles, the amount of charged particles on dielectric support sharply grows, and charging becomes more significant with the growth of both the temperature and the solvent permittivity [1,2].

## OP-7

Based on these results new unusually efficient and stable catalysts for chlorinated wastes processing are developed. Catalysts based on ensembles of Pd and Ni nanoparticles deposited on silicon supports ( $\text{SiO}_2/\text{Si}$ ) or sibunite (C) granules prepared by means of laser electrodispersion technique are very active in gas phase and multiphase hydrodechlorination of chlorobenzenes at 100 – 250 °C. These catalysts with very low metal content are several orders of magnitude superior in activity than usual supported metal catalyst (0.5% Pd/UDD, UDD - ultra dispersed diamond) (Fig. 3).

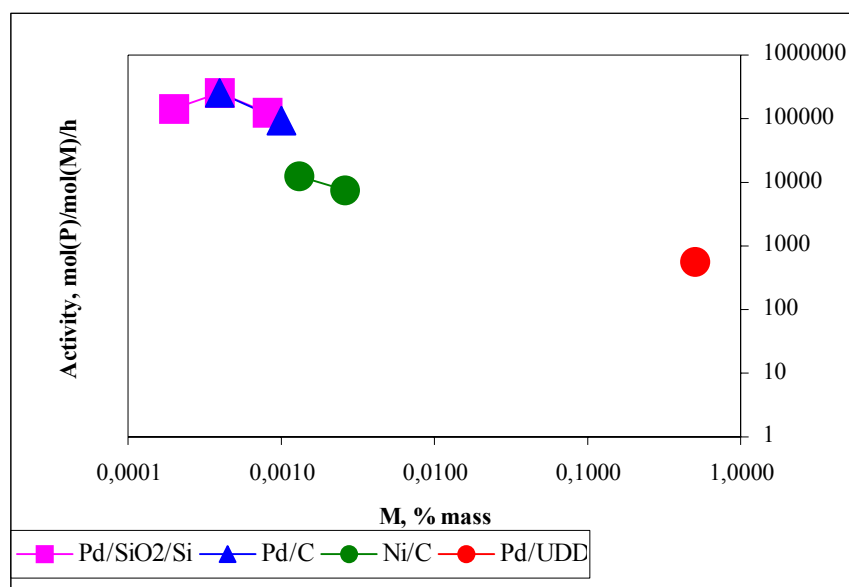


Fig. 3. Catalytic activities of different catalysts in chlorobenzene hydrodechlorination.

The process of hydrodechlorination with new catalysts may be a basis for the environmentally safe and cost effective technology of toxic polychlorinated wastes utilization.

The authors are grateful to ISTC and collaborators of the project 2955 Prof. Ronald Imbihl (Institute of Physical Chemistry and Electrochemistry, Hanover University) and Prof. Nils I. Jaeger (Institute of Applied and Physical Chemistry, Bremen University) for the support.

## References

1. V.M. Kozhevnikov, T.N. Rostovshchikova, D.A. Yavsin, M.A. Zabelin, V.V. Smirnov, S.A. Gurevich, I.N. Yassievich, Doklady Phys. Chem. 387 (2002) 324 (in Russian).
2. T.N. Rostovshchikova, V.V. Smirnov, V.M. Kozhevnikov, D.A. Yavsin, M.A. Zabelin, I.N. Yassievich, S.A. Gurevich, Appl. Catal. A 296 (2005) 70.
3. T.N. Rostovshchikova, V.V. Smirnov, S.A. Gurevich, V.M. Kozhevnikov, D.A. Yavsin, S.M. Nevskaya, S.A. Nikolaev, E.S. Lokteva, Catal. Today 105 (2005) 344.
4. V.M. Kozhevnikov, D.A. Yavsin, V.M. Kouznetsov, V.M. Busov, V.M. Mikushkin, S.Yu. Nikonov, S.A. Gurevich, A. V. Kolobov, J. Vac. Sci. Techn. B 18 (2000)1402.
5. L.I. Trachtenberg, G.N. Gerasimov, E.I. Grigoriev, S.A. Zavjalov, V.Yu. Zufman, V.V. Smirnov, Stud. Surf. Sci. Catal. 130 (2000) 941.

**SIZE-DEPENDENT CATALYTIC BEHAVIOR OF ALUMINA-SUPPORTED PLATINUM NANOPARTICLES IN COMPLETE OXIDATION OF METHANE****Beck I.E.<sup>1</sup>, Pakharukov I.V.<sup>1</sup>, Kriventsov V.V.<sup>1</sup>, Zaikovskiy V.I.<sup>1</sup>,****Nartova A.V.<sup>1,2</sup>, Parmon V.N.<sup>1,2</sup>, Bukhtiyarov V.I.<sup>1,2</sup>**<sup>1</sup>*Boriskov Institute of Catalysis, Novosibirsk, Russia*<sup>2</sup>*Novosibirsk State University, Novosibirsk, Russia**E-mail: [beck@catalysis.ru](mailto:beck@catalysis.ru)*

Catalytic activity of the size-controlled platinum nanoparticles with a narrow particle size distribution (HRTEM data) supported on gamma-alumina has been tested in complete methane oxidation. The mean sizes of platinum particles are varied from 0.6 to 20 nm. The reaction under study has been shown to be strongly size sensitive. The size-dependence of the specific catalytic activity is narrow and bell-shaped, with the maximum reaction rate being observed for the mean particle sizes of 1-2 nm. A pretreatment of the support makes it possible to shift the dependence maximum. EXAFS reveals a direct correlation of the catalytic activity with the formation of unusual complex phases of oxygenated platinum formed via a strong interaction with the support.

Catalytic combustion of hydrocarbons has many applications, for example, as an alternative to the conventional thermal combustion or for the abatement of methane emissions from the natural gas or methane-combustion devices including lean-burn natural gas vehicles. The most-used afterburning catalysts represent inert honeycomb-structured metallic or ceramic supports with an active catalytic washcoat which contains platinum or palladium particles dispersed on silica or alumina surfaces. Thus, supported M/Al<sub>2</sub>O<sub>3</sub> or M/SiO<sub>2</sub> granulated catalysts (where M = Pt or Pd, both of which are well known to be active in total oxidation of hydrocarbons) with the same chemical content and distribution of active component as those in the washcoat could serve as a faithful model of the real monolith catalysts for physicochemical studies of the size effects in the performance of these nanosized catalysts. In spite of the significant interest of many scientists to this system, the question of size-sensitivity of methane oxidation remains under discussion, since a number of contradictory data on this issue is available [1-3].

Monodisperse 1%Pt/ $\gamma$ -Al<sub>2</sub>O<sub>3</sub> catalysts were prepared by the incipient wetness impregnation of the support. Aqueous solutions of oligomeric  $\mu$ -hydroxo Pt(IV) complexes with different acidity were used as active component precursors. The surface elemental composition (Al, O and Pt, in the absence of unexpected impurities) was the same for all the samples that was established by EDX (Energy dispersing X-ray micro-analysis). The size

## OP-8

distribution of Pt particles after calcination at 400 or 600°C in muffle was evaluated from high-resolution transmission electron microscopy (HR-TEM) images (fig.1,2). The effective oxidation state and the local environment of platinum atoms were studied by X-ray absorption methods (XANES and EXAFS, respectively). X-ray photoelectron spectroscopy (XPS) was applied to estimate the oxidation state of platinum atoms and its change during the reaction. The catalytic activity of 1%Pt/ $\gamma$ -Al<sub>2</sub>O<sub>3</sub> samples with the various mean particle size was tested in the total oxidation of methane under oxidizing conditions (1 vol.% CH<sub>4</sub>, 20.8 vol.% O<sub>2</sub>, N<sub>2</sub> as balance gas), at constant reactor temperature 450°C. Flow circulation was applied with the space velocity of the initial gas mixture (IGM) varying from 50 to 1100 ml/min. The catalyst loading was ~ 1 g. The catalytic activity was calculated from the dependence of reaction rate on CH<sub>4</sub> concentration under change of the reaction mixture space velocity. The specific activity per accessible Pt atom was recalculated taking into account the mean Pt particle size.

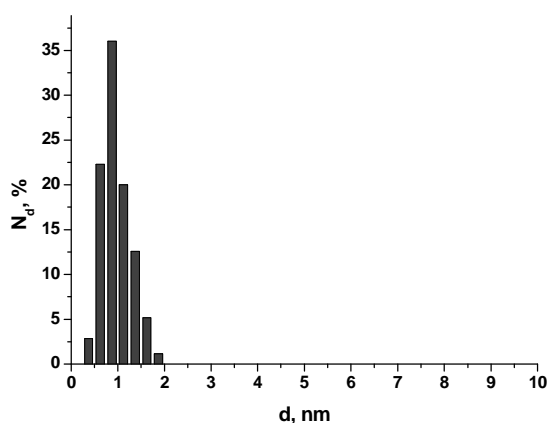
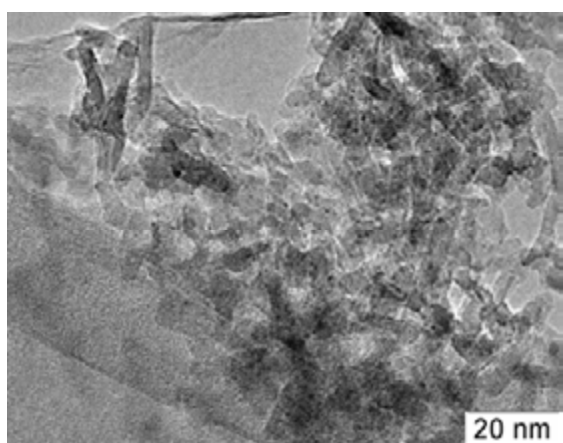


Fig. 1. TEM image and particle size distribution for the most active methane oxidation catalyst prepared on untreated alumina. The mean Pt particle size of 1 nm was evaluated for a sample calcined at 400°C.

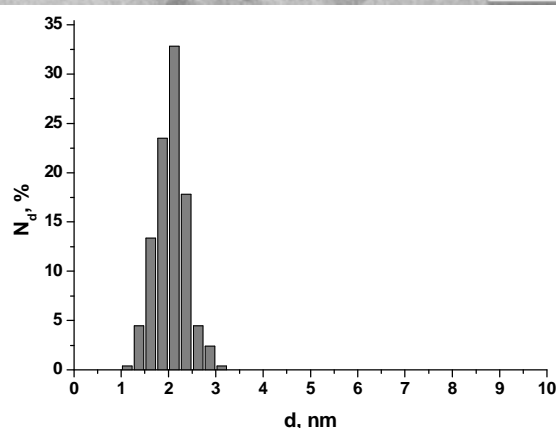
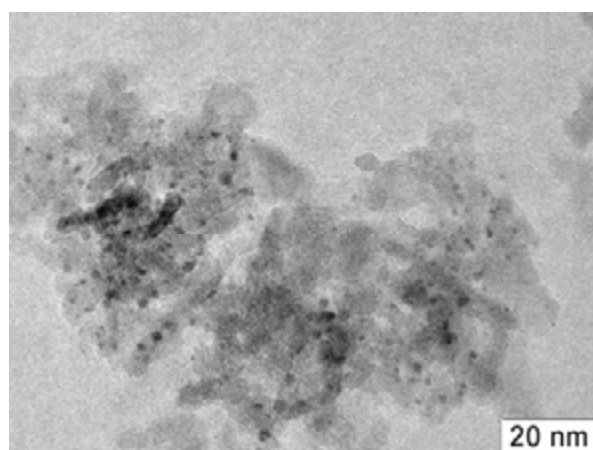


Fig. 2. TEM image and particle size distribution for the most active methane oxidation catalyst prepared on acid-pretreated alumina. The mean Pt particle size of 2 nm was evaluated for a sample calcined at 400°C.

The methane oxidation over platinum nanoparticles with the mean particle size ranging between 0.6 and 20 nm is strongly structure-sensitive, with the maximum reaction rate being

observed for the mean particle sizes of 1-2 nm (fig. 3). Pretreatment of the support with an acid shifts the maximum of the activity-size dependence from 1 to 2 nm. Particles sized below and above 1 or 2 nm, respectively, exhibit a trend of decreasing the reaction rate with the reduction or increase of the mean particle size.

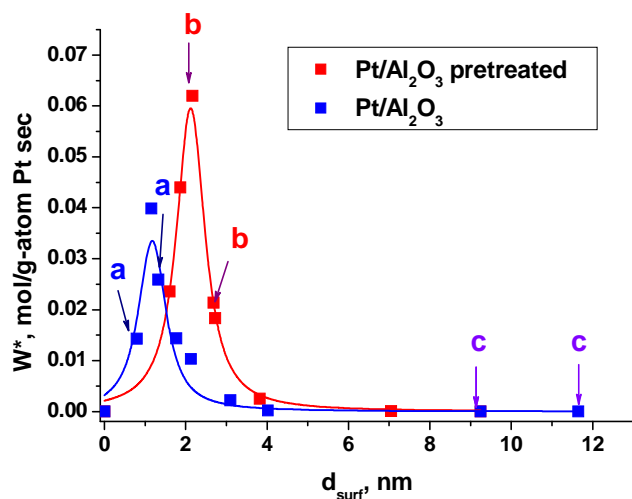


Fig. 3. The effect of particle size on the specific activity of the 1%Pt/Al<sub>2</sub>O<sub>3</sub> catalysts in complete oxidation of methane.

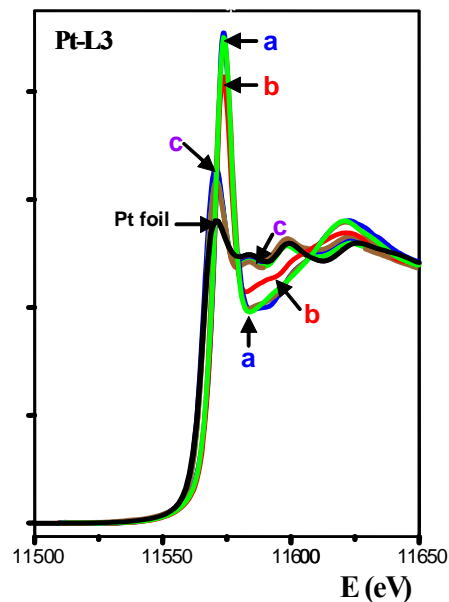


Fig. 4. The difference in average oxidation state of supported Pt particles depending on support pretreatment (a, b) and calcination temperature (c, calcination at 600°C) – XANES Pt-L<sub>3</sub> absorption spectra.

Another important factor affecting the specific activity of the catalyst in the methane oxidation is the chemical state of platinum. The most active catalysts contained small oxygenated platinum nanoparticles strongly bound to the alumina surface (fig. 4). The large nanoparticles of the active component (> 6 nm), which are formed as result of high-temperature (600°C) calcination of catalysts on untreated alumina, were mainly metallic. It should be also noted that the chemical state of platinum particles with similar particle sizes supported on pre-activated and on untreated alumina are different. In addition, the stronger metal-support interaction with the pre-activated carrier resulted in higher thermal stability of oxygenated platinum particles.

The study was partly supported by Russian Science and Innovation Agency (contracts No 02.434.11.2004 and 02.513.11.3203).

## References

1. P. Gelin, M. Primet, Appl. Catal. B 39 (2002) 1.
2. T.F. Garetto, C.R. Apesteguia, Catal. Today 62 (2000) 189.
3. L. Burch, P.K. Loader, Appl. Catal. B 5 (1994) 149.



**OXYGEN REACTIVITY IN CO OXIDATION ON STEPPED  
Rh(410) AND Pt(410) SURFACES**

**Matveev A.V.<sup>1,2</sup>, Weststrate C.J.<sup>3</sup>, Sametova A.A.<sup>1</sup>,  
Gorodetskii V.V.<sup>1</sup> and Nieuwenhuys B.E.<sup>3</sup>**

<sup>1</sup>*Borshkov Institute of Catalysis, Novosibirsk, Russia*

<sup>2</sup>*Novosibirsk State University, Novosibirsk, Russia*

<sup>3</sup>*Leiden Institute of Chemistry, Leiden, the Netherlands*

*E-mail: [matveev@catalysis.ru](mailto:matveev@catalysis.ru)*

The TPR, TDS, LEED methods were used to elucidate the role played by surface defects, subsurface oxygen, surface oxide and CO<sub>ads</sub> concentration in the initiation of the low-temperature CO oxidation on stepped Pt(410) and Rh(410) surfaces. A strong effect of the CO<sub>ads</sub> coverage on the reactivity of atomic oxygen was demonstrated. The CO<sub>ads</sub> layer causes a decrease in the apparent activation energy  $E_{act}$  of the reaction due to changes in the type of coordination and in the energy of binding of O<sub>ads</sub> atoms to the surface.

Model stepped single-crystal surfaces of platinum group metals have played an important role in establishing the key role initiated by defects in the CO + O<sub>2</sub> reaction. No oxygen dissociation was found at ~100 K on the flat surfaces Pt(111), Pt(100)-hex and Pt(110)-1×2. Structural step defects on Pt(100)-1×1 surface, on the other hand, can adsorb O<sub>2</sub> molecules more strongly and accelerate the oxygen dissociation on defect sites at 100 K [1]. Therefore, surface defects create new reaction pathways and multiple CO<sub>2</sub> formation peaks have been observed [2]. The present work aims to contribute to a more profound understanding of the

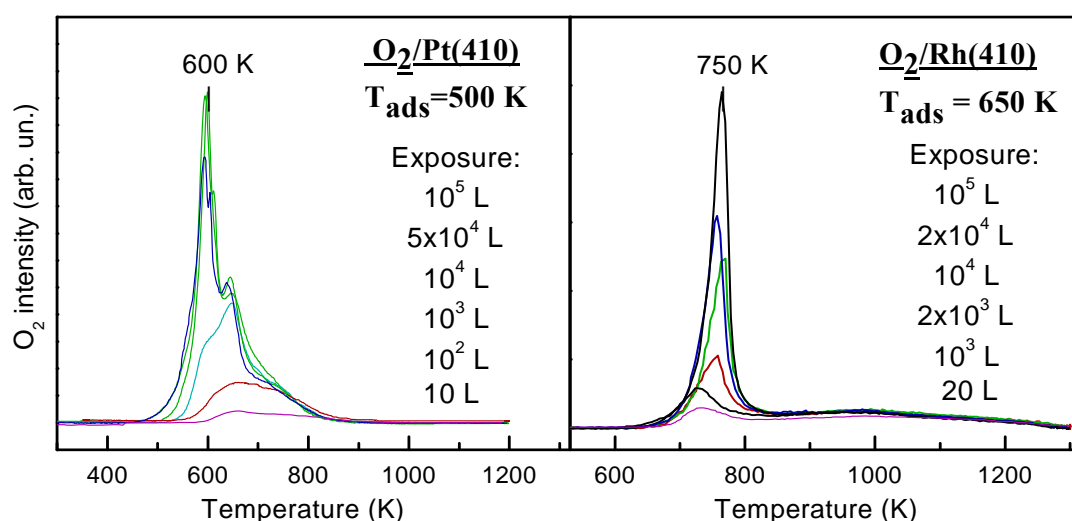


Fig. 1. TD-spectra for O<sub>2</sub> adsorption on Pt(410) and Rh(410) for several initial exposures, 6 K s<sup>-1</sup>.

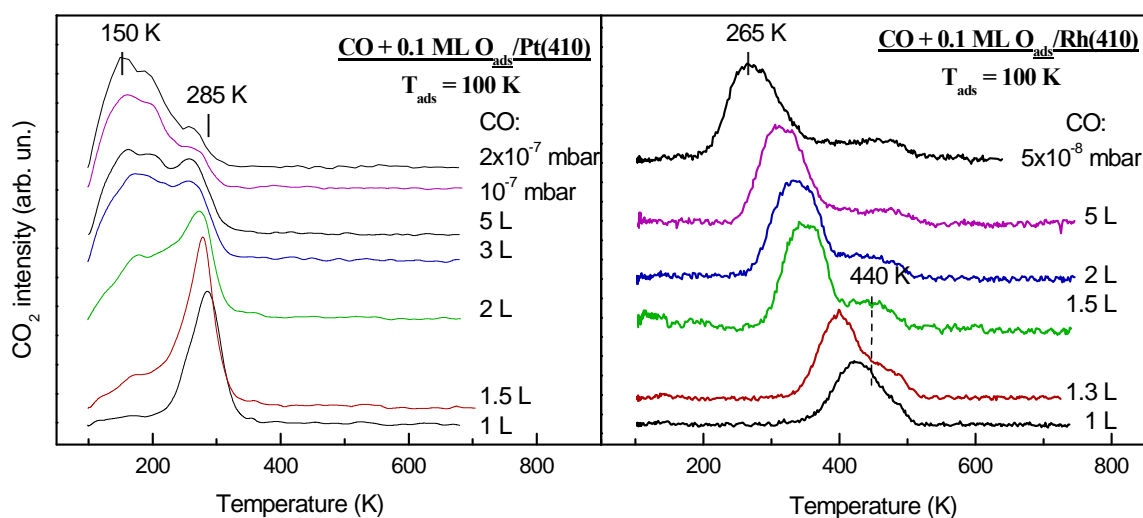


Fig. 2. TPR spectra of  $\text{CO}_2$  formed by reaction of adsorbed oxygen and CO, 3 K s

acceleration of the low-temperature CO oxidation on the stepped Pt(410) and Rh(410) surfaces. In particular, we examined the reactivity of chemisorbed oxygen, subsurface oxygen, and surface oxide on the basis of temperature-programmed reaction (TPR) spectra. The Pt(410) and Rh(410) surfaces consist of (100) terraces with a width of 4 atoms separated by monatomic (110) steps.

*Oxygen adsorption.* Exposure of the Pt(410) or Rh(410) surface to  $\text{O}_2$  at 100 K results in the formation of an adsorbed layer of molecular and atomic oxygen states. The molecularly adsorbed species desorbs at  $\sim 150$  K. The chemisorbed oxygen desorbs in the temperature interval 750-850 K. At  $T_{\text{ads}} > 200$  K oxygen adsorbs dissociatively. In Fig. 1 two oxygen temperature desorption spectra (TDS) are shown for Pt(410) and Rh(410). Two desorption peaks are observed for both surfaces: a sharp saturated peak at 600 K and a broad peak in the 740-850 K temperature range for Pt(410); the sharp peak at  $\approx 750$  K increases with increasing initial coverage and a broad peak at  $\sim 1000$  K for Rh(410). Distinctions between atomic oxygen  $\text{O}_{\text{ads}}$ , subsurface oxygen  $\text{O}_{\text{sub}}$  and surface oxide  $\text{O}_{\text{oxi}}$  may be determined from an analysis of TD spectra [3]. On Rh(410) we made a conclusion about surface oxide formation after  $10^3$ - $10^4$  L exposure to  $\text{O}_2$  at  $T_{\text{ads}}=650$  K. Our LEED patterns of the O/Rh(410) surface correspond to the structure of the surface oxide, observed for Rh(100) [5]. A dramatic effect of the surface temperature on the oxygen coverage was found for  $\text{O}_2$  adsorption on Pt(410) at temperatures 300-500 K. The coverage of oxygen increased by a factor of  $\sim 10$  at 500 K, apparently as a result of subsurface oxygen island formation at defect sites along the (110) steps on (410) surface.

## OP-9

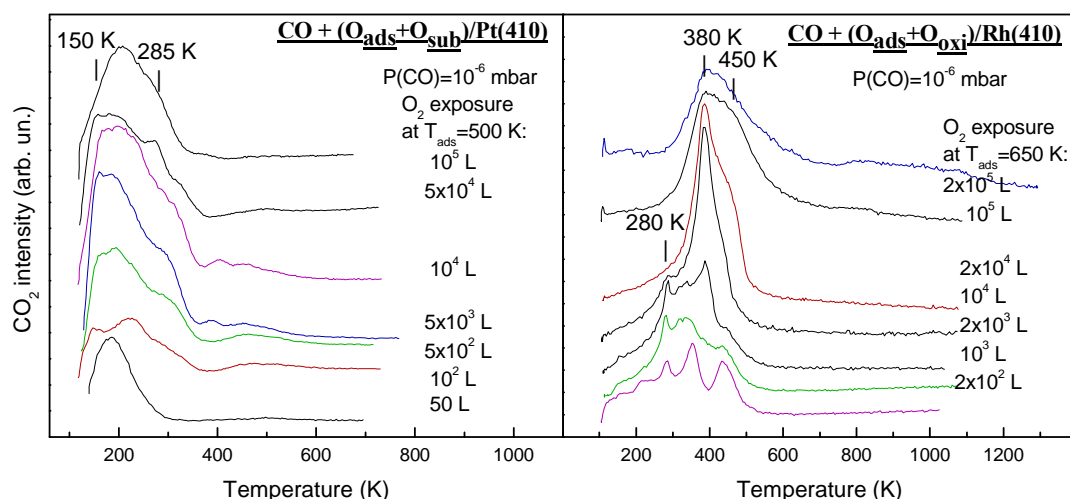


Fig. 3. TPR spectra of  $\text{CO}_2$  formed by reaction of  $\text{O}_{\text{ads}}+\text{O}_{\text{sub}}$  (Pt),  $\text{O}_{\text{ads}}+\text{O}_{\text{oxi}}$  (Rh) and CO,  $3 \text{ K s}^{-1}$ .

*Reaction  $\text{CO}_{\text{ads}} + \text{O}_{\text{ads}}$ .* Fig. 2 shows TPR spectra that contain the dependence of the rate of the  $\text{CO}_2$  formation on Pt(410) and Rh(410) surfaces on  $\text{CO}_{\text{ads}}$  concentration. Upon exposing a clean surface to  $\text{O}_2$  (0.1-0.2 L, 100 K), the  $\text{O}_{2\text{ads}}$  molecular form was removed by heating to 200 K. At low coverages ( $\theta_{\text{O}} \sim 0.1 \text{ ML}$ ,  $\theta_{\text{CO}} \sim 0.2 \text{ ML}$ ), heating of the  $\text{O}_{\text{ads}}+\text{CO}_{\text{ads}}$  mixed layer produced a single  $\text{CO}_2$  peak at 285 K (Pt) and 440 K (Rh). At high coverages,  $\theta_{\text{CO}} \sim 1 \text{ ML}$  ( $\theta_{\text{O}} = \text{const} \sim 0.1 \text{ ML}$ ), the formation of  $\text{CO}_2$  occurs at substantially lower temperatures, 170-200 K. We explain this by an increase in the reactivity of  $\text{O}_{\text{ads}}$  atoms due to the influence of the  $\text{CO}_{\text{ads}}$  layer [4]. As the pressure of CO was increased to  $2 \times 10^{-7} \text{ mbar}$ , the temperature of  $\text{CO}_2$  formation attained its lowest value, 150 K on Pt(410) and 265 K on Rh(410).

*Reaction  $\text{CO}_{\text{ads}} + \text{O}_{\text{sub}}$ ;  $\text{CO}_{\text{ads}} + \text{O}_{\text{oxi}}$ .* Fig. 3 shows the results of a TPR study of the reactivity of subsurface oxygen (Pt) and surface oxide (Rh) compared to that of atomic oxygen. As can be seen, oxygen atoms incorporated into the subsurface layer of the Pt(410), react with carbon monoxide ( $P_{\text{CO}} = 10^{-6} \text{ mbar}$ ) at  $T \sim 250\text{-}300 \text{ K}$  much more slowly compared to  $\text{O}_{\text{ads}}$ . This result clearly shows that the reactivity of  $\text{O}_{\text{ads}}$  is higher than that of  $\text{O}_{\text{sub}}$ . It was also demonstrated that  $\text{O}_{\text{oxi}}$  on Rh(410) reacts with CO only at high temperature to produce a  $\text{CO}_2$  peak at 450 K. The  $\text{O}_{\text{ads}}$  layer reacts with CO at low temperature ( $T \sim 300 \text{ K}$ ) that indicates a high reactivity of  $\text{O}_{\text{ads}}$  atoms.

*Conclusions.* The obtained results allow us to draw two main conclusions: (i) at  $T < 300 \text{ K}$ , chemisorbed oxygen atoms  $\text{O}_{\text{ads}}$  are highly reactive; (ii) there is direct evidence for the action of  $\text{CO}_{\text{ads}}$  layer on the reactivity of atomic oxygen.

This work was supported by the RFBR Grant 05-03-32971, INTAS 05-109-5039 and RSSF.

## References

1. P.R. Norton, P.E. Binder, K. Griffiths, J. Vac. Sci. Technol. A 2 (1984) 1028.
2. J.L. Gland, M.R. McClellan, F.R. McFeely, J. Chem. Phys. 79 (1983) 6349.
3. N. McMillan, T. Lele, C. Snively, J. Lauterbach, Catal. Today 105 (2005) 244.
4. V.V. Gorodetskii, A.A. Sametova, A.V. Matveev, N.N. Bulgakov, Chem. Phys. 2 (2007) 30
5. E. Lundgren, A. Mikkelsen, J. N. Andersen, et al, J. Phys.: Cond. Matter 18 (2006) R4819.

**CO OXIDATION AT GRAPHITE EDGES: A THEORETICAL STUDY****Zhang Aihua***Fritz Haber Institute of Max Planck Society, Department of Inorganic Chemistry,  
Berlin, Germany**E-mail: [aihua@fhi-berlin.mpg.de](mailto:aihua@fhi-berlin.mpg.de)*

Carbon materials have recently been shown to be efficient catalysts for dehydrogenation reactions. This awakes the idea that carbon materials may also be used as catalysts for other elementary reactions. We have therefore studied graphite edges, which are chosen as a model for reactive carbon materials, in a mixture of oxygen and CO. Our ab-initio thermodynamic results indicate that the undercoordinated atoms at the edges would easily be saturated by functional groups, such as carbonyls and ethers, when exposed to an oxygen atmosphere. The coverage is T and p-dependent and already low gas pressures lead to full saturation, but relative concentration of the functional groups may change due to T and p. This puts the large number of cluster calculations in doubt, where usually isolated functional groups are considered individually. Subsequent analysis of CO adsorption indicates that lactones may form due to CO and O adsorption at adjacent sites. This provides a starting point to study elementary oxygen related reactions in carbon materials, such as gasification, CO-oxidation or the Boudouard reaction.

## FIELD ELECTRON AND FIELD ION MICROSCOPY IMAGING OF CATALYTIC SURFACE REACTIONS ON PLATINUM GROUP METALS

**Gorodetskii V.V.<sup>1</sup>, Elokhin V.I.<sup>1</sup>, Nieuwenhuys B.E.<sup>2</sup>**

<sup>1</sup>*Boriskov Institute of Catalysis, Novosibirsk, Russia*

<sup>2</sup>*Leiden Institute of Chemistry, Leiden, The Netherlands*

*E-mail: [Gorodetsk@catalysis.ru](mailto:Gorodetsk@catalysis.ru)*

The obtained results reveal the detailed mechanism of self-organization in chemical reactions on catalytically active surfaces of hundred Angstroms size. New experimental data are obtained, concerning the formation of chemical waves, and new realistic models to describe these phenomena are developed. It becomes possible to study catalysis on a nanoscale level which is necessary for understanding of the mechanism of the action of the high-dispersed supported metal catalysts having metal nanocrystallites  $\sim 300$  Å in size as active part of the catalyst.

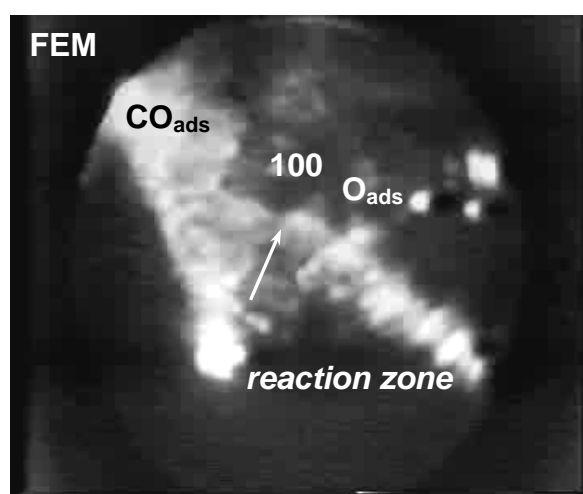
Field electron microscopy (FEM) with a lateral resolution of  $\sim 20$  Å and field ion microscopy (FIM) with a lateral resolution of  $\sim 5$  Å have been developed to investigate the dynamics of the surface phenomena associated with  $\text{CO}+\text{O}_2$ ,  $\text{H}_2+\text{O}_2$  and  $\text{NO}+\text{H}_2$  oxidation on a nanoscale level. Sharp tips of Pt, Rh, Ir and Pd, up to several hundreds Å in size, have been used to perform *in situ* investigations of the real dynamic surface processes simultaneously occurring on different crystallographic nanoplanes of the emitter-tip. The mechanism of local oscillator synchronization is one of the fundamental problems in the study of the oscillatory behaviour of  $\text{CO}+\text{O}_2$ ,  $\text{H}_2+\text{O}_2$  and  $\text{NO}+\text{H}_2$  catalytic reactions. The isothermal kinetic oscillations in different oxidation reactions are observed as a rule [1,2] on the supported metals and on metal tips considered as a superposition of the interrelated single crystal nanoplanes. The following factors should play the dominant role in synchronizing a catalytic system consisting of separate oscillators with different properties, especially in the case of high pressure experiments: i) the global coupling through the gas phase, or/and ii) in the case of the support with the high thermal conductivity, the coupling *via* heat transfer. In the case of single crystals and metal tips studies under UHV conditions the surface diffusion of the adsorbed species can be responsible for the synchronization of local oscillators [3,4].

The present results show that the field electron and field ion microscope can serve as an *in situ* catalytic flow reactor in the  $10^{-7}$  to  $10^{-3}$  mbar total pressure regime. A very fine metal tip (model catalyst, grain diameter  $\sim 700$  Å) exposes particular surface nanoplanes with different structures. The experimental results prove that self-sustained oscillations in the catalytic  $\text{H}_2+\text{O}_2$ ,  $\text{CO}+\text{O}_2$  and  $\text{NO}+\text{H}_2$  reactions are observed on the nanoscale on certain

surface areas of Pd, Rh, Ir and Pt tips as small as a few hundred surface sites while surroundings with different crystallographic nanoplanes stay in a stationary state. With slightly different external control parameters, mixed-mode oscillations caused by sequential reaction steps occur, characterizing a collective ensemble of crystal nanoplanes.

Three fundamentally different feedback mechanisms generating kinetic oscillations have been identified: periodic changes in surface structure (Pt tip:  $\text{CO}+\text{O}_2$ ,  $\text{H}_2+\text{O}_2$ ), subsurface oxygen formation (Pd tip:  $\text{CO}+\text{O}_2$ ) and a strongly non-linear interaction between adsorbed species (Rh and Ir tips:  $\text{NO}+\text{H}_2$ ). Based on experimental results, a model for the  $\text{CO}+\text{O}_2$  reaction on Pt(100) and Pd(110) surfaces is proposed for mathematical Monte Carlo modeling.

**Phase transition.** In order to establish the region in parameter space for oscillations, the



system was studied at  $T = 340$  K in the  $P(\text{CO})$  range from  $10^{-7}$  to  $10^{-5}$  mbar and  $P(\text{O}_2)$  range from  $10^{-6}$  to  $5 \times 10^{-4}$  mbar.

Fig. 1. FEM image showing the surface structures of the oxygen island (black) developed on the CO-precovered surface (light). The preadsorbed  $\text{CO}_{\text{ads}}$  layer in the presence of  $P(\text{CO}) = 1 \times 10^{-5}$  mbar reacts with oxygen ( $P(\text{O}_2) = 1.5 \times 10^{-4}$  mbar), producing a standing sharp  $\text{O}_{\text{ads}}$  wave front. [4].

It has been found that the Pt(100) surface switches reversibly from an inactive state (hex)

into a highly active state ( $1 \times 1$ ) under  $\text{CO}+\text{O}_2$  self-oscillation conditions [4]. A kinetic phase diagram has been established for the Pt(100) nanoplane. In this diagram, the region in which the  $\text{O}_{\text{ads}}$  layer is found at high  $P(\text{O}_2)/P(\text{CO})$  ratio, is separated by a line (reaction zone) from the region of the  $\text{CO}_{\text{ads}}$  layer at a lower partial pressure ratio. In this reaction zone the highest concentration of free Pt-centres is reached which contribute to dissociative adsorption of  $\text{O}_2$  and a rapid reaction with closely arranged  $\text{CO}_{\text{ads}}$  molecules. The direct imaging of catalytic  $\text{H}_2+\text{O}_2$  oxidation on clean Pt tips of small radius ( $\sim 700$  Å) has been studied on an atomic level by FIM [1]. The  $\text{H}_2\text{O}$  molecules produced act as an imaging gas and display the catalytically active surface area *in situ* and in real time. The tip contains a region of the (100) nanoplane, on which the reaction rate displays sustained temporal oscillations. The transition of hex-Pt(100) into ( $1 \times 1$ )-Pt(100) manifests itself by the appearance of fluctuating clusters of Pt atoms ( $\sim 15$  atoms) which can be discerned in the series of FIM images. This process is visible *in situ* in the original video recording. Thus, we can conclude that the catalytic  $\text{H}_2+\text{O}_2$

## OP-11

reaction in this cycle of cluster formation and removal is creating and destroying its own catalytic centres.

**Subsurface oxygen.** On the Pd(110) surface the self-oscillations are connected with periodic formation and consumption of subsurface oxygen  $O_{\text{ads}} \leftrightarrow O_{\text{sub}}$ , that affects the catalytic properties of the metal surface [3,4].  $O_{\text{ads}}$  is highly active compared to  $O_{\text{sub}}$  species due to the rapid reaction with  $\text{CO}_{\text{ads}}$ . On this oxidized surface local oscillations on the Pd(100)<sub>step</sub> nanoplanes can be obtained with fast repetition periods. Analysis of the tip surface shows the availability of a sharp boundary between mobile  $\text{CO}_{\text{ads}}$  and  $O_{\text{ads}}$  fronts. A maximum initial rate has been observed on Pd(110) and two spatially separated adlayers are formed on the tip surface. The oxygen layer forms only on the {110}, {320} and {210} planes, whereas  $\text{CO}_{\text{ads}}$  layers or empty sites form on the {100} and {100}<sub>step</sub> planes. Chemical waves are combined with  $O_{\text{ads}}$  and  $\text{CO}_{\text{ads}}$  layers in a sequence of reaction steps with the back-transition of  $O_{\text{ads}} \leftrightarrow O_{\text{sub}}$ . This process involves the feedback reaction  $O_{\text{sub}} \rightarrow O_{\text{ads}}$  during oscillations. Monte Carlo simulations on the Pd(110) surface demonstrate the appearance of turbulent patterns, spiral and elliptic waves [3].

**"Explosive" reaction.** It has been shown that the mechanism of non-linear behaviour in the  $\text{NO} + \text{H}_2$  over Pt, Rh and Ir surfaces involves the creation of adjacent vacant sites needed for NO dissociation. The products  $\text{N}_2$ ,  $\text{N}_2\text{O}$ ,  $\text{NH}_3$ ,  $\text{H}_2\text{O}$ , leaving the surface facilitate an autocatalytic rise in the concentration of such vacant sites and, hence, the reaction rate increases [4]. The availability of vacant sites near the  $\text{NO}_{\text{ads}}$  and  $\text{N}_{\text{ads}}$  may play a central role in the selectivity towards  $\text{N}_2\text{O}$  and  $\text{N}_2$ . For  $\text{NH}_3$  formation the surface vacant sites are needed for  $\text{H}_2$  dissociation and subsequent reaction of  $\text{H}_{\text{ads}}$  with  $\text{N}_{\text{ads}}$ . Our FEM results indicated a key role of stepped surfaces in initiation of such oscillations.

**Conclusions.** It was learned that the non-linear reaction kinetics is not restricted to macroscopic planes, since: (a) planes  $\sim 200 \text{ \AA}$  in diameter show the same non-linear kinetics; (b) regular waves appear on those nanoplanes under the oscillation conditions; and (c) the propagation of reaction-diffusion waves includes the participation of the different crystal nanoplanes, indicating effective coupling between adjacent planes.

This work is supported in part by RFBR Grant № 05-03-32971 and NWO № 047-015-002.

## References

1. V. Gorodetskii, J. Lauterbach, H.-H. Rotermund, J.H. Block, G. Ertl, *Nature* 370 (1994) 276.
2. J. Lauterbach, G. Bonilla, T.D. Pletcher, *Chem. Eng. Sci.* 54 (1999) 4501.
3. A.V. Matveev, E.I. Latkin, V.I. Elokhin, V.V. Gorodetskii, *Chem. Eng. J.* 107 (2005) 181.
4. V.V. Gorodetskii, V.I. Elokhin, J.W. Bakker, B.E. Nieuwenhuys, *Catal. Today* 105 (2005) 183.

## METHANOL OXIDATION ON Ru CATALYSTS: REACTION PATHWAYS AND CATALYTICALLY ACTIVE STATES

Blume R.<sup>1</sup>, Hävecker M.<sup>1</sup>, Zafeiratos S.<sup>1</sup>, Teschner D.<sup>1</sup>, Vass E.<sup>1</sup>, Schnörch P.<sup>1</sup>, Knop-Gericke A.<sup>1</sup>, Schlögl R.<sup>1</sup>, Lizzit S.<sup>2</sup>, Dudin P.<sup>2</sup>, Barinov A.<sup>2</sup> and Kiskinova M.<sup>2</sup>

<sup>1</sup>*Fritz Haber Institute of the Max Planck Society, Department of Inorganic Chemistry,*

*Faradayweg 4-6, 14195 Berlin, Germany*

<sup>2</sup>*Synchrotron Trieste, AREA Science Park-Basovizza, Trieste-34012, Italy*

*E-mail: [mh@fhi-berlin.mpg.de](mailto:mh@fhi-berlin.mpg.de)*

Surface composition and corresponding catalytic activity and selectivity of model Ru catalysts in methanol oxidation have been studied in the  $10^{-1}$  mbar pressure range for three oxidation regimes, combining in situ synchrotron based X-ray photoelectron spectroscopy (XPS) with simultaneous monitoring by online mass spectrometry the products released to the gas phase. Ru3d<sub>5/2</sub> and O1s XP core level spectra provide clear evidence that the composition of catalytically active steady states exhibiting different activity and selectivity originate from interactions with reactants and are dynamically controlled by the reactants partial pressure and temperature.

### Introduction

Selective oxidation of methanol (CH<sub>3</sub>OH) to formaldehyde (CH<sub>2</sub>O) has attracted a lot of interest because formaldehyde is a primary reagent in many organic syntheses. Along with the most commonly used metallic Ag and Cu or Mo and V oxide catalysts, a remarkable activity for CH<sub>2</sub>O production at rather low temperature (300 K - 400 K) has been recently reported for supported RuO<sub>2</sub> catalysts [1]. Their high catalytic activity is attributed to fast redox cycles. Recent studies focusing on identification of catalytically active states in redox reactions have provided strong evidence that both structure and chemical state of the catalyst can be far different from those of the stoichiometric oxide compounds used as models for explaining Mars-van Krevelen oxidation mechanism. A Ru transient “surface oxide” (TSO) state, Ru<sub>x</sub>O<sub>y</sub>, has been found to be active for CO oxidation at mbar pressures [2]. Extensive structural, photoemission and TPD studies characterized the TSO state as a disordered phase with 1-4 ML oxygen incorporated within the top few Ru layers, which precedes the nucleation and growth of the stoichiometric RuO<sub>2</sub> phase [3,4]. The TSO state exists in a pressure-temperature range, where the formation of the thermodynamically stable RuO<sub>2</sub> is kinetically hindered and it can also coexist with the growing RuO<sub>2</sub> islands.

In contrast to CO oxidation, the reaction mechanism in CH<sub>2</sub>O production from CH<sub>3</sub>OH is complicated by multiple possible reaction pathways. The present study of CH<sub>3</sub>OH oxidation



## OP-12

on model Ru(0001), Ru(10 $\bar{1}$ 0), and polycrystalline Ru catalysts addresses the catalytically active states under different reaction conditions. Ru3d and O1s X-ray photoelectron core level spectra were used as fingerprints for the dynamic response of the catalysts surface active state to changes in temperature and CH<sub>3</sub>OH/O<sub>2</sub> molecular mixing ratio.

### Experimental

The experiments have been performed at the synchrotron facility BESSY in Berlin in the high pressure XPS station designed and constructed in FHI-MPG. The gas phase products were monitored by a differentially pumped HIDEN mass spectrometer. The MS response was used as a measure of the catalytic activity. Ru3d and O1s XP spectra were measured with photon energies of 450 eV and 650 eV, respectively. The results in an effective escape depth for the O1s and Ru3d photoelectrons of  $\sim 5\text{\AA}$ , which limits the probing depth to the top few layers ( $\sim 10\text{\AA}$ ). The catalyst temperature was changed stepwise. The investigations were carried out in the pressure range of  $10^{-2}$  -  $10^{-1}$  mbar using different CH<sub>3</sub>OH/O<sub>2</sub> mixing molecular ratios.

### Results and discussion

Our results clearly show that the CH<sub>3</sub>OH:O<sub>2</sub> mixing ratio controls the Ru reduction-oxidation equilibrium attaining the steady catalyst states independently of the initial pre-catalyst state. Fig. 1A shows Ru3d<sub>5/2</sub> XP spectra taken at steady state conditions corresponding to different catalyst selectivity. The deconvolution of the Ru3d<sub>5/2</sub> core level reveals 3 components that can be assigned to the bulk metallic component Ru<sub>bulk</sub>, Ru with adsorbed oxygen Ru<sub>ad</sub> and transient “surface oxide” Ru<sub>x</sub>O<sub>y</sub> (TSO), respectively. Ru<sub>ad&TSO</sub>/Ru<sub>bulk</sub> abundance ratios higher than 0.3 mark the incorporation of oxygen and the formation of the TSO state. For the catalytically active states favouring partial oxidation of methanol to: CO+H<sub>2</sub>+H<sub>2</sub>O (a) and CH<sub>2</sub>O+H<sub>2</sub>O (b), and full oxidation to CO<sub>2</sub>+H<sub>2</sub>O (c) we evaluated the Ru<sub>ad&TSO</sub>/Ru<sub>bulk</sub> abundance ratios 0.15, 0.46, and 0.56, respectively. Apparently, the only difference in the catalytically active TSO states for partial oxidation to CH<sub>2</sub>O and full oxidation to CO<sub>2</sub> is in the amount of accumulated oxygen, whereas the partial oxidation to CO+H<sub>2</sub>+H<sub>2</sub>O occurs on metallic Ru only with submonolayer of adsorbed oxygen. The established steady states exhibit different activity and favour specific reaction pathways (Fig. 1B). The figure compares the catalytic activities of the three catalyst states elucidated from the total yield of C-containing products (CO, CH<sub>2</sub>O, CO<sub>2</sub>) and from the corresponding methanol consumption.

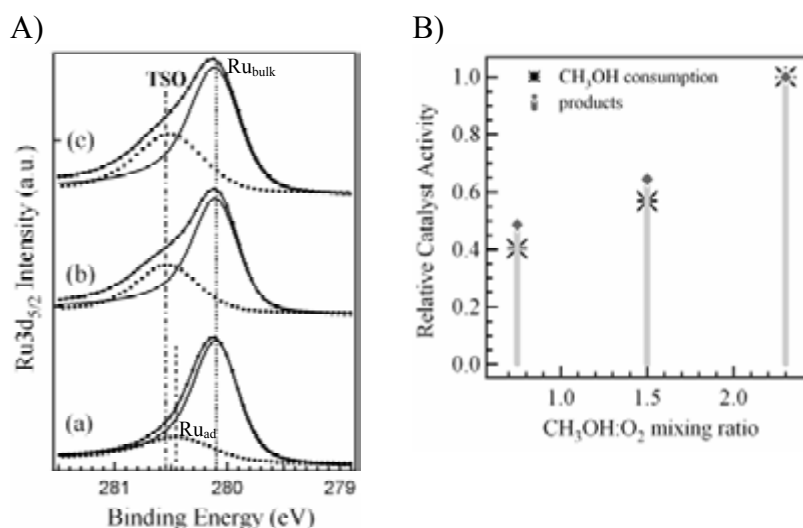


**Figure 1 (A):** Deconvoluted Ru<sub>3d<sub>5/2</sub></sub> XP spectra of the catalyst steady states measured in the temperature range 570-620 K, representing the oxidation regimes favouring oxidation to CO+H<sub>2</sub>+H<sub>2</sub>O (a), CH<sub>2</sub>O+H<sub>2</sub>O (b), and CO<sub>2</sub>+H<sub>2</sub>O (c).

**Figure 1 (B):** Catalyst activity at 580-600 K for the RuO<sub>2</sub> pre-catalyst state as a function of the CH<sub>3</sub>OH:O<sub>2</sub> ratio.

## Conclusions

The catalytically active states of Ru catalysing different CH<sub>3</sub>OH oxidation pathways are formed by interaction with the reactants in the gas phase under specific (T, P<sub>CH<sub>3</sub>OH</sub>, P<sub>O<sub>2</sub></sub>) conditions, independently of the initial pre-catalyst. Non-stoichiometric transient “surface oxide” (“Ru<sub>x</sub>O<sub>y</sub>”), differing only by the amount of accumulated oxygen was found to catalyze both partial oxidation to CH<sub>2</sub>O and total oxidation to CO<sub>2</sub>. The dramatic changes in the selectivity correlate to relatively small differences in catalyst chemical state demonstrate the compositional complexity of the catalyst surface under dynamic reaction conditions and the important role of the T,P range in tuning the catalyst performance.

## Acknowledgements

M. Kiskinova thanks AvH foundation for the Award to pursue research at FHI-Berlin. P. Dudin acknowledges financial support under contract No. NMP3-CT-2003-505670 (NANO2).

## References

1. H. Liu, and E. Iglesias, J. Chem. Phys. B 109 (2005) 2155.
2. R. Blume, M. Hävecker, S. Zafeiratos, D. Teschner, E. Kleimenov, A. Knop-Gericke, R. Schlögl, A. Barinov, P. Dudin, M. Kiskinova, J. Catal. 239 (2006) 354.
3. A. Böttcher, U. Starke, H. Conrad, R. Blume, L. Gregoriatti, B. Kaulich, A. Barinov, M. Kiskinova, J. Chem. Phys. 117 (2002) 8104.
4. R. Blume, H. Niehus, H. Conrad, A. Böttcher, L. Aballe, L. Gregoriatti, A. Barinov, and M. Kiskinova, J. Phys. Chem. B 109 (2005) 14052.

**STABILITY OF STEADY STATES IN NONIDEAL MODELS  
OF SOME DETAILED MECHANISMS OF CATALYTIC REACTIONS**

**Mamash E.A.**

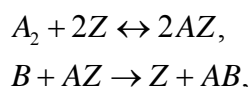
*Tuvianian Institute for the Exploration of Natural Resources, SB RAS, Kyzyl, Russia*

*E-mail: [m\\_elen@rambler.ru](mailto:m_elen@rambler.ru)*

Stability of steady states in nonideal models of typical catalytic reactions with one intermediate occurring in CSTR has been investigated. Explicit expressions for the neutrality curves have been derived. It has been shown that the model of catalytic isomerization mechanism does not permit the self-oscillations of the reaction rate.

The traditional procedure of parametric analysis of a dynamic system describing the processes at catalytic surfaces includes the study of the type and the number of steady states and the investigation of their stability [1]. Construction and analysis of nonideal models of chemical kinetics is of current importance now, because the ideal models does not allow usually the description of such critical phenomena as the multiplicity of steady states, the self-oscillations, etc., observed in experiments. Taking into account the non-ideality of the adsorbed layer of the catalyst the models of catalytic isomerization mechanism and mono- and-bimolecular Eley-Rideal mechanisms have been considered recently [2-4]. In this case the rate constants depend on the adsorbate coverage [5]. It has been shown, that such nonideal models allow to observe in the systems the multiplicity of steady states which is absent in an ideal case.

However the question about the stability remains open; the absence of self-oscillations was supposed usually only by virtue of simplicity of investigated mechanisms. In the present study the exact analytical expressions for the neutrality curves which single out the parameter regions with the various stability types have been obtained for all above mentioned systems. It is proved, that in the model of catalytic isomerization reaction mechanism in CSTR self-oscillations are absent. Also it is shown that for Eley-Rideal mechanisms it is impossible to give such an answer. In particular, for the model of bimolecular Eley-Rideal mechanism



where  $A_2, B, AB$  are the substances in the gas phase,  $AZ$  is an intermediate (adsorbed substance on a surface of the catalyst) the expression for the neutrality curve is of the form

$$L(P_{A_2,0}, P_{B,0}) = \begin{cases} P_{A_2,0} = f(\theta, \mu, P_{00}, k_{a,0}, k_{d,0}, k_{r,0}, P^*, \tau_{r,A_2}, \tau_{r,B}, T), \\ P_{B,0} = g(\theta, \mu, P_{00}, P_{A_2,0}, k_{a,0}, k_{d,0}, k_{r,0}, P^*, \tau_{r,A_2}, \tau_{r,B}, T), \end{cases}$$

Here  $P_{A_2,0}$ ,  $P_{B,0}$  are the pressures of reactants,  $\theta$  is the adsorbate coverage,  $\mu$  is the chemical potential,  $P_{00}$  is the probability that two nearest sites are empty,  $P^*$ ,  $\tau_{r,A_2}$ ,  $\tau_{r,B}$  are the constants, describing the properties of the reactor,  $k_{a,0}$ ,  $k_{d,0}$ ,  $k_{r,0}$  are the rate constants for adsorption, desorption and reaction respectively,  $T$  is the absolute temperature.

Dependence  $\theta$  and  $P_{00}$  on  $\mu$  is calculated by the transfer-matrix method well known in the statistical physics [6]. As a result, the parameters of the model can be chosen in such a manner that the neutrality curve appears in the positive half-plane and lies inside of the area of multiplicity of steady states (fig.1). It shows that we can't approve the absence of self-oscillations in given mechanism. The similar situation takes place in the model of the monomolecular Eley-Rideal mechanism.

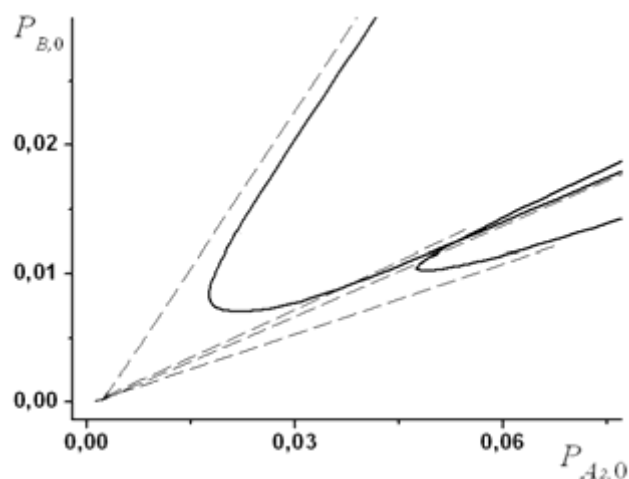


Fig. 1. Bifurcation curves for the model of bimolecular Eley-Rideal mechanism; solid line – the neutrality curve, dashed line – the multiplicity curve.

## References

1. V.I. Bykov. Modeling of the Critical Phenomena in Chemical Kinetics. – Moscow: Komkniga, 2006. – 325 pp.
2. A.V. Myshlyavtsev, R.T. Samdanchap, React. Kinet. Catal. Lett. 53 (1994) 269.
3. E.A. Mamash, A.V. Myshlyavtsev, Vestnik Krasnoyarskogo gos. tech. universiteta. 33 (2004) 118.
4. V.I. Bykov, E.A. Mamash, Vestnik Krasnoyarskogo gos. tech. universiteta 33 (2004) 102 (in Russian).
5. V.P. Zhdanov, Elementary Physicochemical Processes on Solid Surfaces. Plenum Press, New York, 1991.
6. V.I. Bykov, A.V. Myshlyavtsev, M.G. Slinko, Dokl. Akad. Nauk 384 (2002) 650 (in Russian).

**Arrigo R.<sup>1\*</sup>, Wild U.<sup>1</sup>, Lerch M.<sup>2</sup>, Schlögl R.<sup>1</sup> and Su D.S.<sup>1</sup>**

<sup>1</sup>*Fritz-Haber-Institut der Max-Planck-Gesellschaft, Faradayweg 4-6, 14195 Berlin, Germany*

<sup>2</sup>*Technische Universität Berlin, Straße des 17. Juni 135, 10623 Berlin, Germany*

*\*E-mail: [arrigo@fhi-berlin.mpg.de](mailto:arrigo@fhi-berlin.mpg.de)*

Post-synthesis treatments, with nitrogen-containing molecules such as NH<sub>3</sub> or HCN, could be a suitable route for incorporating nitrogen functionalities on the surface of CNTs (carbon nanotubes). In order to introduce nitrogen functionalities on the surface of CNTs, the pre-existence of oxygenated functionalities is favorable. Although this requires treatment with strong oxidizing agents, for instance HNO<sub>3</sub>, the graphitic structure is not largely modified. In this work the effect of NH<sub>3</sub> treatment conditions on the nature of nitrogen functionalities in CNTs have been investigated by temperature programmed mass spectrometry (TPD-MS) and X-ray photoelectron spectroscopy (XPS). The amount of N introduced (up to 5 wt%) is of relevance if considered to be on the surface.

## **Introduction**

Tailoring the electronic mechanical and chemical properties of carbon nanotubes (CNTs) by doping with elements such as N, B, P and S, represents a significant challenge in modern nanotube science [1]. In heterogeneous catalysis, nitrogen-doping of CNTs is especially interesting as it introduces specific surface properties. Among these properties are: increased number of defects and exposed edges, enhanced polarity and basicity. N-CNTs have already been successfully applied in fuel cells [2] and liquid phase base-catalyzed reaction [3]. Most of the studies reported in the literature on the synthesis of N-doped CNTs, have focused on catalytic chemical vapor deposition (CCVD) of N-containing hydrocarbons, the main reason being that it is compatible with a hypothetical scale-up. Although this method might allow introduction of high amounts of nitrogen, the nitrogen will be mostly localized in the internal walls of the CNTs. Consequently, the nitrogen will be inaccessible to reactants. Post-synthesis treatments, with nitrogen-containing molecules such as NH<sub>3</sub> or HCN, could be a suitable route for incorporating nitrogen functionalities on the surface of CNTs. The aim of this work is to investigate the influence of post-synthesis NH<sub>3</sub> treatment conditions on the nature of nitrogen functionalities in CNTs and to gain insight into the mechanism of nitrogen insertion in CNTs. This is addressed by analyzing the effluent gas using temperature programmed mass spectrometry (TPD-MS) and looking at the modification of nitrogen functionalities on the CNTs surface by X-ray photoelectron spectroscopy (XPS). Furthermore chemical surface properties have been investigated by Zeta potential measurements.

## Experimental

Commercial multiwall carbon nanotubes (applied science PR24-PS) have been treated with  $\text{HNO}_3$  at 373 K for 16 h in order to create oxygenated functionalities on the CNT surface. Then,  $\text{NH}_3$  (amination) and  $\text{NH}_3/\text{air}$  (ammoxidation) treatment have been performed at temperature ranging between 473-1073 K ( $\text{NH}_3/\text{H}_2\text{O}$  at 1073 K) on the oxidized MWNT and on the MWNT as received. The samples have been characterized by TPD-MS and XPS. For TPD, the samples were heated at  $2 \text{ Kmin}^{-1}$  in Ar flow, and the evolved gases were continuously analyzed by mass spectrometry. The elemental analysis was performed by hot gas extraction. XPS (Mg  $\text{K}\alpha$  1253.6 eV, 168 W power) was performed using a modified LHS/SPECS EA200 MCD detector. A fixed analyser pass energy of 48 eV was used for the XPS measurements. Quantitative data analysis was performed by subtracting Shirley background [4] and using empirical cross sections [5].

## Results and discussion

In order to create nitrogen functionalities on the surface of CNTs, the pre-existence of oxygenated functionalities is favorable. Although this requires treatment with strong oxidizing agents, for instance  $\text{HNO}_3$ , the graphitic structure is not largely modified. The post-synthesis treatments conditions strongly influence the distribution of nitrogen functionalities and the nitrogen content in the CNTs. The lower the  $\text{NH}_3$  treatment temperature, the higher the nitrogen content (from 5 wt/wt % at 473 K to 1 wt/wt% at 1073 K in  $\text{NH}_3/\text{H}_2\text{O}$ ). The XPS spectrum of the N1s core level for this sample presents a broad peak consisting of two main contributions at 398.3 eV and 399.6 eV (Fig.1). In the TPD mass spectrum of this sample, the NO peaks ( $m/e = 30$ ) occur below 873 K and around 1073 K. Although the nitrogen contents decrease with increasing  $\text{NH}_3$  treatment temperature, it selectively introduces nitrogen functionalities, as is evident by the narrow FWHM of XPS N1s peak at 398.7 eV (not shown).

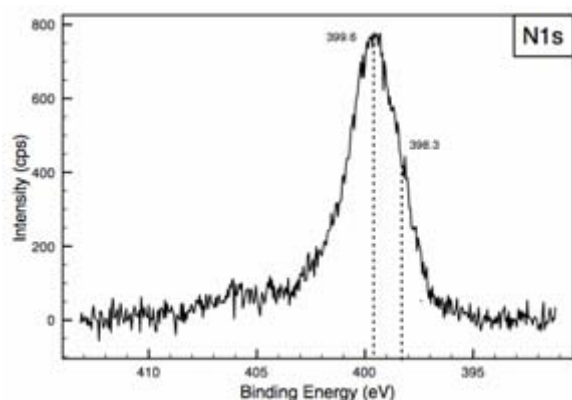


Fig. 1. XPS spectra of N1s core levels from N-CNT.

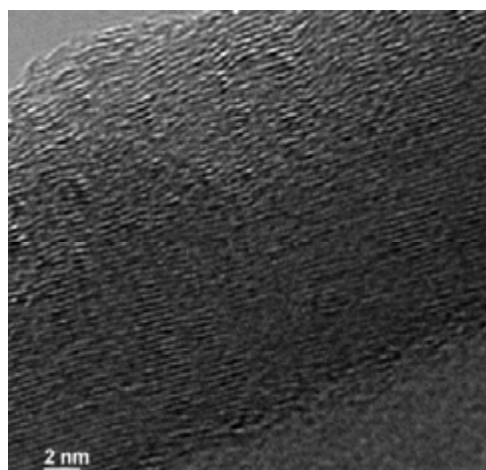


Fig. 2. HRTEM image of MWNTs after  $\text{NH}_3/\text{H}_2\text{O}$  treatment at 1073 K.

## OP-14

In the TPD spectrum of this sample, NO peak occurs only at 1073 K. In the literature [6] both the component centered at 398.3 eV and 399.6 eV have been assigned to species where N is bound to C, probably the former in pyridine-like while the latter can be related to nitrous functionalities. In comparison with the amination treatments, ammoxidation treatments introduce a higher concentration of N functionalities. However, all the post-synthesis procedures, necessary to introduce nitrogen functionalities, do not compromise the graphitic structure of CNTs (Fig. 2).

## Conclusions

Post-synthesis  $\text{NH}_3$  treated have been applied to introduce nitrogen functionalities in large amount on the surface of CNTs with pyridinic nature and nitrous functionalities.

## References

1. M. Terrones, A. Jorio, M. Endo, A.M. Rao, Y.A. Kim, T. Hayashi, H. Terrones, J.-C. Charlier, G. Dresselhaus and M.S. Dresselhaus. *Mat. Today* 7 (2004) 30.
2. Paul H. Matter, Ling Zhang and Umit S. Ozkan, *J. Catal.* 239 (2006) 83.
3. Stefan van Dommele, Krijn P. de Jong and Johannes H. Bitter, *Chem. Comm.* (2006) 4859.
4. D.A. Shirley, *Phys. Rev. B* 5 (1972) 4709.
5. Briggs and Seah "Practical Surface Analysis" second edition, Volume1 - Auger and X-ray Photoelectron Spectroscopy, Wiley, 1990 pp. 635-638 (Appendix 6).
6. J.R. Pels, F. Kapteijn, J.A. Moulijn, Q. Zhu and K.M. Thomas, *Carbon* 33 (1995) 1641.

**EFFICIENT IMPLEMENTATION OF DETAILED SURFACE CHEMISTRY  
INTO REACTOR MODELS BY A SPLINE-REPRESENTATION  
OF PRECOMPUTED RATE DATA**

**Votsmeier Martin**

*Umicore AG & Co. KG, Hanau, Germany*

*E-mail: [martinumi@gmx.de](mailto:martinumi@gmx.de)*

The increasing mechanistic understanding of catalytic processes can frequently not be fully exploited in realistic reactor simulations due to numerical constraints. It is shown that a spline representation of precomputed rate data is well capable of substituting a full numerical simulation of the mechanistic model during runtime of a reactor flow simulation. The approach offers a reduction in computing times by orders of magnitude and will allow the implementation of more complex mechanistic models in detailed flow simulations.

In recent years more and more mechanistic understanding of many catalytic processes becomes available. However, this understanding can frequently not be fully exploited in reactor simulations due to computational limitations. The approach of the current contribution is to substitute the full numerical simulation of the detailed reaction mechanism by the use of precomputed rate data in combination with an adequate mathematical data-representation.

The use of precomputed rate data for the simulation of complex reactive flow situations is fairly developed for gas phase kinetics and is frequently referred to as repro-modeling [1,2]. One major difficulty for the application of repro-modeling in gas phase kinetics is the identification of the species to be treated as quasi-equilibrated. This point is not an issue for heterogeneous catalysis, since the surface species on a reactor length scale do not move and hence, at least for steady state reactor simulations, can be naturally treated as steady state species. In consequence, the remaining task for the application of the repro-modeling approach in heterogeneous catalysis is the representation of the effective reaction rates for the gas species as a function of temperature and bulk gas concentrations.

From a mathematical point of view repro-modeling is a nonparametric regression problem. Different nonparametric regression techniques have emerged from the disciplines of statistics, mathematics and machine learning. Common techniques that have been applied in repro-modeling include high dimensional polynomial regression, partition trees, neural networks and grid-based interpolation. In the current contribution tensor product splines are used for the interpolation of precomputed rate data [3].



## OP-15

A mechanistic model of catalytic combustion on Platinum is used as an example to demonstrate the potential of the approach [4]. The effective rates used for the mapping procedure include the contribution of the surface reactions and the mass transport between gas phase and monolith surface. Rates are computed as a function of temperature, residence time in one volume element, and the concentrations of  $\text{CH}_4$ ,  $\text{CO}$  and  $\text{O}_2$ . This results in a 5-dimensional spline representation of the rate information.

A simple 1D isothermal monolith reactor model is used to demonstrate the performance of the approach. Figure 1 compares results of a full numerical solution to results obtained by the interpolation scheme. In all cases  $\text{CH}_4$  conversion and build up of the intermediate reaction product  $\text{CO}$  are well reproduced. The gain in computational speed is several orders of magnitude.

The methodology presented in this contribution promises an economic way for the implementation of increasingly complex mechanistic models in realistic flow simulations of catalytic reactors.

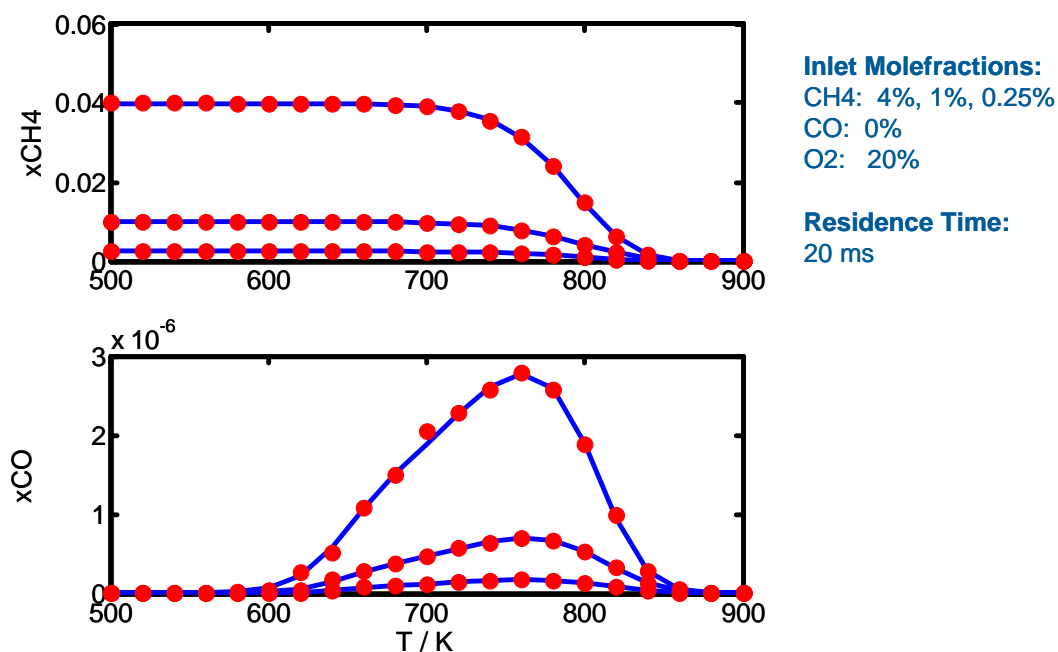


Figure 1. Comparison of outlet concentrations of a monolith reactor computed by a full numerical solution (line) and by the mapping approach (circles).

## References

1. W.S. Meisel, D.C. Collins, IEEE Trans. Syst. Man Cybern. 3 (1973) 349.
2. T. Turanyi, Computers Chem. 18 (1994) 45.
3. C. de Boor, A Practical Guide to Splines, Spribger Verlag, New York (1978).
4. Deutschmann, R. Schmidt, F. Behrendt, J. Warnatz. Proc. Combust. Inst. 26 (1996) 1747.

AN INVESTIGATION OF THE MECHANISM FOR METHANOL OXIDATION TO METHYL FORMATE AND DIMETHOXYMETHANE ON V<sub>2</sub>O<sub>5</sub>/TiO<sub>2</sub> CATALYST

**Kaichev V.V.<sup>1\*</sup>, Popova G.Ya.<sup>1</sup>, Chesalov Yu.A.<sup>1</sup>, Andrushkevich T.V.<sup>1</sup>,  
Bukhtiyarov V.I.<sup>1</sup>, Zemlyanov D.Yu.<sup>2</sup>, Knop-Gericke A.<sup>3</sup>, Schlögl R.<sup>3</sup>**

<sup>1</sup>*Boriskov Institute of Catalysis, Novosibirsk, Russia*

<sup>2</sup>*Purdue University, Birck Nanotechnology Center, West Lafayette, IN, USA*

<sup>3</sup>*Fritz Haber Institute of the Max Planck Society, Berlin, Germany*

\*E-mail: [vvk@catalysis.ru](mailto:vvk@catalysis.ru)

Based on kinetics analysis, *in situ* XPS/FTIR measurements, methanol oxidation to dimethoxymethane and methyl formate is suggested to proceed via the Mars-van Krevelen mechanism.

Vanadia supported on titania is known to be an effective catalyst in the selective oxidation of hydrocarbons, aldehydes, and alcohols, and other industrially important reactions. In particular, the V<sub>2</sub>O<sub>5</sub>/TiO<sub>2</sub> catalyzes methanol oxidation to form dimethoxymethane (DMM) and methyl formate (MF) at near ambient temperatures. Here, we report a study of the mechanism of this reaction, which was performed by *in situ* X-ray photoelectron spectroscopy and *in situ* Fourier transform IR spectroscopy. We show that concurrent formation of DMM and MF mainly occurs in a temperature range of 75-150 °C. At low temperature close to 75-100 °C, DMM is the main reaction product with selectivity of more than 90%. Increasing the temperature leads to the sharp decrease in DMM selectivity and a concurrent formation of MF. At 140-150 °C, the selectivity in MF is about 80%. At higher temperature, the methanol dehydrogenation to CO is dominant. Other products, such as formaldehyde and formic acid, were also observed, but only in small amounts.

The XPS experiments were performed at beam line U49/2-PGM1 at BESSY (Berlin, Germany). The experiments included the step-wise heating of the sample from 50 to 150 °C under near-equimolar CH<sub>3</sub>OH/O<sub>2</sub> mixture. Before *in situ* experiments were started, the catalyst was activated in oxygen at 300 °C. This led to full oxidation of vanadium to V<sup>5+</sup>. Only sharp single peak at 517.6 eV, which corresponds to V<sup>5+</sup> ions, is observed in the V2p<sub>3/2</sub> spectrum (Fig. 1). Under influence of the reaction mixtures, V<sup>5+</sup> ions are reduced to V<sup>4+</sup> that is identified on appearance of a wide V2p<sub>3/2</sub> peak at 516.4 eV. Increasing the temperature led to partial oxidation of V<sup>4+</sup> ions and two peaks at 516.4 eV (V<sup>4+</sup>) and 517.6 eV (V<sup>5+</sup>) are observed. The fraction of V<sup>5+</sup> ions are increased with temperature, but significant part of V<sup>4+</sup>

## OP-16

ions were remained on the catalyst surfaces even after methanol switch off. On the other hand, switch off oxygen at 150 °C resulted in further reduction of vanadium and two peaks at 515.6 and 516.6 eV, which correspond to  $V^{3+}$  and  $V^{4+}$ , were observed. It should be noted that no changes in Ti2p spectra were detected *in situ* by XPS which corresponded to  $Ti^{4+}$  ions only (spectra not shown).

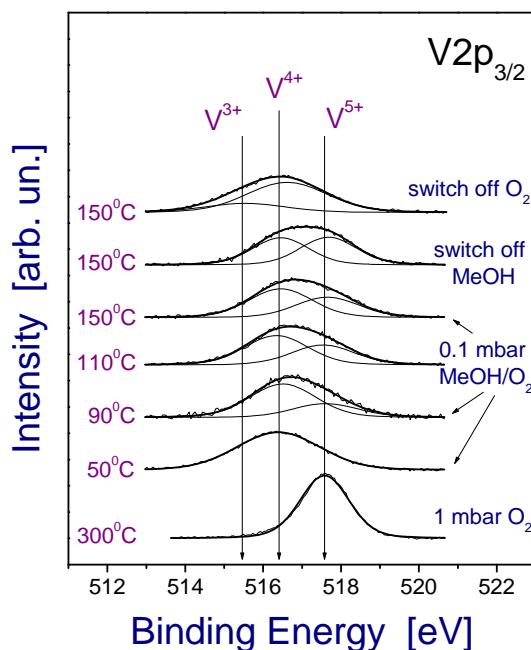


Figure 1. *In situ*  $V2p_{3/2}$  core level spectra.

*In situ* FTIR studies were performed to identify the reaction intermediates involved in the methanol oxidation. Figure 2 shows the FTIR spectra of the  $V_2O_5/TiO_2$  catalyst surface during methanol oxidation in the temperature range of 70-160 °C. At low temperature, observed two  $\nu(CH_3)$  bands at 2951 and 2842  $cm^{-1}$  as well as two  $\delta(CH_3)$  bands at 1445 and 1433  $cm^{-1}$  were assigned to methoxy ( $CH_3O$ ) species [1,2]. Another band at 1150  $cm^{-1}$  corresponding to  $\nu(CO)$  mode, as well as, two bands at 2923 and 2884  $cm^{-1}$  corresponding to  $\nu(CH_2)$  mode were assigned to dioximethylene ( $CH_2O_2$ ) species.

We suggest that the methanol oxidation proceeds via dehydrogenation to methoxy as a first intermediate, which is likely adsorbed on  $V^{5+}$  cations. The subsequent oxidation of these methoxy species by surface oxygen leads to dioximethylene formation and reduction of  $V^{5+}$  to  $V^{4+}$ . The dioximethylene decomposition results in the formation of formaldehyde and dioximethane, which quickly desorb from the surface. Dioximethane is also formed via an interaction of dioximethylene species with methanol. The low rates of reoxidation of the active center ( $V^{5+}$ ) at temperatures below 100 °C are the reason for the significant decrease in

the activity with time. An increase in temperature above 100 °C results in an intense oxidation of methoxy and dioximethylene into formates ( $\nu_s(\text{COO}^-)$  at  $1360\text{ cm}^{-1}$  and  $\nu_{as}(\text{COO}^-)$  at  $1550\text{ cm}^{-1}$ ) and in a partial reoxidation of  $\text{V}^{4+}$  to  $\text{V}^{5+}$ . The interaction of surface formates with methanol leads to MF formation. As a result, the  $\nu(\text{C}=\text{O})$  band at  $1654\text{ cm}^{-1}$  corresponding to molecularly adsorbed MF is observed in the FTIR spectra at 120-160 °C.

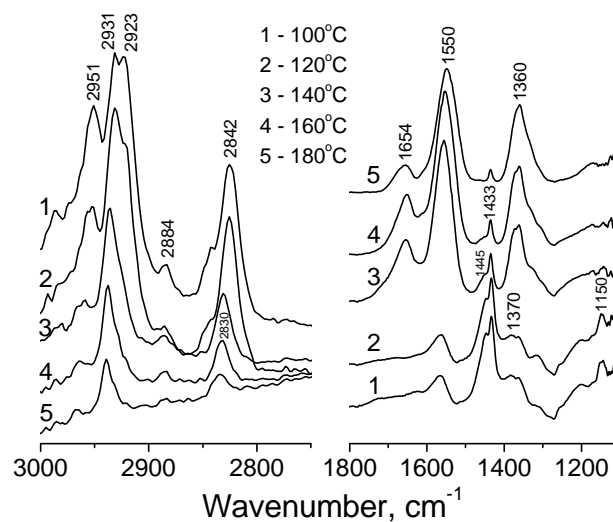


Figure 2. *In situ* FTIR spectra obtained in methanol oxidation on  $\text{V}_2\text{O}_5/\text{TiO}_2$  catalyst.

## Conclusions

Thus, our data testify that the lattice oxygen of vanadium oxide takes part in the methanol oxidation via the Mars-van Krevelen mechanism, which consists in reduction of the oxide catalyst surface by methanol and subsequent reoxidation by gas phase oxygen.

## Acknowledgements

This work was partially supported by the RFBR grant № 06-03-08137.

## References

1. G.Ya. Popova, Yu.A. Chesalov, T.V. Andrushkevich, I.I. Zakharov, E.S. Stoyanov, *J. Mol. Catal. A* 158 (2000) 345.
2. G.Ya. Popova, T.V. Andrushkevich, Yu.A. Chesalov, V.N. Parmon, *J. Mol. Catal. A* 268 (2007) 251.

## SIMULATION OF ALKANES DEHYDROGENATION PROCESS

Kravtsov A.V., Ivanchina E.D., Ivashkina E.N., Yuriev E.M., Fetisova V.A.

*Tomsk Polytechnical University, Tomsk, Russia*

*E-mail: [v1205f@list.ru](mailto:v1205f@list.ru)*

A new method for computer prediction of the catalytic activity dependence on service life and technological conditions for Pt catalysts has been proposed. The proposed method is based on physical and chemical laws of multicomponent hydrocarbon transformations on Pt catalysts and takes into account deactivation of metallic (Pt) sites. It allows calculating the product composition and catalytic activity level for real industrial units as a function of their technological parameters and raw material characteristics.

Petrochemical processes are very complex for the computer simulation as they include a number of parallel and successive stages. Industrial realization of these processes requires the determination of optimal unit parameters. Our task was to analyze systematically physical and chemical information. In this case, mathematical modeling is an efficient instrument. Models formed on the basis of hydrocarbon transformation laws permit to compute quantitative process characteristics and predict an optimal operating mode for industrial units [1, 2].

A specific feature of petrochemical processes is the fact that oil and oil refining products have complex hydrocarbon composition. So, the mathematical description would be very intricate in case of all reactions and substances were considered. On the other hand, a pseudokinetic model can be created for pseudocomponents constructed from hydrocarbons belonging to one homologous group. In this case, kinetic information is lost.

This problem has been solved due to creation of a mathematical description for an industrial dehydrogenation process, which includes stages shown on a fig. 1.

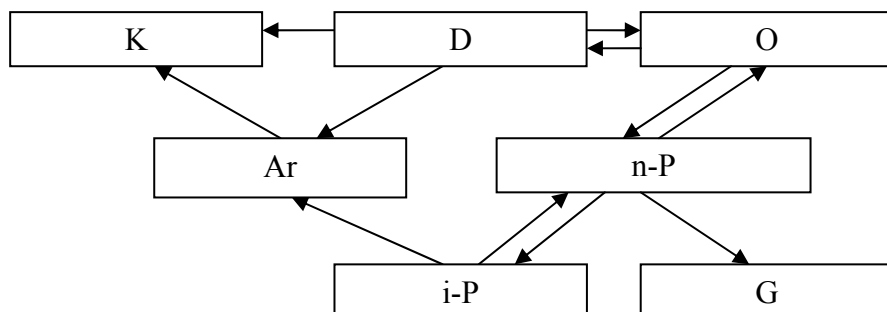


Fig. 1. Scheme of an industrial dehydrogenation process

Ar are aromatic hydrocarbons, n-P are normal alkanes (C<sub>9</sub>-C<sub>14</sub>), i-P are isoalkanes (C<sub>9</sub>-C<sub>14</sub>), K is coke, G are gaseous substances, D are diolefins C<sub>9</sub>-C<sub>14</sub>, O are olefines C<sub>9</sub>-C<sub>14</sub>.

Relationship between hydrocarbon molecular dimension, molecular structure and quantitative and qualitative characteristics of its conversion, such as conversion mechanism, activation energy, chemisorption heat and probability of bond dissociation, has been investigated. The results of this investigation permit to aggregate certain components used in construction of the mathematical model.

The proposed model contains material and heat balances equations:

$$G \frac{\partial C_i}{\partial z} + G \frac{\partial C_i}{\partial V} = (1 - \varepsilon) \sum_j w_j, \quad z=0: C_i=0, \quad V=0: C_i=C_{input} \quad (1)$$

$$G \frac{\partial T}{\partial z} + G \frac{\partial T}{\partial V} = -(1 - \varepsilon) \frac{\sum_j \Delta H_j r_j}{c_p \rho}, \quad z=0: T=T_0, \quad V=0: T=T_{input} \quad (2)$$

$$r_i = \sum_j w_j \quad (3)$$

where  $j$  is the reaction number according to the process mechanism,  $i$  is the number of an individual component or a hydrocarbon group,  $Z$  is the quantity of raw material processed after last regeneration,  $V$  is the catalyst volume,  $G$  is the unit flow rate of crude oil,  $C_i$  is the concentration of the  $i$ -th individual hydrocarbon or hydrocarbon group,  $T$  is the reactor temperature,  $C_p$  is the mixture heat capacity,  $\Delta H_j$  is the enthalpy of the  $j$ -th reaction,  $w_j$  is the rate of the  $j$ -th reaction,  $\rho$  is the density of mixture,  $\varepsilon$  is the fractional void volume.

The model created takes into account catalyst deactivation because of blocking of the active surface by adsorbed coke molecules.

Experimental data of industrial dehydrogenation process obtained on the Kirishy refinery (Russia) were used for computation. The refinery has one dehydrogenation unit. The process flowsheet contains three reactors for each unit.

The unit use Pt catalysts. The structure of Pt catalysts can be described as  $\text{Al}_2\text{O}_3\text{-Pt}$ .

A block of computer programs for calculation of the industrial dehydrogenation unit based on the proposed model has been worked out. Results of computation depend on the technological conditions and raw material quality. Some computational results are presented in Table 1.

The programs also allow: (1) to choose the most efficient process flowsheet for different dehydrogenation variants; (2) to find an optimal construction solutions for nontraditional flow charts; (3) to predict activity and service life of industrial catalysts; (4) to investigate the influence of the raw material composition, moisture and harmful impurities on the dehydrogenation product outcome and its quality; (5) to predict the emergency conditions and

## OP-17

give recommendations for their treatment; (6) to determine conditions which restore the catalytic activity; (7) to evaluate efficiency of different catalysts used in the alkanes dehydrogenation process.

Table 1. Influence of raw material hydrocarbon composition on quality of a product

Components	Content, mass %						
	1	2	3	4	5	6	7
<b>Raw materials</b>							
Paraffin C <sub>9</sub>	0,01	0,01	0,01	0,01	0,01	0,01	0,01
Paraffin C <sub>10</sub>	13,3	10,95	10,76	14,67	11,8	11,69	14,46
Paraffin C <sub>11</sub>	28,93	28,94	32,59	29,14	27,28	28,7	26,23
Paraffin C <sub>12</sub>	24,85	28,91	26	24,79	26,07	28,33	26,3
Paraffin C <sub>13</sub>	19,62	19,75	18,17	19,25	21,57	18,55	19,64
Paraffin C <sub>14</sub>	0,33	0,32	0,43	0,33	0,46	0,29	0,35
Iso-paraffin C <sub>10</sub>	3,77	2,72	3,43	3,17	3,33	3,42	4,05
Iso-paraffin C <sub>11</sub>	0,1	0,09	0,11	0,1	0,1	0,1	0,09
Iso-paraffin C <sub>12</sub>	0,09	0,09	0,09	0,08	0,1	0,1	0,09
Iso-paraffin C <sub>13</sub>	0,07	0,06	0,06	0,06	0,08	0,06	0,07
<b>Products</b>							
Olefines	7,61	7,09	7,2	7,25	7,84	7,5	7,41
Diolefins	0,49	0,44	0,45	0,46	0,51	0,48	0,47
Aromatic hydrocarbons	0,83	0,61	0,7	0,68	0,84	0,77	0,82
Coke	5	7,04	6,62	6,28	4,55	5,68	5,62
Gaseous substances							
C <sub>4</sub>	6,05	5,5	8,55	6,01	6,09	8,23	6,91
Isoparaffins	4,03	2,97	3,68	3,42	3,61	3,68	4,3
Hydrogen, % vol.	93,95	94,5	91,45	93,99	93,91	91,77	93,09

## References

1. G.K Boreskov. Catalysis, Problems of Theory and Practice. Nauka, Novosibirsk 1987 (in Russian).
2. A.V. Kravtsov, E.D. Ivanchina and A.V. Kornienko, React. Kinet. Catal. Lett. 61 (1997) 161.

**EFFECT OF THE STRUCTURAL ARRANGEMENT OF (MoVW)<sub>5</sub>O<sub>14</sub>-BASED  
CATALYSTS ON THEIR CATALYTIC PROPERTIES IN THE REACTION  
OF THE ACROLEIN OXIDATION INTO ACRYLIC ACID**

**Zenkovets G.A.<sup>1</sup>, Kryukova G.N.<sup>2</sup>, Richter K.<sup>2</sup>**

<sup>1</sup>*Boreshkov Institute of Catalysis of SB RAS, pr. Lavrenteva 5, Novosibirsk, 630090, Russia*

<sup>2</sup>*GNF eV, Volmerstrasse 7B, D-12489 Berlin-Adlershof, Germany*

*E-mail: [gnf-berlin@t-online.de](mailto:gnf-berlin@t-online.de)*

The relationship between the structure of (MoVW)<sub>5</sub>O<sub>14</sub>-based catalysts and their catalytic behavior in the reaction of the acrolein oxidation has been studied. It was found that (MoVW)<sub>5</sub>O<sub>14</sub> catalyst possessing nanocrystalline state shows improved activity in this reaction comparing to that of the catalyst with regular structural ordering owing to the higher accessibility of the active centers stabilized inside the channels in the structure of nanocrystalline complex oxide.

### **Introduction**

V-Mo-W-O mixed oxide catalysts, pure and modified with different elements, are characterized by high activity and selectivity in the reaction of acrolein oxidation [1-3]. It was shown that the selectivity for acrylic acid depends on the amount of mixed oxide phase of (MoVW)<sub>5</sub>O<sub>14</sub> type while the structure of this mixed oxide may affect the catalyst activity. This paper reports results of the structural study of catalysts of this composition in relation to their catalytic properties in the reaction of acrolein oxidation.

### **Experimental**

Nanocrystalline and well-ordered single phase (MoVW)<sub>5</sub>O<sub>14</sub> oxide with Mo<sub>0.68</sub>V<sub>0.23</sub>W<sub>0.09</sub> ratios were prepared by spray-drying of the salt solutions followed by thermal treatment of the as-prepared powders. Catalysts have been characterized by using XRD, HRTEM and thermal desorption of acrolein and acrylic acid. Catalytic testing was performed at 290 °C in the reaction mixture of C<sub>3</sub>H<sub>4</sub>O (4%), O<sub>2</sub> (8%), H<sub>2</sub>O (20%), He (rest) at the velocity of 2 ml/sec in the flow reactor. Analysis of all reaction products was carried out chromatographically.

### **Results and discussion**

Fig. 1 shows HRTEM micrographs of (MoVW)<sub>5</sub>O<sub>14</sub> oxide in the regular and nanocrystalline states. As evident from Fig. 1a, single crystals of the well-crystalline ternary oxide is pseudolamellar with alternating layers along [010] direction and have a strongly developed (010) faces. Molybdenum and tungsten ions are in the hexavalent state and coordinated in an octahedral environment. Furthermore, the octahedral sites are partially



## OP-18

occupied by  $V^{4+}$  ions, whereas a highly distorted trigonal pyramidal coordination indicates that the  $V^{5+}$  ions could be accommodated in pentagonal bipyramids of the  $Mo_5O_{14}$  structure, however, displaced away from the center [2-4]. Morphology of nanocrystalline catalyst of the same composition is represented by nanometer-sized (5-7 nm) particles with internal regular  $Mo_5O_{14}$  structure joined into bigger (about 1000 nm)

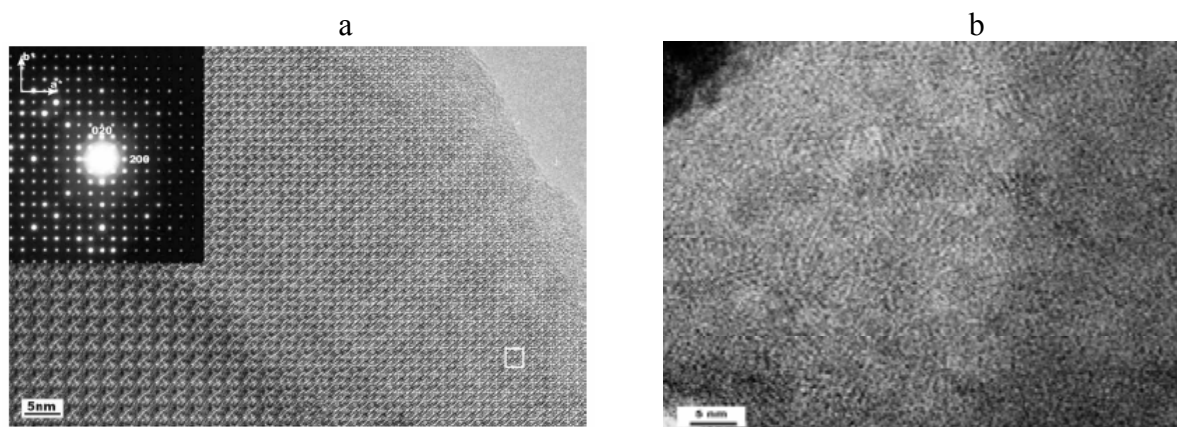


Figure 1. HRTEM micrographs of the structure of regular (a) and nanocrystalline (b)  $(MoVW)_5O_{14}$

aggregates with formation of intergrained boundaries. Oxide structure in the vicinity of these boundaries is highly distorted and looks almost amorphous (Fig. 1b), therefore, it is highly expected that concentration of the active centers in the nanocrystalline oxide will be bigger than those in the catalyst with perfect crystal ordering.

**Table 1.** Catalytic properties of  $(VMoW)_5O_{14}$  catalysts ( $\tau=0.15$  sec).

Type of $(VMoW)_5O_{14}$ structure	Acrolein conversion, %	Selectivity, %	
		$S_{\text{acrylic acid}}$ , %	$S_{\text{CO}+\text{CO}_2}$ , %
Regular	3.7	84.6	13.6
Nanocrystalline	32.3	98.6	1.4

Table 1 lists results of the catalytic testing and provides the evidence that nanocrystalline oxide shows better catalytic properties in the reaction of acrolein oxidation that indicate the small size of the primary oxide particle and their regular internal structure as two features necessary for maintaining of good catalytic properties. Study of these catalysts using thermal desorption method revealed distinctively higher concentration of weakly bounded forms of acrolein and acrylic acid in the case of nanocrystalline oxide that enables us to suggest that activation of the acrolein molecule proceeds on the active centers stabilized in the channels of  $(MoVW)_5O_{14}$  structure.

## Conclusion

Results obtained in this study unambiguously show that structural arrangement (regular or distorted) of  $(\text{MoVW})_5\text{O}_{14}$  catalysts strongly affect their catalytic behaviors in the oxidation reaction of acrolein into acrylic acid.

## References

1. A. Tenten, F.-G. Martin, H. Hibst, L. Marosi, V. Kohl (BASF AG), EP 668104 B 1 (1995).
2. O. Ovsitser, Y. Uchida, G. Mestl, G. Weinberg, A. Blume, M. Dieterle, H. Hibst and R. Schlögl, *J. Mol. Catal. A* 185 (2002) 291.
3. S. Knobl, G.A. Zenkovets, G.N. Kryukova, O. Ovsitser, D. Niemeyer, R. Schlögl, G. Mestl, *J. Catal.* 215 (2003) 177.
4. G.A. Zenkovets, G.N. Kryukova, V.Yu. Gavrilov, S.V. Tsybulya, V.F. Anufrienko, T. Larina, D.F. Khabibulin, O.B. Lapina, E. Roedel, A. Trunschke, T. Ressler, R. Schlögl, *Mater. Chem. Phys.* (in press).

**CATALYTIC ETCHING OF NICKEL IN PROPANE OXIDATION**

**Sorokin A.M., Kaichev V.V., Gladky A.Yu., Rudina N.A., Prosvirin I.P.,  
Bukhtiyarov V.I.**

*Boreskov Institute of Catalysis, Novosibirsk, Russia*

*E-mail: [sorokin@catalysis.ru](mailto:sorokin@catalysis.ru)*

Two stages of morphological changes of the surface of nickel foil in the course of propane oxidation to synthesis-gas are identified by scanning electron microscopy (SEM) and scanning tunneling microscopy (STM).

The phenomenon of catalytic etching (strong morphological changes of metal surfaces) is often observed in catalytic studies. The primary focus of this study is the investigation of the catalytic etching of a nickel foil used as catalyst for propane oxidation. It has been previously found that in mbar pressure range the propane oxidation over nickel occurs in an auto-oscillation regime [1-3]. The oscillations in concentrations of both reactants and product, as well as in temperature, were generally observed in a temperature range of 650-750°C under oxygen-deficient conditions. It was been also found that the stable and repeatable oscillations appear after an induction period of tens minutes, when catalyst did not exhibit a detectable activity in the propane oxidation. When the catalyst is activated, the self-sustained oscillations are observed immediately in the subsequent experiments after temperature reaches a certain critical value. These observations clearly indicate that there are some initial processes on the nickel surface, which are essential for development of the oscillation regime. Operating the catalyst under reaction conditions is accompanied by a strong restructuring of the surface, resulting in development of rough and highly porous structure. Obviously, such modification can lead to significant increasing of the surface area and can changes catalytic activity. In order to obtain detailed information about the reaction-induced morphological changes scanning electron microscopy and scanning tunneling microscopy were used in this study. The catalyst surface before and after exposure of nickel foils to a propane/oxygen mixture was also characterized by X-ray photoelectron spectroscopy (XPS). These data together with kinetics measurements provide new insight into the reaction mechanism of the propane oxidation over nickel catalysts.

Pieces of rectangular nickel foil (0.125×8×10 mm, 99.99 % Ni – Advent Research Materials Ltd) were used as a catalyst for propane oxidation. These pieces denoted as fresh catalysts were preliminary cleaned in a UHV chamber of VG ESCALAB HP spectrometer by

a sequence of ion bombardment ( $\text{Ar}^+$  - 2 keV, 30  $\mu\text{A}$ , 20 min), heating to 1200 K, oxidation at 700 K in  $1 \times 10^{-6}$  mbar  $\text{O}_2$  for 10 minutes, ion bombardment for 3 minutes, followed by a final flash to 1250 K in UHV. After a few cycles, no contaminants were detected by XPS. Three types of catalysts were examined by SEM and STM: the fresh nickel foils, the activated nickel foils which were treated in the propane oxidation for 50 min, and the worked nickel foils which were used in the propane oxidation for 13 h.

SEM shows that the fresh catalyst surface is mainly smooth and flat. Some textural damage caused by the manufacturing process is seen as well. High resolution SEM images show irregular hill-and-valley structures. Flat terraces with an average width of 100-200 nm separated by steps are clearly observed in the STM images. The activated catalyst surface is characterized by randomly spaced irregular pits of  $\sim 300$  nm in diameter and large ( $\sim 1 \mu\text{m}$ ) cavities which cover most of the surface. Furthermore, well-defined terrace structures and crystalline domains are observed in STM images as well. Prolongation of the reaction in auto-oscillation mode forms another type of the surface structures. The surface becomes smoother and large circular islands with a diameter of  $\sim 10 \mu\text{m}$  are observed after several hours of the propane oxidation. At the same time, defects like pinhole and shallow pits are observed on the surface, but with substantially smaller concentration. STM images show also well-defined steps and terraces as well as grain boundary grooves. Based on these observations, intensive faceting of the nickel surface during the oscillation regime can be concluded.

Comparison of the activated catalyst surface with the worked catalyst surface indicates that the catalytic etching of the nickel foil proceeds in two sequential stages, where different surface structures are formed. The first stage which associates with the induction period is the formation of a lot of irregular pits and their coalescence into large cavities. When the oscillation regime starts (second stage), formation of circular islands that accompany with faceting and dissipation of the pits occur. The reasons of these morphological changes are discussed.

We acknowledge with pleasure the support of this work by Russian Foundation for Basic Research, grant No. 04-03-32667.

## References

1. A.Yu. Gladky, V.K. Ermolaev, V.N. Parmon, *Catal. Lett.* 77 (2001) 103.
2. A.Yu. Gladky, V.V. Ustugov, A.M. Sorokin, A.I. Nizovskii, V.N. Parmon, V.I. Bukhtiyarov, *Chem. Eng. J.* 107 (2005) 33.
3. A.Yu. Gladky, V.V. Kaichev, V.K. Ermolaev, V.I. Bukhtiyarov, V.N. Parmon, *Kinet. Catal.* 46 (2005) 251.

**ACTIVE ELECTROCATALYSTS BY MODULAR DESIGN****Roth C.<sup>1</sup>, Mazurek M.<sup>1</sup>, Benker N.<sup>1</sup>, Scott F.J.<sup>2</sup>, Ramaker D.E.<sup>2</sup>**<sup>1</sup>*Institute for Materials Science, TU Darmstadt, Petersenstr. 23, D-64287 Darmstadt*<sup>2</sup>*Chemistry Department, George Washington University, Wash., DC 20052**E-mail: [c\\_roth@tu-darmstadt.de](mailto:c_roth@tu-darmstadt.de)*

A modular design approach has been developed as an alternative way to obtain multi-phasic (electro)catalyst systems by the controlled mixing of different monometallic catalysts. This procedure might be of significant interest for industrial applications, since the catalyst suppliers need only supply the monometallic components and leave it to their customers to assemble the best possible catalyst for their respective application. Moreover, the modular concept allows for an additional degree of freedom, as the catalyst components can be modified individually and independent of each other.

The idea of a modular design approach is best described by combining an arbitrary number of single components into an optimum electrocatalyst system. However, for this concept to work, it must be the case that the products obtained by simply mixing the individual components have an activity comparable to that of the typical “alloyed” multi-phasic catalysts. In the case of carbon-supported Pt-Ru, a prominent system in fuel cell electrocatalysis, it has been shown that a mixture catalyst obtained via the modular approach is as active - or even better - than its partially “alloyed” counterpart. Within this work, a novel Pt/Ru mixture catalyst has been prepared by intimately mixing and grinding respective amounts of a pure carbon-supported Pt and a pure carbon-supported Ru catalyst. The chosen mixing procedure of monometallic catalysts should render more flexibility to the preparation of catalysts, which could thus easily be adjusted to the optimal working conditions. A modular approach is of significant interest for industrial applications - not only with respect to fuel cells - since the producing companies need only supply the monometallic components and leave it to their customers to assemble the catalyst system that suits their application best. Moreover, the modular concept gives an additional degree of freedom, as the catalyst components can be tuned individually, e. g. with respect to their particle size or their degree of oxidation.

The catalyst morphology resulting from the novel mixing procedure has been investigated using X-ray absorption spectroscopy (EXAFS), and the results obtained compared to a traditional “alloyed” Pt-Ru bimetallic electrocatalyst.

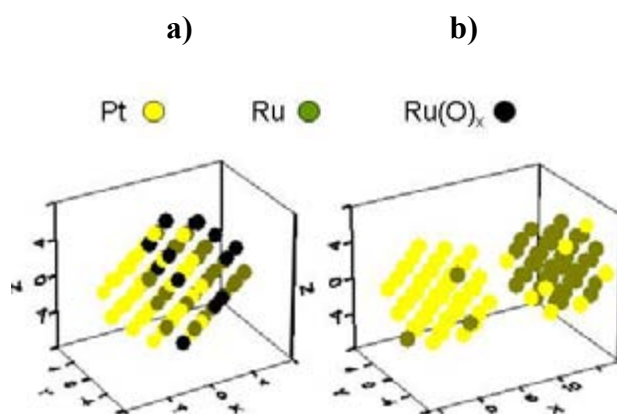


Figure 1. Proposed models for a) Pt-Ru partially “alloyed”, and b) Pt/Ru mixture sample. Black atoms indicate  $\text{Ru(O)}_x$ , green atoms indicate Ru, yellow atoms indicate Pt.

As shown schematically in Figure 1, mechanically mixing the respective amount of carbon-supported Pt and carbon-supported Ru results in Pt nanoparticles with a small Ru surface component and similarly composed Ru particles with some Pt on the surface. The model configuration for the Pt-Ru alloyed sample is composed of 80 atoms, 40 Pt and 40 Ru, with approximately 1/3 of the Ru atoms present as  $\text{Ru(O)}_x$  islands when under fuel cell conditions at 0.4 V vs RHE. This sample appears to be only partially “alloyed” with a relatively small number of Pt-Ru contact sites. In contrast, the Pt/Ru catalyst is a mixture of Pt nanoparticles (50 atoms) with a small (3 atoms) surface Ru substituent, coincident with similar Ru nanoparticles (40 atoms) with a parallel Pt surface component (8 atoms). Obviously, as the coordination numbers predicted by the EXAFS fit are an average per metal atom and as the mechanical mixing method is unlikely to produce completely identical nanoparticles, it is not suggested that this model indicates the full morphological range of the sample.

Taking into account the above results, it is apparent, that in a binary system atoms or clusters of component 1 are transferred onto nanoparticles of component 2 and vice versa by the mixing procedure, thereby creating contact sites between both monometallic components. Consequently, it appears feasible to control the cluster size on the host nanoparticle by an appropriate design of the mixing process. Catalyst design should thus become far more flexible, since nanoparticle sizes of both components can be varied independently by individual heat-treatment, whereas it should be possible to affect the number of contact sites (atoms transferred) by the chosen mixing parameters.

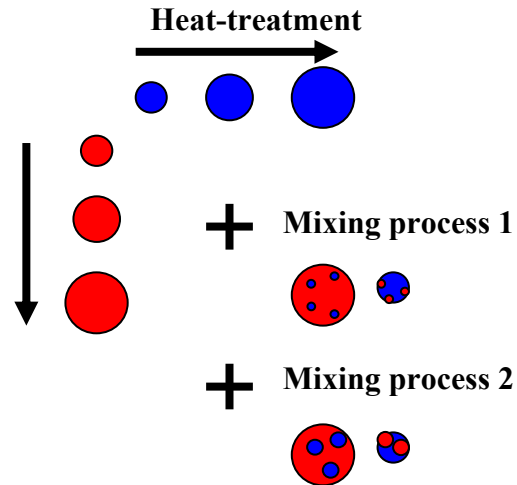


Figure 2. Concept of the modular approach and additional parameters to be controlled; two likely examples are shown.

This concept and its possible implications are pictured schematically in Figure 2. However, further work is required to obtain additional insight into particle size and cluster size effects as well as to learn more about the optimal mixing parameters, which are crucial in a controlled mixing process.

## HYDROISOMERISATION OF *n*-HEXANE ON LAYERED ARRANGEMENTS OF H-ERIONITE AND Pt/Al<sub>2</sub>O<sub>3</sub>

**Frank Roessner, Arne Kuhlmann**

*Industrial Chemistry II, University of Oldenburg, Oldenburg, Germany*

*E-mail: [frank.roessner@uni-oldenburg.de](mailto:frank.roessner@uni-oldenburg.de)*

The mobility of activated hydrogen on the surface can be used to create new catalytic composite catalysts containing different phases. One of them contains the hydrogen activating component whereas the other phase is characterized by acidic centers. Surprisingly, the composite system shows the same catalytic behavior as classical bifunctional catalysts. This effect is explained in terms of the spillover concept.

### **Introduction**

Metal supported zeolites play an important role in bifunctional catalysis. In the early 50ies Mills and Weiz proposed a consecutive model to describe the bifunctionally catalysed conversion of hydrocarbons. According to this model a *n*-alkanes is dehydrogenated to a *n*-olefin on a metal, *e.g.* platinum. Than, it isomerizes on the acidic center and, finally, the *iso*-olefin is hydrogenated on the metal resulting in a saturated *iso*-alkane. The transport between metallic and acidic centers proceeds via gas phase.

However, in the literature a few experiments are described questioning the classical model, especially when both active sites are spatially separated. So, only hydroisomerisation takes place in sandwich-like systems, when both phases are in intimate contact. Otherwise, acidic cracking was observed entirely. The same phenomenon was observed for hydroisomerisation of cyclohexane.

Furthermore, the influence of carrier gas on the conversion of *n*-hexane on bifunctional catalysts cannot be explained satisfactorily. According to the classical mechanism the carrier gas (hydrogen or nitrogen) should not have any influence on the selectivity of the products. Only strong coking could be changed the reaction path. However, the influence of carrier gas was recently demonstrated both in plug flow and recirculation reactors. According to these results hydroisomerisation was observed only in the presence of hydrogen whereas in nitrogen acidic cracking dominated.

Based on these results an extended model including surface diffusion of activated hydrogen was developed to explain the mentioned above results. This model involves the following steps: (i) activation of hydrogen on the metal, (ii) surface diffusion to the acidic



## OP-21

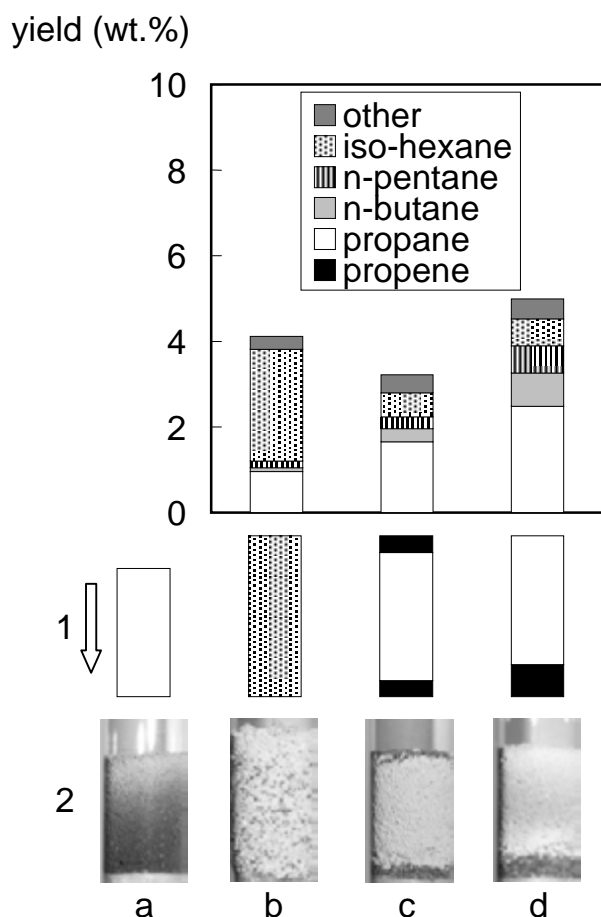


Figure 1. Conversion of n-hexane on different catalyst arrangements in plug flow reactor (50 mL/min  $H_2$ , 573 K). Yields after 3 min time on stream. (1: scheme, 2: image after 240 min time on stream), black:  $Pt/Al_2O_3$ , white: H-erionite, speckled: mechanical mixture).

center and (iii) conversion of hydrocarbon adsorbed preferentially on the acidic center accompanied with consumption of activated hydrogen.

On the acidic H-form coking takes place (Fig. 1, 1a and 2 a). In the presence of metal the coking is suppressed (Fig 1, 1b and 2b). For validation of the extended model different layered arrangements of  $Pt/Al_2O_3$  and Pt/Ilerite and H-erionite were realized (Fig. 1, 1c and 1d).

The key experiment is arrangement (d), where  $Pt/Al_2O_3$  is placed under the layer of H-erionite. The feed passes firstly the zeolite and only after this it contacts the metal containing phase, *i.e.* the first step of the classical mechanism cannot proceed. Nevertheless, the system works bifunctionally and the coking is suppressed. The diffusion zone of the activated hydrogen, even against the

current of the carrier gas, is clearly seen (white zone in Fig. 1, 2d).

This experiment clearly demonstrates the limitation of the classical model for the description of the results obtained by layered arrangement of the monofunctional catalyst components. The application of the extended model opens new routes for synthesis of composite catalyst as demonstrated for application of Pt/ilerite, a layered silicate hosting platinum clusters, in n-hexane conversion. Despite, that platinum was encapsulated in the layered silicate *ilerite*, the mechanical mixture with H-erionite was active in hydroisomerization, what supports the arguments for the extended model.

## REGULATION OF PROPERTIES OF CATALYSTS OF DIMETHYL ETHER CONVERSION TO LIGHT OLEFINS BY ZEOLITES MODIFICATION

**Abramova A.V., Kulumbegov R.V.**

*A.V. Topchiev Institute of Petrochemical Synthesis, Russian Academy of Sciences,  
Moscow, Russia*

*E-mail: [abramova@ips.ac.ru](mailto:abramova@ips.ac.ru)*

Catalytic conversion of dimethyl ether to olefins was investigated using zeolite catalyst ZSM-5 and SAPO-34 type.  $\text{Me}_x\text{O}_y/\text{ZSM-5}/\text{Al}_2\text{O}_3$  (Me = Zn, Fe, Co) catalyst have been obtained. The testing of catalyst in DME conversion has been done in a fixed bed reaction setup at 0.1 MPa, from 350 to 450 °C. Maximum yield of light olefins was received on Zn-catalyst at 350 and 375 °C, thereupon increasing of temperature to 450 °C leads to considerable growth of methane in hydrocarbon gas. The study of the influence of zeolite modification by phosphorus and zirconium has shown that yield of  $\text{C}_2=\text{C}_4=$  most increased under P modification, as well as joint modification by P and Zr. Conversion of DME equals 94-96% at the same time. Zeolite modification by P and Zr changes both general acidity of zeolites and spectrum of acidity and nature of acid sites that leads to changing of activity and selectivity of catalysts. Yield of  $\text{C}_2=\text{C}_4=$  olefins equals ~52-61%,  $\text{C}_2\text{H}_4$  ~12%,  $\text{C}_3\text{H}_6$  ~23-32% and  $\text{C}_4\text{H}_8$  ~16% accordingly. Pentasil-based catalysts are characterized by more high stability. SAPO-34-based catalyst reached comparatively high yields of light olefins  $\text{C}_2=\text{C}_4=$  at temperatures 350-375°C: ~74-83%, of them  $\text{C}_2=$  ~29-35%,  $\text{C}_3=$  ~38-47%,  $\text{C}_4=$  ~7-3% in DME conversion ~96%. Yield of  $\text{C}_{5+}$  hydrocarbons doesn't exceed 1%, and yield of methane ~1% basically.

### Introduction

Natural gas is an alternative source oil to obtain of synfuels and valuable products of the petrochemical synthesis. One of the most rational ways of converting natural gas is its conversion to syngas with the following conversion to the valuable hydrocarbons. Industrial processes of production of light olefins from non-oil raw build up by the Mobil (MTO), UOP and Norsk Hydro, and Lurgi (GTP) on the basis of zeolite catalyst ZSM-5 and SAPO-34 type. [1, 2]. There are investigations of influence of active metal nature, method of metal adding, way of zeolite modification in composition of ZVM-based catalysts and conditions of dimethyl ether conversion on the catalytic activity and yield of light  $\text{C}_2\text{-C}_4$  olefins were conducted at present work.

### Experimental

Commercial zeolite Na-ZVM, analogue of ZSM-5, Nizhniy Novgorod's Sorbents, Russia ( $\text{SiO}_2/\text{Al}_2\text{O}_3=30$ ) was carried over to  $\text{NH}_4^+$ -form by ion-exchange method. The zeolite H-ZVM was obtained by calcination of zeolite  $\text{NH}_4^+$ -form at 500 °C during 6 hours.

## OP-22

Commercial SAPO-34 (Zeolyst) used for experiment. There are catalysts by means of molding zeolite with aluminium hydroxide used as binder and by means of the salts of the active metals injection were obtained. The mixture of aluminium hydroxide, zeolite and solution of II-VIII group metal salt, was repulped mixed constantly in the aqueous suspension, and evaporated until reaching conditions suitable for the extrudates molding. The extrudates were dried up at 110 °C and calcinated at 500 °C during 6 hours.

The zeolite structure was characterized by XRD on diffractometer DRON-3M with a Cu K $\alpha$  radiation with application Si as internal standard. Total acidity and zeolite acidity spectrum were investigated by NH<sub>3</sub>-TPD method. Measurement of acid properties was carried out in Laboratory of kinetics and catalysis at Chair of physical chemistry of Chemical Faculty MSU.

Catalytic properties of synthetic samples were studied on the pilot flowing setup of high pressure with fixed bed. 6 ml catalyst loaded into reactor between layers of quartz. Before testing of catalyst, we carried out priory activation of catalyst. The samples were treatment by hydrogen during 6 hours at 400 °C and atmospheric pressure. Further decrease of temperature to 350 °C and started of DME feeding in N<sub>2</sub> or He. The testing of catalyst in DME conversion have been done at the following conditions: pressure 0.1 MPa, temperatures from 350 to 450 °C,  $v_{N_2} = 4000$  l/l cat\*h,  $v_{DME\ gas} = 500$  l/l cat \*h.

A sampling of products of the reaction was carried out after two hours of experiments at each temperature. The gaseous products analyzed by gas-chromatograph.

## Results and discussion

It is shown, that yield of light olefins C<sub>2</sub>=-C<sub>4</sub>= depends of zeolite type, metal nature and method of its adding to catalyst composition, and also conditions of experiments. Gaseous products of reaction have C<sub>1</sub>-C<sub>8</sub> hydrocarbons, as paraffins, as olefins, with linear and furcated chains. Liquid hydrocarbons practically weren't formed.

Zinc, iron and cobalt catalysts behavior was explored into conversion of DME on the ZVM-based systems. Introduction of metal to catalyst composition leads to increasing of the olefins yield. The comparison of data from sample of non-modified zeolite H-ZVM/Al<sub>2</sub>O<sub>3</sub> and modified by Zn, Fe and Co catalyst in DME conversion shows that nature of the metal in catalyst composition doesn't changed the general nature of the DME conversion dependencies and yield of the target products of reactions, but rendered the significant influence upon factors of the olefins yield. Total yield of light olefins slightly increased with growing of the temperature, but then under 450 °C decreased due to intensive cracking of products for all

samples except of Zn-containing catalyst. Maximum yield of light olefins was received on Zn-catalyst at condition of the comparative test.

The study of the influence of zeolite modification by phosphorus and zirconium has shown that yield of  $C_{2=}$ - $C_{4=}$  at the temperature 350-375 °C most increased under phosphorus modification, as well as joint modification by phosphorus and zirconium, yield of ethylene and propylene has formed near 20%, yield of butenes - 10-12 %. Yield of methane at the temperature before 400 °C didn't exceed 3%. Conversion of DME equals 94-96% at the same time. Zeolite modification by phosphorus and zirconium changes both general acidity of zeolites and spectrum of acidity and nature of acid sites that leads to changing of activity and selectivity of catalysts. Modifying of zeolites by diluted solution of  $H_3PO_4$  leads to chemical interaction of P with zeolite framework without detectable destruction of crystal phase. The processing zeolite by a phosphoric acid has resulted in removal of the strong acid centers, but thus the occurrence of the acid centers of average force is possible at the expense of P-OH groups, located on polyphosphate chains. Modifying of zeolites by solution of  $H_3PO_4$  and zirconyl nitrate leads to chemical interaction of P and Zr with zeolite framework to formation zirconium phosphate chemical bonded with zeolite framework. But thus treatment makes it possible to modify at desirable way the acidic and catalytic properties in the conversion of dimethyl ether to olefins. Pentasil-based catalysts are characterized by more high stability.

SAPO-34-based catalyst at  $v_{N_2} = 1000-2000$  l/cat\*h and temperatures 350-375 °C reached yields of light olefins  $C_{2=}$ - $C_{4=}$ : ~ 75–80%, of them  $C_{2=}$  ~24-30%,  $C_{3=}$  less 37%,  $C_{4=}$  less 14% in DME conversion ~96%. Yield of  $C_{5+}$  hydrocarbons doesn't exceed 1%, and yield of methane ~1% basically.

We acknowledge the financial support of this work by 7th Program for basic researches of Presidium Russian Academy of Sciences and the partial financial support of this work by the Haldor Topsoe as personal PhD grant for support of young talented scientists in Russia.

## References

1. F.J. Keil, *Microporous and Mesoporous Materials* 29 (1999) 49.
2. M. Stöcker, *Microporous and Mesoporous Materials* 29 (1999) 3.

**STUDY OF THE CONNECTION BETWEEN ACIDIC AND CATALYTIC PROPERTIES OF ZEOLITES IN THE DIMERIZATION OF  $\alpha$ -METHYLSTYRENE**

**Grigorieva N.G.<sup>1</sup>, Galyautdinova R.R.<sup>1</sup>, Kutepov B.I.<sup>1</sup>, Dzhemilev U.M.<sup>1</sup>,  
Paukshtis E.A.<sup>2</sup>**

<sup>1</sup>*Institute of Petrochemistry and Catalysis, Ufa, Russia*

<sup>2</sup>*Boreskov Institute of Catalysis, Novosibirsk, Russia*

*E-mail: [ink@anrb.ru](mailto:ink@anrb.ru)*

$\alpha$ -Methylstyrene dimerization was studied on Y, X, Beta, ZSM-12, ZSM-5 zeolites. The acid properties of the zeolites were studied by IR spectroscopy. It was revealed that the catalytic properties of the zeolites in  $\alpha$ -methylstyrene dimerization depend on both acidic and structural characteristics of the catalysts. The highest activity in the reaction was exhibited by Beta zeolite, as the maximum amount of acid sites were found in its structural units (inside channels, on the outer surface). Zeolite ZSM-12 had the highest selectivity for linear dimers.

$\alpha$ -Methylstyrene dimers are known to be practically important oil-producing compounds. Their hydrogenated derivatives are of interest as a base for synthetic oil lubricants, a high-grade plastificators, growth regulators of polymer chains and heat-bearers.

The main products of  $\alpha$ -methylstyrene dimerization on Y, Beta, ZSM-12, ZSM-5 zeolites are linear (4-methyl-2,4-diphenylpent-1- and -2-enes) and cyclic (1,1,3-trimethyl-3-phenylindane) dimers. The amount of trimers does not exceed 15%.

The zeolites can be arranged in the following order in terms of  $\alpha$ -methylstyrene conversion (10wt% catalyst, 80°C): ZSM-5 < 0.50 HNaY<sup>6.0</sup> < 0.96HNaY<sup>6.0</sup>  $\approx$  ZSM-12  $\approx$  Beta.

An increase in temperature and catalyst concentration results in decrease of  $\alpha$ -methylstyrene conversion. The  $\alpha$ -methylstyrene conversion on zeolite ZSM-12 is determined to a great extent by the reaction temperature and on zeolites ZSM-5 and HNaY<sup>6.0</sup> – by the catalyst concentration. The selectivity for dimers also depends on reaction conditions. The selective synthesis of linear dimers (85-90%) on zeolite Beta is possible only at low temperatures (20-40°C) and catalyst concentrations up to 5wt%. For all other test catalysts this temperature consist 60-80°C. An increase in temperature, as well as in the catalyst concentration, results in a sharp decrease in the selectivity for linear dimers and increases the yield of the cyclic dimer.

The catalytic properties of the zeolites in the  $\alpha$ -methylstyrene dimerization depend on both acidic and structural characteristics of the catalysts.

The acid properties of the zeolites, such as nature of acid sites, its concentration and strength, were studied by IR spectroscopy.

From the data obtained it follows that the highest concentration of Brønsted acid sites (BAS) (bridging Al-OH-Si groups in channels, bridging OH groups on the outer surface of crystals, AlOH groups of extra-framework aluminum) is on zeolite Y type: the total concentration of BAS is 220 mmol/g on 0.50HNaY<sup>6.0</sup> and 450 mmol/g on 0.96HNaY<sup>6.0</sup>. The strength of this BAS is 1170-1220 kJ/mol.

On the surface high-silica zeolites Beta, ZSM-12, ZSM-5 are situated only bridging Al-OH-Si groups and strength of this BAS is the same – 1165 kJ/mol. In terms of concentration of this BAS zeolites can be arranged in the following order: Beta (179 mmol/g) > ZSM-5 (135 mmol/g) > ZSM-12 (106 mmol/g). It should be noted the high concentration of Lewis acid sites on Beta zeolite – 370 mmol/g whereas on other catalysts consist 4,9-70 mmol/g. The obtained low catalytic activity of ZSM-5 may mean that either not all acid sites of ZSM-5 are accessible to  $\alpha$ -methylstyrene molecules or the formed products cannot be desorbed onto the outer zeolite surface and block the zeolite channels that contain the main amount of acid OH groups inside. Zeolite ZSM-5 has a porous structure consisting of channels of two types: straight channels with a round 10-membered ring of 0.56 nm in diameter and sinusoidal channels with a pore opening diameter of 0.51×0.55 nm. Obviously, it is difficult for  $\alpha$ -methylstyrene molecules. Which has dimensions of 0.43×0.72 nm, to penetrate inside zeolite channels, and is particularly impossible for  $\alpha$ -methylstyrene dimers to diffuse inside the channels.

It was found that the conversion of  $\alpha$ -methylstyrene increases proportionally to the strength and concentration of BAS. An increase of strength and concentration acid sites results in decrease in selectivity for linear dimers. The different selectivity for linear and cyclic dimers on zeolites is also associated with their porous structure. Apparently, the cyclic dimer more readily forms and diffuses from wide straight channels of Y and Beta zeolites than from narrower channels of ZSM-12. However, the pore size of zeolite ZSM-12 is optimal for the formation and diffusion of linear dimers.

So, it was showed that the catalytic properties of zeolites (0.96HNaY<sup>6.0</sup>, 0.50HNaY<sup>6.0</sup>, Beta, ZSM-12, ZSM-5) in  $\alpha$ -methylstyrene dimerization are determined by differences in concentration and strength of acid sites, as well as by the molecular-sieve properties of the catalysts (channel size, location of acid sites inside the channels or on the outer surface of crystals).

**TARGET MODIFICATION OF ACID PROPERTIES ZEOLITES FOR OBTAINING OF EFFECTIVE CATALYSTS OF n-HEXANE AND FISCHER-TROPSCH SYNTHETIC GASOLINE ISOMERIZATION****Abramova A.V., Panin A.A.***A.V. Topchiev Institute of Petrochemical Synthesis, Moscow, Russia**E-mail: [abramova@ips.ac.ru](mailto:abramova@ips.ac.ru)*

It is shown that dependence of work efficiency and factors of isomerization processes of model and real raw (the product of the Fisher-Tropsch synthesis) from structure and composition of heterogenic zeolite catalysts and way of their modification. The best conditions are determined for optimum run of these catalysts. The presented data point to relationship between efficiency of the catalyst in isomerization of model and real mixtures and its acidity, hanging from chemical structure and composition. Zeolite structure, its nature, quantity and distribution of acid sites on strength in great degree provide isomerization activity of bifunctional heterogenic catalysts. Modification of USY zeolite by boron and phosphorus allows to control of isomerization and cracking activity of modified catalysts.

Natural gas is alternative petroleum raw material for production gasoline and diesel fuels, and also products for petrochemical synthesis. At the first stage natural gas is converted to syngas, at the second stage syngas is converted to hydrocarbons by method of Fischer-Tropsch mainly on iron or cobalt catalysts. Carrying out of Fischer-Tropsch synthesis on bifunctional zeolite catalytic systems unlike traditional metal catalysts is allows to considerably decreasing of high-molecular hydrocarbons C<sub>22+</sub>. The fuel from syngas by Fischer-Tropsch synthesis, is ecologic pure, and doesn't contain sulfur and aromatic hydrocarbons. Application of zeolites in catalyst composition leads to formation of isomers which increasing of octane value in the fuel. However hydrocarbons of gasoline fraction which produced in Fischer-Tropsch synthesis on iron catalysts contain olefins that lower stability of gasolines. The content of isomers in gasoline fraction is not enough for compensation of decreasing of octane value at only hydrogenation of olefins of gasoline fraction. The gasoline fraction which produced in Fischer-Tropsch synthesis on cobalt catalysts contains mainly n-paraffins, and share of isomers is low.

The purpose of the present work consist of investigation of influence of type and content of zeolite (ZSM-5, Y, USY, Beta, mordenite) in composition of Pt-catalysts on isomerization and cracking activity of catalysts in reaction of n-hexane conversion as model raw and gasoline hydrocarbons of Fischer-Tropsch synthesis in real conditions at pressure 3 MPa, temperature 250-400°C, space velocity 1 h<sup>-1</sup>, G.H.S.V. – 2800 l\*cat\*h<sup>-1</sup>.

Zeolites were characterized by XRD, IRS, and TPD  $\text{NH}_3$ . It is shown, that the isomerization activity of bifunctional catalysts are determined substantially by zeolite nature, its content in catalyst composition, temperature of process.

$\text{n-C}_6\text{H}_{14}$  conversion increases with growth of zeolite content and temperature in line  $\text{Y} < \text{MOR} < \beta < \text{ZVM}$  for all catalytic samples. Catalysts, based on the large-pored zeolites Y, USY and Beta shown high  $\text{i-C}_6\text{H}_{14}$  selectivity. Iso- $\text{C}_6$  selectivity grows in line  $\text{Y} > \text{MOR} > \beta > \text{ZVM}$  for catalysts with same content of zeolite. Higher isomerization activity of Y- and  $\beta$ -zeolite based catalysts in comparison with ZVM may be explained by different structural and acidic characteristics of these zeolites.

Using of ultrastable zeolites USY in catalysts composition, modified by solutions of the acids and alkalis, and also phosphorus and boron compounds, provides the more high  $\text{n-C}_6\text{H}_{14}$  conversion, iso- $\text{C}_6$  selectivity and content of 2,3-dimethylbutane in comparison with Y-zeolite based catalyst.

Ultrastable zeolite-based catalysts shows more high cracking activity than Y-based catalyst due to USY zeolite has higher content of strong acid sites as zeolite Y. Catalysts based on non-modified USY and modified by boron and phosphorus have most cracking activity. Probably, such behavior of catalysts is conditioned that most accessibility of acid sites for reacting molecules in non-modified USY in contrast with modified USY.

As we know, modifying of zeolite by boron leads to increasing of Lewis acidity. So, probably, zeolite sample modified by boron and phosphorus has also Lewis acid sites, and as effect of enlargement of cracking catalytic activity.

Ultrastable zeolite-based catalysts modified by boron and phosphorus show more high iso- $\text{C}_6$  selectivity in contrast with non-modified USY due to more high content of acid sites of medium strength, whose provides isomerization activity of zeolites.

USY-B/P modified zeolite sample has maximum of  $\text{n-C}_6\text{H}_{14}$  conversion is 82% at  $300^\circ\text{C}$ , and  $\text{i-C}_6$  selectivity reaches 56%, content of 2,3-dimethylbutane is 10,8%, 2-methylpentane – 33,3%, 3-methylpentane – 18%.

Test of these Pt-catalysts in hydrotreatment of gasoline fractions of Fischer-Tropsch synthesis shown that isomerization of  $\text{C}_5\text{-C}_{10}$  hydrocarbons proceeds on Y, USY and Beta catalysts, while isomerization mainly  $\text{C}_5$  proceeds on ZSM-5 and  $\text{Pt/Al}_2\text{O}_3$  catalyst.

Modified USY based catalysts show most isomerization activity under small cracking. For example,  $\text{i-C}_8/\text{n-C}_8$  rate reaches 6,5 in products of gasoline fractions of Fischer-Tropsch synthesis on USY-modified catalysts, but on Y-based catalysts only 2,4.



## **OP-24**

Zeolite structure, its nature, quantity and distribution of acid sites on strength in great degree provide isomerization activity of bifunctional heterogenic catalysts. Modification of USY zeolite by boron and phosphorus with chemical interaction of modifier and zeolite structure allows to control of nature, quantity and distribution of acid sites and, consequently, isomerization and cracking activity of modified zeolite based catalysts.

Laws installed for model reaction of n-hexane isomerization, correlate with results, obtained on real gasoline fraction of Fisher-Tropsch synthesis.

## WET PEROXIDE OXIDATION OF ORGANIC POLLUTANTS IN AQUEOUS MEDIA IN PRESENCE OF CARBON MATERIALS

**Pestunova O., Ogorodnikova O., Kuznetsov V., Moseenkov S.**

*Boreskov Institute of Catalysis, Novosibirsk, Russia*

*E-mail: [oxanap@catalysis.ru](mailto:oxanap@catalysis.ru)*

Comparative study of the H<sub>2</sub>O<sub>2</sub> destruction and adsorption of phenol and ethanol and their oxidation by H<sub>2</sub>O<sub>2</sub> in the presence of various carbon materials (nano-diamonds (ND), onion-like carbon (OLC), porous graphite-like carbon Sibunit and catalytic filamentous carbon (CFC)) and/or Fe<sup>3+</sup> salts was carried out. Influence of carbon morphology on the process of oxidation and the mechanism of this influence will be discussed.

### **Introduction**

Adsorption by active carbons is widely used in processes of purification of wastewater from toxic organic compounds. However the adsorption only provides the transfer of toxic substances from one phase into another, and does not destruct adsorbed molecules. It seems very promising to combine the sorption and destruction of sorbate through catalytic oxidation (for example with H<sub>2</sub>O<sub>2</sub>) [1]. The development of such complex processes requires clear understanding of how the presence of a carbon material affects various stages of the process.

In the literature, this problem is interpreted in three different manners. 1) The pure carbon materials can catalyze oxidation of organic substrates in aqueous solutions by hydrogen peroxide [2,3]. 2) The presence of active carbon and adsorption of substrate on its surface increases the rate of the oxidation reaction catalyzed by transition metals [4,5]. 3) Point of view is quite the contrary, i.e. carbon in the solution is thought to behave as a free radical scavenger, hence, to slow down free-radical oxidation processes [6].

In these works, because of their applied nature, the active carbon produced from natural raw materials and, therefore, containing transition metal impurities in significant amounts were used that could lead to inaccurate conclusions about the intrinsic catalytic activity of carbon. Actually, these carbon materials were obtained from different sources; they had rather complex structure, apparently various in different works. This can explain distinction in the conclusions.

This work is aimed to answer the above questions. For this purpose influence of various types of carbon materials on kinetics of H<sub>2</sub>O<sub>2</sub> destruction and oxidation of model substrates by hydrogen peroxide at presence of carbon materials and/or salts Fe is regularly investigated.

## OP-25

The principal moment of our research was that we used the "pure" synthetic carbon materials free of metals impurities. The morphology and an electronic structure of these carbon materials were appreciably different.

We chose well-known reactions of oxidation of phenol and ethanol with hydrogen peroxide as model reactions. Adsorption of these substrates and kinetics of their oxidation were studied.

### Experimental

Following carbon materials have been used in this work. 1) Detonation nano-diamonds (ND) containing mainly oxygenate surface groups in total amount 0.025 mmol/g. ( $sp^3$ -carbon material).  $S_{BET} = 345 \text{ m}^2/\text{g}$ . 2) Onion-like carbon (OLC) was prepared via ND thermal heating in vacuum and consisting of defective closed graphite shells enclosed each other ( $sp^2$ -carbon).  $S_{BET} = 582 \text{ m}^2/\text{g}$ . 3) Porous graphite-like carbon Sibunit-4 ( $sp^2$ -carbon).  $S_{BET} = 588 \text{ m}^2/\text{g}$ . This material is produced via hydrocarbons pyrolysis and therefore it contains few amount of impurities of transition metals ( $C(Fe) < 0.02$  weight. %). 4) Two types of catalytic filamentous carbon (CFC) ( $sp^2$ -carbon).  $S_{BET} = 119$  and  $194 \text{ m}^2/\text{g}$ . Carbon morphology was characterized by TEM and nitrogen adsorption. Quantity and chemical nature of surface groups on the surface of ND were studied with IR-spectroscopy. Acid-base titration according [7] was used for estimation of amount and nature of species on the surface of Sibunit.

The conditions of the experiments are listed in Table.

Reaction	$C_C$ (g/L)	$C_{\text{substrate}}$ (mol/L)	$C_{\text{H}_2\text{O}_2}$ (mol/L)	$C_{\text{Fe}^{3+}}$ (mol/L)	$t$ ( $^{\circ}\text{C}$ )	pH
EtOH adsorption	250	0.01	0	0	30	3
PhOH adsorption	5	0.01	0	0	21	6
EtOH oxidation	5	0.01	0.06	$5 \cdot 10^{-4}$	30	3
PhOH oxidation	5	0.01	0.7	$1 \cdot 10^{-4}$	30	3
	“	“	0.2	$5 \cdot 10^{-5}$	50	6

### Results and discussion

*Adsorption properties.* The results obtained show ND containing only  $sp^3$ -carbon and surface species ( $-\text{COOH}$ ,  $-\text{COC}-$ ,  $-\text{COH}$ ,  $-\text{C=O}$ ) does not noticeably adsorb neither phenol nor ethanol. Graphite-like  $sp^2$ -carbon samples (Sibunit-4, OLC, ND) have adsorbability proportional to  $S_{BET}$  which are higher for phenol and lower for ethanol.

*Catalytic activity of carbon.* ND and Sibunit were found to be inactive to oxidation of EtOH in absence of iron. OLC and CFC have very low activity in this reaction. Conversion of ethanol was about 90% after 70 and 110 hours, respectively. All carbon samples have shown very low catalytic activity in PhOH oxidation. 90% conversion of PhOH was after 150 hours for Sibunit and 650 hours for ND, OLC and CFC.

*Oxidation with  $Fe^{3+}$  & C.* In case of oxidation catalyzed by homogeneous  $Fe^{3+}$ -ions the conversion ~90% was achieved after 170 min for ethanol and 30 min for phenol. Outstanding results were obtained for ethanol oxidation in presence of carbon samples. The rate of the reaction decreases in the presence of ND in the solution but increases in the presence of all  $sp^2$ -carbon samples (Sibunit, OLC, CFC). More complex effect of Sibunit, OLC and CFC was revealed in case on phenol oxidation. No influence or minor acceleration was observed for high  $H_2O_2$  concentration (0.7 M,  $C_{PhOH}/C_{H_2O_2} = 1/70$ ) and  $t = 30^\circ C$ . Deceleration was monitored for lower concentration of  $H_2O_2$  (0.2 M,  $C_{PhOH}/C_{H_2O_2} = 1/20$ ) and  $t = 50^\circ C$ .

### Conclusions

Adsorbability of carbon material strongly depends on the electron configuration of carbon. This is essentially lower for  $sp^3$ - carbon in comparison with  $sp^2$ - carbon despite of comparable amount of surface species. All types of carbon samples are inactive or low-active to oxidation of both phenol and ethanol in absence of iron. Presence of  $sp^3$ -carbon slows down oxidation as phenol as ethanol catalyzed by  $Fe^{3+}$ . It is possibly due to surface oxygenate species behaving as a free radical scavenger.  $sp^2$ - carbon can both decelerate free-radical oxidation and to accelerate it depending on reaction conditions. Acceleration apparently is caused by ability to transfer electron due to  $\pi$ -conjugation in graphene layer [8].

### Acknowledgements

This research was supported by the RFBR (grants 05-03-22004, 05-03-32995, 06-03-32969).

### References

1. L.C. Toledo, A.C.B. Silva, R. Augusti, R.M. Lago, Chemosphere 50 (2003) 1049.
2. N.H. Ince, I.G. Apikiyan, Wat. Res. 34 (2000) 4169.
3. J.M. Austin, T. Groenewald, M. Spiro, JCS, Dalton (1980) 854.
4. F. Lücking, H. Köser, M. Jank, A. Ritter, Wat. Res. 32 (1998) 2607.
5. A.A. Ryazantsev, A.A. Batoeva, D.B. Zhalsanova, Patent Russian Federation No. 2135419 (1999).
6. A. Georgi, F.-D. Kopinke, Appl. Catal. B 58 (2005) 9.
7. C.A. Toles, W.E. Marshal, M.M. Johns, Carbon 37 (1999) 1207.
8. V.V. Strelko, N.T. Kartel, I.N. Dukhno, et al., Surf. Sci. 548 (2004) 281.

## LIST OF PARTICIPANTS

### **Abramova Anna V.**

A.V. Topchiev Institute of Petrochemical  
Synthesis, RAS  
Leninsky Prosp., 29  
119991 Moscow

#### **Russia**

**Tel.:** +7(495) 955 41 24

**Fax:** +7(495) 954 47 98

**E-mail:** [panin@jps.ac.ru](mailto:panin@jps.ac.ru)

### **Arrigo Rosa**

Fritz-Haber-Institut  
der Max-Planck-Gesellschaft  
Faraday weg, 4-6  
14195 Berlin

#### **Germany**

**Tel.:** +49(30) 8413 4482

**E-mail:** [arrigo@fhi-berlin.mpg.de](mailto:arrigo@fhi-berlin.mpg.de)

### **Beck Irene E.**

Boreskov Institute of Catalysis, SB RAS  
Prosp. Akad. Lavrentieva, 5  
630090 Novosibirsk

#### **Russia**

**Tel.:** +7(383) 326 94 60

**Fax:** +7(383) 330 80 56

**E-mail:** [beck@catalysis.ru](mailto:beck@catalysis.ru)

### **Bukhtiyarov Valerii I.**

Boreskov Institute of Catalysis, SB RAS  
Prosp. Akad. Lavrentieva, 5  
630090 Novosibirsk

#### **Russia**

**Tel.:** +7(383) 330 67 71

**Fax:** +7(383) 330 80 56

**E-mail:** [vib@catalysis.ru](mailto:vib@catalysis.ru)

### **Elokhin Vladimir I.**

Boreskov Institute of Catalysis, SB RAS  
Prosp. Akad. Lavrentieva, 5  
630090 Novosibirsk

#### **Russia**

**Tel.:** +7(383) 330 97 70

**Fax:** +7(383) 330 80 56

**E-mail:** [elokhin@catalysis.ru](mailto:elokhin@catalysis.ru)

### **Fetisova Veronika A.**

Tomsk Polytechnical University  
Lenina street, 30  
634050 Tomsk

#### **Russia**

**Tel.:** +7(3822) 56 34 43

**Fax:** +7(3822) 56 34 35

**E-mail:** [v1205f@list.ru](mailto:v1205f@list.ru)

### **Gieshoff Juergen**

Umicore AG & Co. KG  
Rodenbacher Chaussee, 4  
63457 Hanau

#### **Germany**

**Tel.:** +49(6181) 59 28 32

**Fax:** +49(6181) 59 37 15

**E-mail:** [juergen.gieshoff@eu.umicore.com](mailto:juergen.gieshoff@eu.umicore.com)

### **Golovleva Anna V.**

Boreskov Institute of Catalysis  
Prosp. Akad. Lavrentieva, 5  
630090 Novosibirsk

#### **Russia**

**Fax:** +7(383) 330 80 56

**E-mail:** [gav@catalysis.ru](mailto:gav@catalysis.ru)

### **Gorodetskii Vladimir V.**

Boreskov Institute of Catalysis, SB RAS  
Prosp. Akad. Lavrentieva, 5  
630090 Novosibirsk

#### **Russia**

**Tel.:** +7(383) 339 73 15

**Fax:** +7(383) 330 80 56

**E-mail:** [gorodetsk@catalysis.ru](mailto:gorodetsk@catalysis.ru)

### **Grigorieva Nelli G.**

Institute of Petrochemistry and Catalysis, RAS  
Prosp. Oktyabrya, 141  
450075 Ufa

#### **Russia**

**Tel.:** +7(3472) 31 27 50

**Fax:** +7(3472) 31 27 50

**E-mail:** [greg-79@mail.ru](mailto:greg-79@mail.ru)

### **Gürtler Christoph**

Bayer Material Science AG, BMS-SIP-CAT  
Leverkusen, B211

#### **Germany**

**Tel.:** +49(214) 30 217 71

**Fax:** +49(214) 30 285 64

**E-mail:** [christoph.guertler@bayermaterialscience.com](mailto:christoph.guertler@bayermaterialscience.com)

### **Häevecker Michael**

Fritz-Haber-Institut der MPG  
Faradayweg, 4-6  
14195 Berlin

#### **Germany**

**Tel.:** +49(30) 8413 4422

**Fax:** +49(30) 8413 4401

**E-mail:** [mh@fhi-berlin.mpg.de](mailto:mh@fhi-berlin.mpg.de)

**Kaichev Vasilii V.**

Boreskov Institute of Catalysis, SB RAS  
Prosp. Akad. Lavrentieva, 5  
630090 Novosibirsk

**Russia**

**Tel.:** +7(383) 339 72 86

**Fax:** +7(383) 330 80 56

**E-mail:** [vvk@catalysis.ru](mailto:vvk@catalysis.ru)

**Kalinkin Alexander V.**

Boreskov Institute of Catalysis, SB RAS  
Prosp. Akad. Lavrentieva, 5  
630090 Novosibirsk

**Russia**

**Tel.:** +7(383) 339 73 53

**Fax:** +7(383) 330 80 56

**E-mail:** [avkalinkin@mail.ru](mailto:avkalinkin@mail.ru)

**Kazansky Vladimir B.**

Zelinsky Institute of Organic Chemistry, RAS  
Leninsky prosp., 47  
117913 Moscow

**Russia**

**Tel.:** +7(495) 137 74 00

**E-mail:** [vbk@ioc.as.ru](mailto:vbk@ioc.as.ru)

**Knop-Gericke Axel**

Fritz-Haber-Institut der Max-Planck-Society,  
Dept. Inorganic Chemistry  
Faradayweg, 4-6  
14195 Berlin

**Germany**

**Tel.:** +49(30) 8413 44 22

**Fax:** +49(30) 8413 44 05

**E-mail:** [knop@fhi-berlin.mpg.de](mailto:knop@fhi-berlin.mpg.de)

**Kryukova Galina N.**

GNF eV  
Volmerstrasse, 7B  
D-12489 Berlin-Adlershof

**Germany**

**E-mail:** [gnf-berlin@t-online.de](mailto:gnf-berlin@t-online.de)

**Lercher Johannes A.**

Technische Universitet Muenchen,  
Institut fuer Technische Chemie  
Lichtenbergstr., 4  
D-85748 Garching

**Germany**

**Tel:** +49(89) 289 135 40

**Fax:** +49(89) 289 135 44

**E-mail:** [johannes.lercher@ch.tum.de](mailto:johannes.lercher@ch.tum.de)

**Lindner Stefan**

Bayer Material Science AG, BMS-NB-NT  
Leverkusen, B211  
51368 **Germany**

**Tel:** +49(214) 30 445 43

**Fax:** +49(214) 30 96 344 34

**E-mail:** [stefan.lindner@bayerbms.com](mailto:stefan.lindner@bayerbms.com)

**Mamash Elena A.**

Tuvinian Institute for Exploration  
of Natural Resources, SB RAS  
Internatsionalnaya, 117-a  
667000 Kyzyl

**Russia**

**E-mail:** [m\\_elen@rambler.ru](mailto:m_elen@rambler.ru)

**Martyanov Oleg N.**

Boreskov Institute of Catalysis, SB RAS  
Prosp. Akad. Lavrentieva, 5  
630090 Novosibirsk

**Russia**

**Tel.:** +7(383) 330 87 67

**Fax:** +7(383) 330 80 56

**E-mail:** [oleg@catalysis.ru](mailto:oleg@catalysis.ru)

**Matveev Andrey V.**

Boreskov Institute of Catalysis, SB RAS  
Prosp. Akad. Lavrentieva, 5  
630090 Novosibirsk

**Russia**

**Tel.:** +7(383) 339 73 15

**Fax:** +7(383) 330 80 56

**E-mail:** [matveev@catalysis.ru](mailto:matveev@catalysis.ru)

**Mitina Liudmila M.**

International Science and Technology Center  
Krasnoproletarskaya ul., 32-34  
127473 Moscow

**Russia**

**Tel.:** +7(495) 982 31 85

**Fax:** +7(495) 978 36 03

**E-mail:** [mitina@istc.ru](mailto:mitina@istc.ru)

**Mleczko Leslaw**

Bayer Technology Services GmbH  
Leverkusen, E 41  
51368 **Germany**

**Tel.:** +49(214) 30 239 20

**Fax:** +49 (214) 30 502 61

**E-mail:** [leslaw.mleczko@bayertechnology.com](mailto:leslaw.mleczko@bayertechnology.com)

**Mutas Inna Yu.**

Boreskov Institute of Catalysis, SB RAS  
Prosp. Akad. Lavrentieva, 5  
630090 Novosibirsk

**Russia**

**Tel.:** +7 (383) 339 72 93

**Fax:** +7(383) 330 62 97

**E-mail:** [mutas@catalysis.ru](mailto:mutas@catalysis.ru)

**Nartova Anna V.**

Boreskov Institute of Catalysis, SB RAS  
Prosp. Akad. Lavrentieva, 5  
630090 Novosibirsk

**Russia**

**Tel.:** +7(383) 339 72 64

**Fax:** (383) 330 80 56

**E-mail:** [nartova@catalysis.ru](mailto:nartova@catalysis.ru)

**Nasluzov Vladimir**  
Institute of Chemistry and Chemical  
Technology, SB RAS  
ul. Marxa, 42  
660042 Krasnoyarsk  
**Russia**  
**Tel.:** +7(3912) 23 93 19  
**E-mail:** [nasluzova@4net.ru](mailto:nasluzova@4net.ru)

**Panin Alexander A.**  
A.V. Topchiev Institute of Petrochemical  
Synthesis, RAS  
Leninsky prosp., 29  
119991 Moscow  
**Russia**  
**Tel.:** +7(495) 955 41 24  
**Fax:** +7(495) 954 47 98  
**E-mail:** [panin@jps.ac.ru](mailto:panin@jps.ac.ru)

**Pestunova Oxana P.**  
Boreskov Institute of Catalysis, SB RAS  
Prosp. Akad. Lavrentieva, 5  
630090 Novosibirsk  
**Russia**  
**Tel.:** +7(383) 330 75 63  
**Fax:** +7(383) 330 80 56  
**E-mail:** [oxanap@catalysis.ru](mailto:oxanap@catalysis.ru)

**Popkova Vera Ya.**  
AO Bayer  
B. Tryokhgornyy per., 1, build. 1  
123022 Moscow  
**Russia**  
**Tel.:** +7(495) 234 20 36  
**Fax:** +7(495) 234 20 04  
**E-mail:** [vera.popkova.vp@bayer-ag.de](mailto:vera.popkova.vp@bayer-ag.de)

**Roessner Frank**  
University of Oldenburg,  
Institute of Pure and Applied Chemistry  
Ammerlaender Heerstr., 114-118  
D-26111 Oldenburg  
**Germany**  
**Tel.:** +49(441) 798 33 55  
**Fax:** +49(441) 798 33 60  
**E-mail:** [frank.roessner@uni-oldenburg.de](mailto:frank.roessner@uni-oldenburg.de)

**Rostovshchikova Tatyana N.**  
Lomonosov Moscow State University,  
Chemistry Department  
Vorobievyy Gory  
119899 Moscow  
**Russia**  
**Tel.:** +7(495) 939 34 98  
**Fax:** +7(495) 932 88 46  
**E-mail:** [rtn@kinet.chem.msu.ru](mailto:rtn@kinet.chem.msu.ru)

**Roth Christina Maria**  
TU Darmstadt  
Petersenstr., 23  
64287 Darmstadt  
**Germany**  
**Tel.:** +49(61) 51 164 391  
**Fax:** +49(61) 51 166 377  
**E-mail:** [c\\_roth@tu-darmstadt.de](mailto:c_roth@tu-darmstadt.de)

**Savinova Elena R.**  
Boreskov Institute of Catalysis, SB RAS  
Prosp. Akad. Lavrentieva, 5  
630090 Novosibirsk  
**Russia**  
**Tel.:** +7(383) 330 75 63  
**E-mail:** [elensav@catalysis.ru](mailto:elensav@catalysis.ru)

**Schlögl Robert**  
Fritz-Haber-Institut  
der Max-Planck-Gesellschaft  
Faradayweg, 4-6  
14195 Berlin  
**Germany**  
**Tel.:** +49(30) 8413 44 00  
**Fax:** +49(30) 8413 44 01  
**E-mail:** [acsek@fhi-berlin.mpg.de](mailto:acsek@fhi-berlin.mpg.de)

**Shaikhutdinov Shamil K.**  
Fritz-Haber-Institut  
der Max-Planck-Gesellschaft  
Faradayweg, 4-6  
14195 Berlin  
**Germany**  
**Tel.:** +49(30) 8413 41 14  
**Fax:** +49(30) 8413 44 01  
**E-mail:** [shaikhutdinov@fhi-berlin.mpg.de](mailto:shaikhutdinov@fhi-berlin.mpg.de)

**Shiryaev Alexandr**  
Umicore Automotive Catalysts  
ul. Gubkina, 14, office 96  
117312 Moscow  
**Russia**  
**Tel.:** +7(495) 244 38 28, +7(495) 244 40 27,  
916-805 89 75  
**Fax:** +7(495) 926 58 88  
**E-mail:** [alex.service@list.ru](mailto:alex.service@list.ru)

**Shor Elena**  
Institute of Chemistry and Chemical  
Technology, SB RAS  
ul. Marxa, 42  
660042 Krasnoyarsk  
**Russia**  
**E-mail:** [ei@icct.ru](mailto:ei@icct.ru)

**Sorokin Alexei M.**

Boreskov Institute of Catalysis, SB RAS  
Prosp. Akad. Lavrentieva, 5  
630090 Novosibirsk

**Russia**

**Tel.:** +7(383) 339 72 64

**E-mail:** [sorokin@catalysis.ru](mailto:sorokin@catalysis.ru)

**Spiridonov Alexei A.**

Boreskov Institute of Catalysis, SB RAS  
Prosp. Akad. Lavrentieva, 5  
630090 Novosibirsk

**Russia**

**Tel.:** +7(383) 326 97 15

**E-mail:** [spiridonov@catalysis.ru](mailto:spiridonov@catalysis.ru)

**Stakheev Aleksandr Yu.**

Zelinsky Institute of Organic Chemistry, RAS  
Leninsky Pr., 47  
119991 Moscow

**Russia**

**Tel.:** +7(495) 135 63 42

**Fax:** +7(495) 137 29 35

**E-mail:** [st@ioc.ac.ru](mailto:st@ioc.ac.ru)

**Startseva Lyudmila Ya.**

Boreskov Institute of Catalysis, SB RAS  
Prosp. Akad. Lavrentieva, 5  
630090 Novosibirsk

**Russia**

**Tel./Fax:** +7(383) 330 62 97

**E-mail:** [star@catalysis.ru](mailto:star@catalysis.ru)

**Sudakov Ivan A.**

Ural State University, Physics Department  
Lenin ave., 51  
620083 Ekaterinburg

**Russia**

**Tel./Fax:** +7(343) 261 67 78

**E-mail:** [ivan.sudakov@e1.ru](mailto:ivan.sudakov@e1.ru)

**Telegina Natalia S.**

Zelinsky Institute of Organic Chemistry, RAS  
Leninsky Pr., 47  
119991 Moscow

**Russia**

**Tel.:** +7(495) 135 63 42

**Fax:** +7(495) 137 29 35

**E-mail:** [nt@ioc.ac.ru](mailto:nt@ioc.ac.ru)

**Votsmeier Martin**

Umicore AG & Co. KG  
Rodenbacher Chaussee, 4  
63457 Hanau

**Germany**

**Tel.:** +49(6181) 59 23 11

**Fax:** +49(6181) 59 37 15

**E-mail:** [martin.votsmeier@eu.umicore.com](mailto:martin.votsmeier@eu.umicore.com)

**Wiese Klaus-Diether**

Leiter FE Projekte  
OXENO Olefinchemie GmbH  
Paul-Baumann-Strasse, 1  
D-45772 Marl

**Germany**

**Tel.:** +49(2365) 49 20 87

**Fax:** +49(2365) 49 62 15

**E-mail:** [klaus-diether.wiese@degussa.com](mailto:klaus-diether.wiese@degussa.com)

**Wolf Aurel**

Bayer Technology Services GmbH  
Leverkusen, E 41  
51368 **Germany**

**Tel.:** +49(214) 30 61 102

**Fax:** +49(214) 30 50 261

**E-mail:** [aurel.wolf.aw@bayertechnology.com](mailto:aurel.wolf.aw@bayertechnology.com)

**Yudanov Ilya V.**

Boreskov Institute of Catalysis, SB RAS  
Prosp. Akad. Lavrentieva, 5  
630090 Novosibirsk

**Russia**

**Tel./Fax:** +7(383) 330 60 64

**E-mail:** [ilya@catalysis.ru](mailto:ilya@catalysis.ru)

**Zhang Aihua**

Fritz Haber Institute of Max Planck Society,  
Department of Inorganic Chemistry  
Faradayweg, 4-6  
14195 Berlin

**Germany**

**Fax:** +49(30) 8413 4401

**E-mail:** [aihua@fhi-berlin.mpg.de](mailto:aihua@fhi-berlin.mpg.de)

**Zamulina Tatiana V.**

Boreskov Institute of Catalysis, SB RAS  
Prosp. Akad. Lavrentieva, 5  
630090 Novosibirsk

**Russia**

**Tel./Fax:** +7(383) 330 62 97

**E-mail:** [zam@catalysis.ru](mailto:zam@catalysis.ru)

**Zilberberg Igor L.**

Boreskov Institute of Catalysis, SB RAS  
Prosp. Akad. Lavrentieva, 5  
630090 Novosibirsk

**Russia**

**Tel.:** +7(383) 333 05 53

**E-mail:** [I.L.Zilberberg@catalysis.ru](mailto:I.L.Zilberberg@catalysis.ru)



## CONTENT

<b>PLENARY LECTURES</b> .....	3
<b>PL-1</b> <b>Zilberberg I.L.</b> OXYGEN ELECTRONIC STATES ON THE SURFACE OF CATALYSTS: A QUANTUM-CHEMICAL VIEW .....	4
<b>PL-2</b> <b>Shaikhutdinov S.K.</b> TOWARDS AN UNDERSTANDING OF STRUCTURE-REACTIVITY RELATIONSHIPS IN CATALYSIS: MODEL STUDIES .....	5
<b>PL-3</b> <b>Kazansky V.B., Subbotina I.R., Jentoft F.C., Schlögl R.</b> INTENSITIES OF IR STRETCHING BANDS AS A NEW SPECTRAL CRITERION OF CHEMICAL ACTIVATION OF ADSORBED MOLECULES VIA THEIR POLARIZATION BY THE ACTIVE SITES IN THE ACID HETEROGENEOUS CATALYSIS .....	6
<b>PL-4</b> <b>Hävecker M., Teschner D., Vass E., Knop-Gericke A., Zafeiratos S., Gabasch H., Schnörch P., Schlögl R.</b> THE ROLE OF SUBSURFACE SPECIES IN HETEROGENEOUS CATALYTIC REACTIONS .....	8
<b>PL-5</b> <b>Lercher J.A.</b> ACTIVATING LIGHT ALKANES – NEW OPPORTUNITIES THROUGH MOLECULAR UNDERSTANDING .....	10
<b>PL-6</b> <b>Savinova E.R.</b> APPLICATION OF IN SITU METHODS FOR THE INVESTIGATION OF ELECTROCATALYTIC REACTIONS .....	13
<b>PL-7</b> <b>Stakheev A.</b> REVEALING STRUCTURE-ACTIVITY RELATIONSHIP IN SUPPORTED METAL CATALYSTS BY ANALYSIS OF XPS LINE SHAPE .....	15
<b>ORAL PRESENTATIONS</b> .....	16
<b>OP-1</b> <b>Yudanov I.V., Neyman K.M., Rösch N.</b> QUANTUM CHEMICAL MODELING OF NANOSIZED TRANSITION METAL CATALYSTS: DENSITY FUNCTIONAL CALCULATIONS OF Pd AND Cu NANOCCLUSERS .....	17
<b>OP-2</b> <b>Martyanov O.N., Risse T., Freund H.-J.</b> ON THE IMPACT OF Pd ON THE MAGNETIC PROPERTIES OF Co PARTICLES ON A THIN ALUMINA FILM ON NiAl(110) .....	19
<b>OP-3</b> <b>Kalinkin A.V., Smirnov M.Yu., Bukhtiyarov V.I.</b> THE OXIDATION OF RHODIUM SUPPORTED ON ALUMINA IN REACTION WITH NO <sub>x</sub> STUDIED BY XPS .....	22
<b>OP-4</b> <b>Shor E.I., Shor A.M., Laletina S.M., Shulimovich T.A., Nasluzov V.A., Rösch N.</b> MODELING ACTIVE CENTERS ON OXIDE SURFACES IN CLUSTER APPROACH OF DENSITY FUNCTIONAL METHOD .....	25

<b>OP-5</b> <b><u>Nartova A.V., Beck I.E., Bukhtiyarov A.V., Kvon R.I., Bukhtiyarov V.I.</u></b> STM AND XPS STUDY OF Pt/Al <sub>2</sub> O <sub>3</sub> AND Pt-Sn/Al <sub>2</sub> O <sub>3</sub> MODEL CATALYSTS PREPARED BY “WET CHEMISTRY” METHODS ON ALUMINA THIN FILMS .....	28
<b>OP-6</b> <b><u>Elokhin V., Kovalyov E., Myshlyavtsev A.</u></b> SIMULATION OF CATALYTIC PROCESSES OVER METAL NANOPARTICLES: STATE OF THE ART .....	31
<b>OP-7</b> <b><u>Rostovshchikova T.N., Smirnov V.V., Lokteva E.S., Gurevich S.A., Kozhevin V.M., Mitina L.M.</u></b> NEW CATALYSTS BASED ON ENSEMBLES OF NANOPARTICLES: FROM MODEL TO REAL CATALYSIS .....	34
<b>OP-8</b> <b><u>Beck I.E., Pakharukov I.V., Kriventsov V.V., Zaikovskiy V.I., Nartova A.V., Parmon V.N., Bukhtiyarov V.I.</u></b> SIZE-DEPENDENT CATALYTIC BEHAVIOR OF ALUMINA-SUPPORTED PLATINUM NANOPARTICLES IN COMPLETE OXIDATION OF METHANE .....	37
<b>OP-9</b> <b><u>Matveev A.V., Weststrate C.J., Sametova A.A., Gorodetskii V.V., Nieuwenhuys B.E.</u></b> OXYGEN REACTIVITY IN CO OXIDATION ON STEPPED Rh(410) AND Pt(410) SURFACES .....	40
<b>OP-10</b> <b>Zhang Aihua</b> CO OXIDATION AT GRAPHITE EDGES: A THEORETICAL STUDY .....	43
<b>OP-11</b> <b><u>Gorodetskii V.V., Elokhin V.I., Nieuwenhuys B.E.</u></b> FIELD ELECTRON AND FIELD ION MICROSCOPY IMAGING OF CATALYTIC SURFACE REACTIONS ON PLATINUM GROUP METALS .....	44
<b>OP-12</b> <b><u>Blume R., Hävecker M., Zafeiratos S., Teschner D., Vass E., Schnörch P., Knop-Gericke A., Schlögl R., Lizzit S., Dudin P., Barinov A., Kiskinova M.</u></b> METHANOL OXIDATION ON Ru CATALYSTS: REACTION PATHWAYS AND CATALYTICALLY ACTIVE STATES .....	47
<b>OP-13</b> <b>Mamash E.A.</b> STABILITY OF STEADY STATES IN NONIDEAL MODELS OF SOME DETAILED MECHANISMS OF CATALYTIC REACTIONS .....	50
<b>OP-14</b> <b><u>Arrigo R., Wild U., Lerch M., Schlögl R., Su D.S.</u></b> N-DOPING OF CARBON NANOTUBES VIA AMMOXIDATION AND AMINATION .....	52
<b>OP-15</b> <b>Votsmeier M.</b> EFFICIENT IMPLEMENTATION OF DETAILED SURFACE CHEMISTRY INTO REACTOR MODELS BY A SPLINE-REPRESENTATION OF PRECOMPUTED RATE DATA .....	55
<b>OP-16</b> <b><u>Kaichev V.V., Popova G.Ya., Chesalov Yu.A., Andrushkevich T.V., Bukhtiyarov V.I., Zemlyanov D.Yu., Knop-Gericke A., Schlögl R.</u></b> AN INVESTIGATION OF THE MECHANISM FOR METHANOL OXIDATION TO METHYL FORMATE AND DIMETHOXYMETHANE ON V <sub>2</sub> O <sub>5</sub> /TiO <sub>2</sub> CATALYST .....	57

<b>OP-17</b>	
<b><u>Kravtsov A.V., Ivanchina E.D., Ivashkina E.N., Yuriev E.M., Fetisova V.A.</u></b>	
SIMULATION OF ALKANES DEHYDROGENATION PROCESS .....	60
<b>OP-18</b>	
<b><u>Zenkovets G.A., Kryukova G.N., Richter K.</u></b>	
EFFECT OF THE STRUCTURAL ARRANGEMENT OF (MoVW) <sub>5</sub> O <sub>14</sub> -BASED CATALYSTS ON THEIR CATALYTIC PROPERTIES IN THE REACTION OF THE ACROLEIN OXIDATION INTO ACRYLIC ACID .....	63
<b>OP-19</b>	
<b><u>Sorokin A.M., Kaichev V.V., Gladky A.Yu., Rudina N.A., Prosvirin I.P., Bukhtiyarov V.I.</u></b>	
CATALYTIC ETCHING OF NICKEL IN PROPANE OXIDATION .....	66
<b>OP-20</b>	
<b><u>Roth C., Mazurek M., Benker N., Scott F.J., Ramaker D.E.</u></b>	
ACTIVE ELECTROCATALYSTS BY MODULAR DESIGN .....	68
<b>OP-21</b>	
<b><u>Roessner F., Kuhlmann A.</u></b>	
HYDROISOMERISATION OF n-HEXANE ON LAYERED ARRANGEMENTS OF H-ERIONITE AND Pt/Al <sub>2</sub> O <sub>3</sub> .....	71
<b>OP-22</b>	
<b><u>Abramova A.V., Kulumbegov R.V.</u></b>	
REGULATION OF PROPERTIES OF CATALYSTS OF DIMETHYL ETHER CONVERSION TO LIGHT OLEFINS BY ZEOLITES MODIFICATION .....	73
<b>OP-23</b>	
<b><u>Grigorieva N.G., Galyautdinova R.R., Kutepov B.I., Dzhemilev U.M., Paukshtis E.A.</u></b>	
STUDY OF THE CONNECTION BETWEEN ACIDIC AND CATALYTIC PROPERTIES OF ZEOLITES IN THE DIMERIZATION OF α-METHYLSTYRENE.....	76
<b>OP-24</b>	
<b><u>Abramova A.V., Panin A.A.</u></b>	
TARGET MODIFICATION OF ACID PROPERTIES ZEOLITES FOR OBTAINING OF EFFECTIVE CATALYSTS OF n-HEXANE AND FISCHER-TROPSCH SYNTHETIC GASOLINE ISOMERIZATION.....	78
<b>OP-25</b>	
<b><u>Pestunova O.P., Ogorodnikova O., Kuznetsov V., Moseenkov S.</u></b>	
WET PEROXIDE OXIDATION OF ORGANIC POLLUTANTS IN AQUEOUS MEDIA IN PRESENCE OF CARBON MATERIALS .....	81
<b>LIST OF PARTICIPANTS</b> .....	84
<b>CONTENT</b> .....	88

Russian-German Seminar on Catalysis  
“Bridging the Gap between Model and Real Catalysis”

**ABSTRACTS**

**Editors:** Prof. Valerii I. Bukhtiyarov  
Dr. Vasilii V. Kaichev

The most of abstract are printed as presented in camera-ready texts and all responsibilities we address to the authors. Some abstracts underwent a correction of misprints and rather mild editing procedure.

Compilers: Lyudmila Ya. Startseva  
Irene E. Beck

Computer processing of text: Natalia A. Tsygankova

Cover design & disk-maker: Aleksei A. Spiridonov

Подписано в печать 25.05.2007

Формат 60x84/8

Печ. л. 11

Заказ

Тираж 80

---

Отпечатано на полиграфическом участке издательского отдела

Института катализа СО РАН  
Просп. Академика Лаврентьева, 5,  
Новосибирск, 630090